UNIVERSITY OF ALBERTA

A STUDY OF CDMA USING GOLD CODES FOR AN OPTICAL FIBER COMMUNICATION SYSTEM

by

ZHIJING CHRISTINE CHEN

A THESIS

SUBMITTED TO THE FACULTY OF GRADUATE STUDIES AND RESEARCH

IN PARTIAL FULFILMENT OF THE REQUIREMENTS FOR THE DEGREE OF

MASTER OF SCIENCE

DEPARTMENT OF ELECTRICAL ENGINEERING

EDMONTON, ALBERTA

SPRING 1990

ISBN 0-315-60266-X

UNIVERSITY OF ALBERTA

RELEASE FORM

NAME OF AUTHOR: ZHIJING CHRISTINE CHEN

TITLE OF THESIS: A STUDY OF CDMA USING GOLD CODES FOR AN OPTICAL FIBER COMMUNICATION SYSTEM

DEGREE: MASTER OF SCIENCE

YEAR THIS DEGREE GRANTED: SPRING 1990

Zhijing C. Chen

(STUDENT SIGNATURE)

Dept. of Electrical Engineering

(STUDENT PERMANENT ADDRESS)

University of Alberta

Edmonton, Canada T6G 2G7

Date: Dec. 19, 1989

UNIVERSITY OF ALBERTA

FACULTY OF GRADUATE STUDIES AND RESEARCH

The undersigned certify that they have read, and recommend to the Faculty of Graduate Studies and Research for acceptance, a thesis entitled A STUDY OF CDMA USING GOLD CODES FOR AN OPTICAL FIBER COMMUNICATION SYSTEM submitted by ZHIJING CHRISTINE CHEN in partial fulfilment of the requirements for the degree of MASTER OF SCIENCE in ELECTRICAL ENGINEERING.

Colin G. Englefield.

Supervisor

Supervisor

Wo-Sang Young

Date....................1989

ABSTRACT

An implementation of the code division multiple access (CDMA) technique in an optical fiber multi-user system is described in this thesis. CDMA encoding/decoding techniques are discussed first, followed by the characteristics that the address codes should possess. Several types of sequence have been examined theoretically, and Gold codes have been chosen as the address sequences to be used.

With the aid of computer simulations, the system capacity and the BER caused by interference from other signals have been discussed and calculated, and illustrative examples of CDMA transmission under various conditions have been presented. It has been verified that, by using what is referred to as "synchronous data slot transmission", a CDMA system utilizing N-chip Gold codes can support more than N users, with error-free transmission being maintained for up to N users.

An experimental system has been designed and constructed in order to verify the properties of CDMA using 31-chip Gold codes. It consists of two transmitters, an optical fiber channel and a receiver decoder. Synchronous data slot transmission was used, which can in principle support up to 31 users with error free transmission. A novel correlator circuit, which use a 4-quadrant multiplier, was implemented in the decoder, allowing an increase of the data rate compared to a previously used correlation method. For the system tested in this thesis, which was operated at the DS-3 chip rate of 44.736 Mb/s (a data rate of 1.40 Mb/s), a BER of less than 10^{-9} was obtained.

The results obtained in this project indicate that CDMA using Gold

codes is a suitable method for achieving multi-user access in an optical fiber communication system.

ACKNOWLEDGEMENTS

I would like to express my appreciation and respect to Dr. C. G. Englefield and Dr. P. A. Goud for their encouragement, advice and help throughout the course of this research project. I wish to thank Mr. B. Telder, Mr. D. Rudyk and Mr. K. Campbell for their technical assistance and suggestions. Thanks are also expressed to the examining committee for reviewing this work.

As well, appreciation is extended to the following:

- -Dr. R. Lowe (Northern Telecom, Saskatoon) for supplying the optical fiber.
- -Dr. J. McMullin, Mr. K. Teo, Ms. A. Somani, Dr. J. Binder and Mr. S. Lohtia for their useful suggestions and discussions.
- -My fellow students Mr. S. Vandenbrink, Mr. V. A. Anand and Mr. A. Pande in the Optical and Microwave Communication group.
- -Dr. Kingma and Dr. Gourishankar for the use of their computers.
- -The Alberta Telecommunications Research Centre for the occasional use of their equipment.
- -The National Sciences and Engineering Research Council of Canada for their support of this research work through NSERC grants.
- -The Department of Electrical Engineering for the award of a teaching assistantship.

I wish to thank my parents, sister, friends and teachers, whose love and help have made it possible to complete the work reported here.

TABLE OF CONTENTS

LIST OF TABLES

LIST OF FIGURES

LIST OF SYMBOLS

$\mathcal{A}_i$	Logic data of 1 or 0 transmitted to station i
A_i	Electrical signal representing the logic data $\mathcal{A}_i$
$a(t)$	M-sequence
$a(t-\ell)$	The ℓ phase-shifted replica of M-sequence
$a(t)T^i$	An i-chip shift operator which shifts a sequence cyclically to the left by i chips
C_j	The correlation output of receiver j
C_{mj}	Attenuation factor between transmitter m and receiver j
$\mathbb{E}(x)$	The mean value of x
$n(t)$	The channel noise at time t
N	Number of chips per sequence
$p(\Phi_{ij}(T_l))$	Probability of $\Phi_{ij}(T_l)$ occurring
R_j	The received input signal at receiver j
$\mathcal{X}_i(t_n)$	The n^{th} chip of the logic sequence $\mathcal{X}_i$
$X_i(t_n)$	The n^{th} chip of the electrical sequence representing the logic sequence $\mathcal{X}_i(t_n)$
$X_i(t_n-T_l)$	The ℓ chip-shifted replica of $X_i(t_n)$
$\sigma^2(x)$	The variance of x
Φ_{ab}	The correlation of sequences a and b
$\Phi_a(i)$	The correlation of m-sequences a and $T^i a$
$\Phi_{jj}(0)$	The in-phase auto correlation of the j^{th} sequence $X_j(t_j)$,
$\Phi_{ij}(T_l)$	The ℓ chips out-of-phase cross correlation between the i^{th} and the j^{th} sequences $X_i(t_n)$ and $X_j(t_m)$, $t_n = t_m+T_l$,

LIST OF ABBREVIATIONS

APD	Avalanche photo diode
BER	Bit error rate
CCD	Charge-coupled device
CDMA	Code division multiple access
dBμ	dB relative to 1 micro-watt
DS	Direct sequence
ECL	Emitter coupled logic
E-O	Electro-optical
FDM	Frequency division multiplexing
IC	Integrated circuit
I-D	Integrate-and-dump
LAN	Local area network
LED	Light emitting diode
LD	Laser diode
M-SEQUENCE	Maximal linear sequence
M-TPC	Modified time polarity control
NEP	Noise equivalent power
NRZ	Non return to zero
O-E	Opto-electrical
OFC	Optical fiber communication
OFDM	Optical frequency division multiple access
OTDM	Optical time division multiple access
PN	Pseudo-noise
PRBS	Pseudo-random binary sequence

$pW/Hz^{1/2}$	Pico-watt(s) per square root Hertz
RZ	Return to zero
SAW	Surface-acoustic-wave
SCM	Sub-carrier multiplexing
SNR	Signal to noise ratio
TDM	Time division multiplexing
TE	Temperature
TF	Time-frequency
TTL	Transistor-transistor logic
WDMA	Wavelength division multiple access

1. INTRODUCTION

1.1 Optical Fiber Communication Systems

During the last decade, optical fiber has been replacing coaxial cable and microwave waveguides in many applications. Optical fiber communication (OFC) uses a carrier at an optical frequency (infra-red range), and an optical fiber as the channel medium to transmit information. It has several unique advantages [1], such as: enormous potential bandwidth, immunity to interference and cross-talk, electrical isolation, signal security, low transmission loss, small size and light weight, potential low cost, etc. Because of these properties, OFC is widely used today and will be even more widely used in future transmission and communication systems.

An OFC system is normally composed of three parts: the transmitter, the optical fiber channel, and the receiver. In a digital OFC system (see Fig.1.1), the transmitter consists of a data encoder, a modulator and an electro-optical (E-O) converter such as a laser diode (LD) or a light emitting diode (LED) [2]. The transmission channel could be either single mode or multi-mode optical fiber. The receiver consists of an opto-electrical converter, possibly an optical local oscillator, an amplifier and a decoder. During transmission over the fiber channel, the signal is degraded due to attenuation, dispersion, noise, and cross-talk. This degradation decreases the signal to noise ratio (SNR), and causes bit errors. To regenerate and reshape the signal waveform, one or more repeaters (a back-to-back receiver-transmitter unit) may be necessary, depending on the total

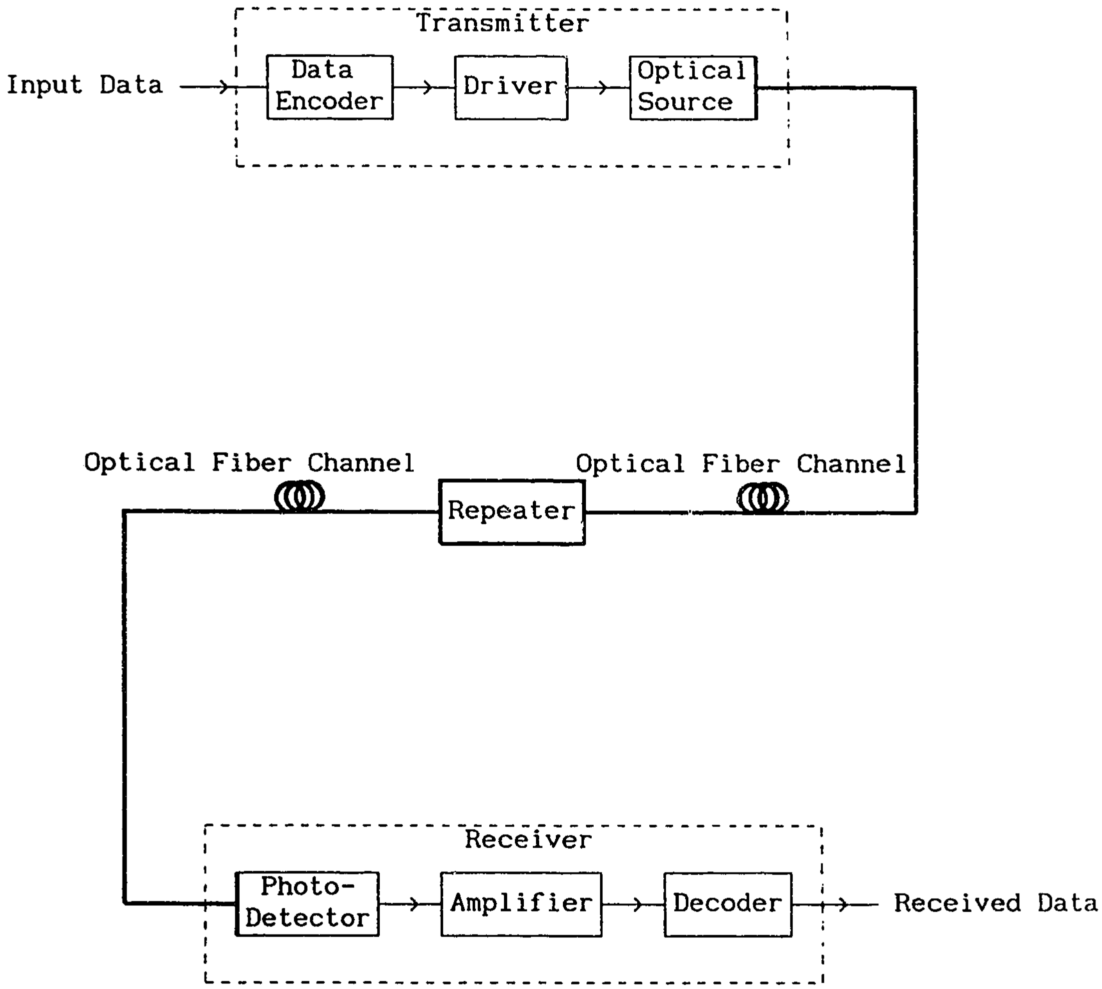

Fig. 1.1 An optical fiber digital communication system.

amount of degradation that has occurred in the link.

The two most important technical parameters of a communication channel are the maximum distance that the signal can be sent without a repeater, and the information-carrying capacity that the channel can provide. Research and development in OFC is aiming at, on the one hand, higher bit rates and longer repeater distances. On the other hand, there is an increasing need for low cost lower bit rate local area networks (LANs) covering shorter distances (ranging from a few meters to about ten kilometers), transmitting multiple sources of digitized information such as voice, video, images, and data traffic, with provision for frequent access by a large number of users to the system [3, 4, 5]. This kind of network has several stations connected within a room, a building, or several buildings (e.g., a campus), and a multi-user transmission method needs to be used here.

1.2 Multi-User Access Techniques

An optical fiber multi-user transmission system can be coherent or incoherent. A coherent system can, in principle, support a large number of users, but it requires high quality single-mode LDs with good phase stability [6, 7]. An incoherent system can also support many users by choosing a suitable method of multiplexing. Since LEDs or ordinary LDs can be used as the optical source, the cost of an incoherent LAN system is much lower than that of a coherent one.

In an incoherent multi-user LAN system, signals can be multiplexed electrically or optically. When electrical multiplexing is used, an optical source is driven by electrically multiplexed signals [8] (e.g., time division multiplexing — TDM, frequency division multiplexing — FDM, time-frequency matrix — TF, or subcarrier multiplexing — SM, etc.). In an optically multiplexed system, optical signals from different users are combined and fed into a common channel by passive optical couplers.

Optical multiplexing has several attractive properties compared with electrical multiplexing. It has a large potential bandwidth and very high signal processing speed. It also avoids the problem of queuing in TDM.

So far, several multiple access methods have been used to achieve incoherent optical multiplexing. These are optical frequency division multiplexing (OFDM), optical time division multiplexing (OTDM), wave length division multiple access (WDMA), passive optical packet transmission, and code division multiple access (CDMA) [9, 10]. The difficulty of OFDM is that it requires a highly stabilized optical source, and a narrow band optical filter in the receiver. The OTDM requires a high degree of synchronization, hence asynchronous access is not possible. The WDMA method cannot support a large number of stations or terminals (addresses), because different stations must use different optical wavelengths and their spacing is limited among other factors by the laser frequency drift impairment. The use of WDMA also leads to a difficulty in distribution control [11]. The optical packet transmission method needs some measurements to avoid signal packet collisions, and this may cause the transmitted packet to experience an unbounded delay, especially under heavy traffic [12]. Considering all of these options and their properties, it was decided to explore the properties of the CDMA method for optical multiplexing in this project.

1.3 Spread Spectrum and Code Division Multiple Access

The spread spectrum coding technique is a means of coding for transmission in which the signal occupies a bandwidth in excess of the minimum necessary to send the information. The band spreading is accomplished by means of a code which is independent of the data, and synchronized reception with the code at the receiver is used for despreading and subsequent data recovery [13]. Fig.1.2 shows a communication system using spread spectrum techniques.

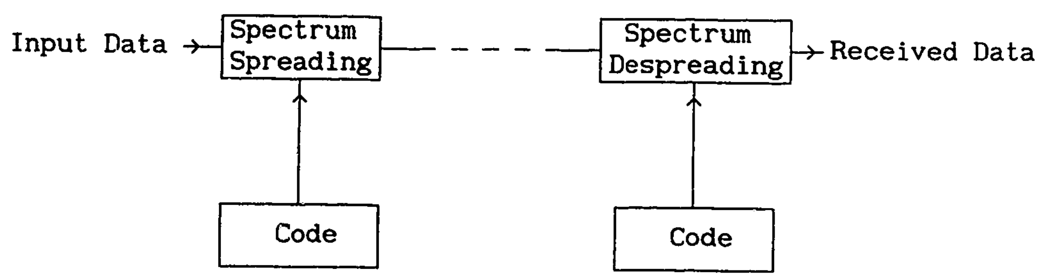

Fig.1.2 A communication system using spread spectrum.

The code division multiple access (CDMA) method used in this project is one of the spread spectrum techniques called direct sequence (DS) modulation CDMA. In a DS modulation system, a carrier is modulated by a digital code sequence whose bit rate is much higher than the information signal bandwidth [14]. DS CDMA is an engineering compromise between the transmission bandwidth, which is abundant in an OFC system, and the multi-address switching ability, which is not so strong in OFC.

A DS modulation optical fiber CDMA system is illustrated in Fig. 1.3.

In this system, each station is assigned a fixed code sequence, which serves as its address. Any station transmitting data encodes each data bit 0 using the address code sequence of its intended receiver, and each data bit 1 using the complement of this code sequence. For example, sequence $\mathcal{X}_i$ or $\mathcal{X}_j$ is assigned to station i or j as the address, respectively; the station k transmitter wishing to send data to station i uses binary keywords $\mathcal{X}_i$ to encode each data bit. Code word $\mathcal{X}_i$ or $\overline{\mathcal{X}}_i$ is transmitted, corresponding to the data 0 or 1 ($\overline{\mathcal{X}}_i$ is the complement of $\mathcal{X}_i$, obtained by the inversion of $\mathcal{X}_i$).

At each transmitter, an electro-optical source (E-O) is intensity modulated by the coded signal. The optical signals from different transmitters are combined and coupled onto a common optical fiber channel by optical couplers. The resulting multi-level signal is transmitted through the common channel, and split by another optical coupler at the receiver end.

Each receiver first converts the multi-level optical signal into an electrical one by an opto-electrical (O-E) converter, then uses its particular address sequence to correlate with the multi-level signal. The i^{th} receiver is able to decode the signal into a data bit 1 or 0 by knowing and using the code sequence $\mathcal{X}_i$.

If the address or code sequences were orthogonal with respect to each other, there would not be any interference between stations. However, the different code sequences being used are usually pseudo-orthogonal [15], therefore, transmissions intended for other

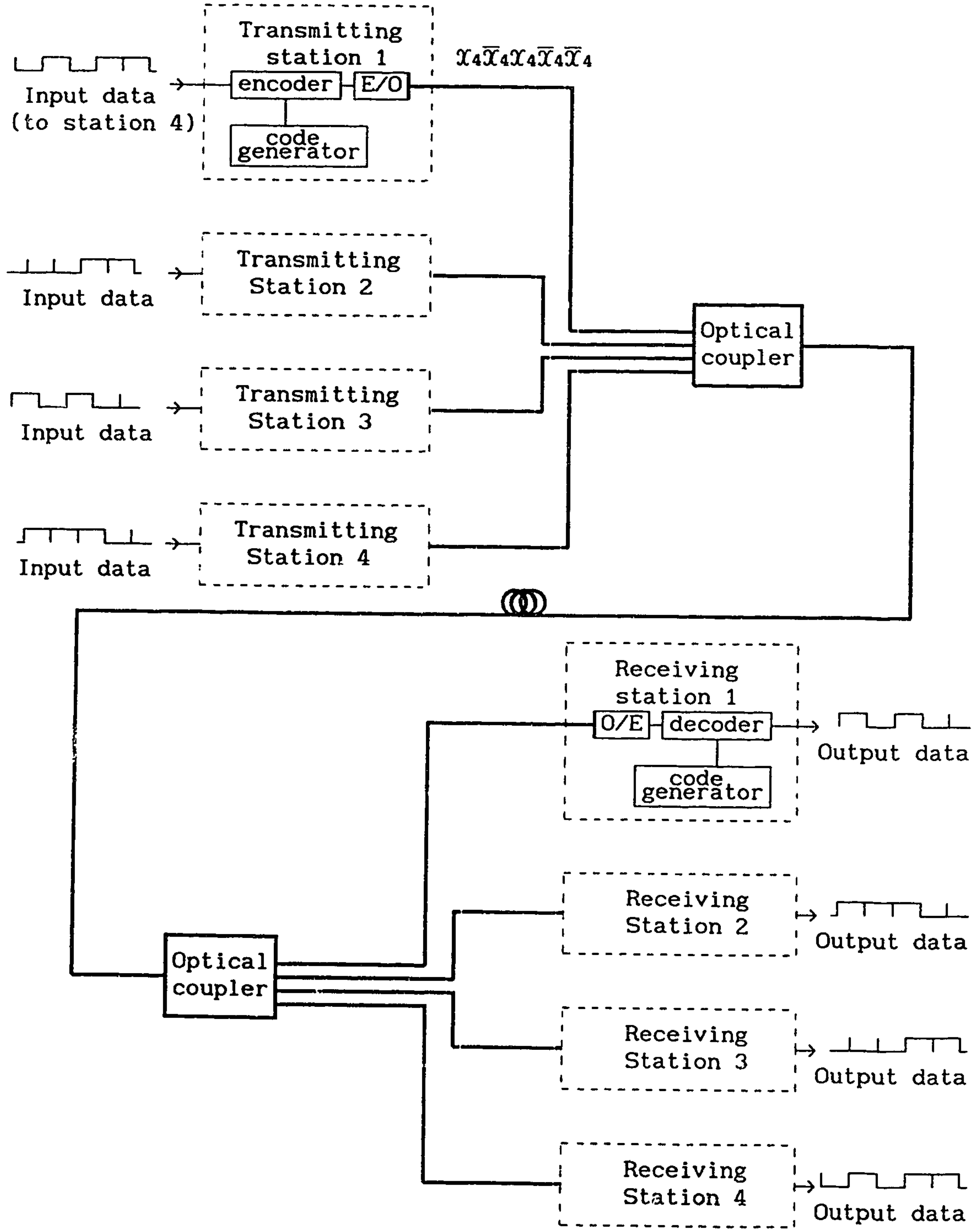

Fig. 1.3 The DS modulation optical fiber CDMA system.

stations, coded by different keywords, will appear as interference (or cross-talk) for this i^{th} receiver. Generally speaking, for a certain receiver station, other received signals intended for other stations will be partially rejected by the correlator and cause only a small amount of interference noise. Each receiver, using its own code sequence, will only decode the data intended for it. Provided that no two simultaneous users attempt to send data to the same destination, using a set of properly chosen code sequences can enable a number of stations to access the channel simultaneously.

In order to decode the data signal, the desired station (station i) must maintain synchronism with the intended signal (from the station k transmitter). This can be obtained in two ways. One is to use a clock recovery technique, initial acquisition and tracking [16, 17]. The other method is to distribute a master clock to both transmitter and receiver, meanwhile sending trigger pulses to the receiver to trigger the local code generator. The latter method is used in this project.

Optical fiber CDMA transmission has several advantages in an optical fiber local area network (LAN):

(1) It offers potentially high speed. The high bit rate allows for great flexibility in terms of the type of service that a station can provide.

(2) It allows each bursty user to share the entire transmission channel (this occurs quite often in local area networks) by providing ...onous access to each user, so that it makes more efficient use ...channel.

(3) It allows new users to be easily added to the network by simply connecting them to the channel using a passive optical coupler.

(4) It provides multi-user simultaneous access to the channel with no waiting time; therefore, there is no need for the user to wait for the right frame slot (as in TDMA), or to wait until the channel is idle (as in carrier sense multiple access) to gain access.

(5) Forward error correction is more effective when it is used with CDMA, than when it is used with FDMA [18].

1.4 Electrical Processing and Optical Processing

For a receiver in an optical DS CDMA system, there are two basic ways to process (i.e. to spectrum despread) the received signal so as to decode the data. These two methods are electrical and optical signal processing. Optical signal processing today is usually equivalent to power measurement (incoherent), due to the lack of low cost, highly coherent lasers which would allow coherent optical detection [19]. Since, unlike voltages or currents, power cannot be negative, if coherent effects (phase information) are eliminated, signals in such a positive system cannot be optically manipulated to add to zero. In electrical processing, since +1 and -1 (normalized voltage) signals are used, selection of suitable code word takes advantage of the ability to sum voltages to zero in the electrical domain. Therefore, codes or sequences that satisfy the pseudo-orthogonal properties in electrical processing do not necessarily maintain those properties in optical processing, and optical orthogonal codes need to be introduced.

Up to now, there have been several papers describing incoherent optical fiber transmission using CDMA. A system using Gold codes, electrical processing, optical multiplexing, and asynchronous data slot transmission has been reported [20]. In other systems [21, 22, 32], optical processing and new CDMA sequences which were designed specifically for this kind of processing were used. A 16-channel digital CATV multiple optical transmission system using a modified time polarity control (M-TPC) line code has been presented [24]. A system using the Alberta Code and an electro-optical combined CDMA technique has also been proposed [25].

In this project, CDMA using electrical processing has been selected for the following reasons:

Firstly, there has been no work reported discussing electrically processed CDMA using a synchronous data slot transmission pattern so far. It is shown in this investigation, which includes both simulation and experimental verification, that this kind of transmission is able to minimize user interference, thus increasing the allowable number of simultaneous users.

Secondly, although optical processing can in principle provide better system performance (faster data rate and more efficient bandwidth usage) than electrical processing, the special facilities required to construct the necessary optical integrated experimental system were not available. In addition, traditional codes are not suitable for positive signal processing [19] and research on new codes is needed for optical processing.

Finally, there is another method of decoder correlation, namely, optical switches and electro-optical signal processing. The basic concepts of electrical and electro-optical signal processing are quite similar since each of them uses both the positive and negative part of the signal for correlation. Therefore, if the coding, transmitting, and decoding methods work for electrical processing, they will also in principle work for electro-optical processing. So, today's research on CDMA using electrical processing may be useful for other signal processing methods in the future.

1.5 Thesis Objectives and Organization

1.5.1 Objectives

An OFC network using CDMA is attractive for a LAN. By using different code sequences, different transmission patterns or different signal processing methods, there are several possible ways of realizing multi-user access. The main objectives of this thesis are:

(1) to investigate the properties of an optical fiber CDMA system both theoretically and experimentally,

(2) to set up an experimental transmission system,

(3) to optimize the performance of a CDMA system in an optical fiber LAN application.

The following steps have been taken to achieve the above objectives:

(1) a theoretical investigation of code sequences was carried out, so that a set of code words used as the address codes in CDMA could be chosen to maintain minimum interference noise,

(2) a theoretical investigation of the transmitting pattern being used in CDMA was conducted, to obtain the maximal number of stations that the system could support for a given chip rate,

(3) a computer simulation for the system BER caused by the

interference of other users and for the channel capacity under a certain system BER has been presented,

(4) computer simulations for transmission under different conditions have been demonstrated,

(5) an experimental system was set up, including: Gold code generators, encoders, lasers and modulators, fiber link and coupler, photo-detector and decoder,

(6) experimental measurements of system BER, channel capacity, the near-far problem, and the signal spectrum, were obtained under the conditions of single station transmission as well as multi-user environments,

(7) a comparison between computer simulation and experimental results has been made,

(8) analysis, discussion of the results, and conclusions have been presented.

1.5.2 Organization

The first chapter has given a brief description of OFC systems, and the concepts of the CDMA spread spectrum technique. Discussions about the different multiple access techniques, and the state-of-the art in the area of multi-user communications, has been presented.

Chapters 2 and 3 concern the first stage of this project; i.e., the theoretical investigation and computer simulation. Chapter 2 discusses in detail the auto-correlation and cross-correlation concepts, the CDMA encoding/decoding process, and the network configurations. The properties of codes which can possibly be used as address sequences are investigated next. It is concluded that Gold sequences are the best choice, and the method for the generation of Gold sequences is discussed.

The computer simulation results of interference noise and system BER are presented in Chapter 3. The asynchronous and synchronous data slot transmission patterns are investigated first, then multi-user behavior and interference are discussed. The relations between the bit error rate (BER) and the length of the Gold code and the number of simultaneous users are illustrated. The computer simulations for several different transmission conditions are demonstrated.

Chapters 4 and 5 deal with the second stage of this project; i.e., the experimental system operation and measurements. Chapter 4 describes the design and construction of each part of the experimental system, which consists of two transmitters, the optical coupler, the fiber channel, and the receiver. All the circuit diagrams are given in detail, and many problems concerning the circuits and the system configuration are discussed.

In Chapter 5, the performance of different parts of the system, especially the operation of the electronic coder and decoder, are demonstrated first. Next, the system transmission properties such as signal waveforms, transmission error and the system capacity, have been measured and illustrated for the case of single station and multi-station transmission. The relation between the BER and various system parameters are presented. The power spectrum of the transmitted and received signals are also illustrated. A discussion of the various sources of error is given at the end of this chapter.

In Chapter 6, the results and conclusions of this thesis work are outlined, Several areas in which this project can be continued are pointed out. Possible future research topics in the area of optical CDMA are also outlined.

2. CODE DIVISION MULTIPLE ACCESS

2.1 CDMA Coding and Decoding

In a CDMA communication system the multiplexing is accomplished by means of a code which is independent of the data, and synchronized reception with the code at the receiver is used for the data decoding. The important properties of the code sequences and the basics of the CDMA technique are discussed in the following sections.

2.1.1 Auto-Correlation and Cross-Correlation of Codes

Auto-correlation is the measure of similarity between a code $X_i(t)$ and a phase-shifted replica of itself $X_i(t-\tau)$. It is defined by the integral

$$\Phi_{ii}(\tau) = \int_{-\infty}^{+\infty} X_i(t)\, X_i(t-\tau)\, dt \qquad (2.1.1)$$

for a continuous signal, or defined by the sum

$$\Phi_{ii}(T_n) = \sum_{k=1}^{N} X_i(t_k)\, X_i(t_k-T_n) \qquad (2.1.2)$$

for the discrete case. It is equal to the number of agreements minus the number of disagreements for the overall length of the code $X_i(t_k)$ and $X_i(t_k-T_n)$ $(k = 1, 2, \cdots, N)$, when the codes are compared chip by chip. An auto correlation function is a plot of the auto-correlation over all phase shifts T_n $(n = 0, 1, \cdots N-1)$ of the code.

Similarly, cross-correlation is defined by the integral

$$\Phi_{ij}(\tau) = \int_{-\infty}^{+\infty} X_i(t)\, X_j(t-\tau)\, dt, \qquad (2.1.3)$$

for a continuous signal, or defined by the sum

$$\Phi_{ij}(T_n) = \sum_{k=1}^{N} X_i(t_k)\, X_j(t_k - T_n) \qquad (2.1.4)$$

for the discrete case, which is a measure of the similarity between two different code sequences $X_i(t_k)$ and $X_j(t_k-T_n)$. It also gives a cross-correlation function over all phase shifts T_n ($n = 0, 1, \cdots N-1$) of the two codes. Fig.2.1 illustrates the auto-correlation of a 12-chip binary sequence ($N = 12$) and the cross-correlation of two 12-chip binary sequences.

$\Phi_{ii}(0) = 12$ $\qquad$ $\Phi_{ii}(2) = -2$

(a) Auto-correlation of a code.

$\Phi_{ij}(0) = 6$ $\qquad$ $\Phi_{ij}(3) = 2$

(b) Cross-correlation of two codes.

Fig.2.1 Auto-correlation and cross-correlation of codes.

When a large number of users using different codes are sharing a common channel, the code sequence must be carefully chosen to avoid interference between users. A high degree of auto-correlation and a low degree of cross-correlation between the local reference code and a received undesired code, will increase the signal and decrease the interference, improving the error rate performance [26].

2.1.2 Code Division Multiple Access

Suppose that data $\mathcal{A}_i$ (logic) of 1 or 0, corresponding to the electrical signal A_i of 1 or -1, is transmitted to station i. Using the address sequence $\mathcal{X}_i(t_k)$ (the logic sequence representing the electrical sequence $X_i(t_k)$) to encode the data by using a modulo-2 addition, the transmitted signal is:

$$\mathcal{A}_i \oplus \mathcal{X}_i(t_k) = \begin{Bmatrix} \overline{\mathcal{X}_i(t_k)}, & \text{for } \mathcal{A}_i = 1 \\ \mathcal{X}_i(t_k), & \text{for } \mathcal{A}_i = 0 \end{Bmatrix} = \mathcal{A}_i \ \overline{\mathcal{X}_i(t_k)} \qquad (2.1.5)$$

ie., electrical signal $A_i(-X_i(t_k))$. Meanwhile, data A_1, A_2, $\cdots$, A_j, $\cdots$, A_k, are encoded and transmitted to station 1, 2, $\cdots$, j, $\cdots$, k. These encoded data A_i $(-X_i(t_k))$ are summed and transmitted by a common channel. Thus, the input of receiver j is the multi-level signal

$$I_j(t_k) = \sum_{\substack{i \\ m}} \left[C_{mj} A_i \ (-X_i(t_k)) \right] + n(t_k) \qquad (2.1.6)$$

where C_{mj} is the attenuation factor between transmitter m (m=1, 2, $\cdots$, k) and receiver j (j=1, 2, $\cdots$, k, $j \neq m$), and $n(t_k)$ is channel noise.

Assume that the receiver j is synchronized with respect to the signal sent to it by transmitter n. Using its key sequence $X_j(t_k)$, the correlation of this receiver can be expressed as

$$C_j(t_k) = \left[\sum_{\substack{i \\ m}} C_{mj}\ A_i\ (-X_i(t_k)) + n(t_k) \right]\left[-X_j(t_k) \right] \qquad (2.1.7)$$

It can then be expressed as

$$C_j(t_k) = C_{nj}\ A_j X_j(t_k) X_j(t_k)$$

$$+ \sum_{\substack{i \neq j \\ m \neq n}} C_{mj}\ A_i X_i(t_o) X_j(t_k) - n(t_k)\ X_j(t_k) \qquad (2.1.8)$$

The signal received by station j would be

$$R_j = \sum_{k=1}^{N} C\ (t_k)$$

$$= C_{nj} A_j\ \Phi_{jj}(0) + \sum_{\substack{i \neq j \\ m \neq n}} C_{mj}\ A_i\ \Phi_{ij}(T_l) + \bar{n} \qquad (2.1.9)$$

where, $\Phi_{jj}(0)$ is the in-phase auto correlation of the j^{th} keyword $X_j(t_k)$,

$$\Phi_{jj}(0) = \sum_{k=1}^{N} X_j(t_k)\ X_j(t_k) \qquad (2.1.10)$$

$\Phi_{ij}(T_l)$ is the ℓ chips out-of-phase cross correlation between the i^{th} and the j^{th} keywords $X_i(t_o)$ and $X_j(t_k)$, $t_k = t_o + T_l$,

$$\Phi_{ij}(T_l) = \sum_{o=1}^{N} X_i(t_o)\ X_j(t_o + T_l) \qquad (2.1.11)$$

A_i or A_j is the data to the i^{th} or the j^{th} receiver, and, $\bar{n}$ is the averaged noise.

The processes of data encoding and decoding are illustrated in Fig. 2.2.

In order to decode the data signal, the desired receiver (station j) must maintain synchronism with the intended transmitter signal (from station n). This can be obtained in two ways. One is to use a clock recovery technique, initial acquisition and tracking. The other method is to use a master clock to drive both the transmitter and receiver,

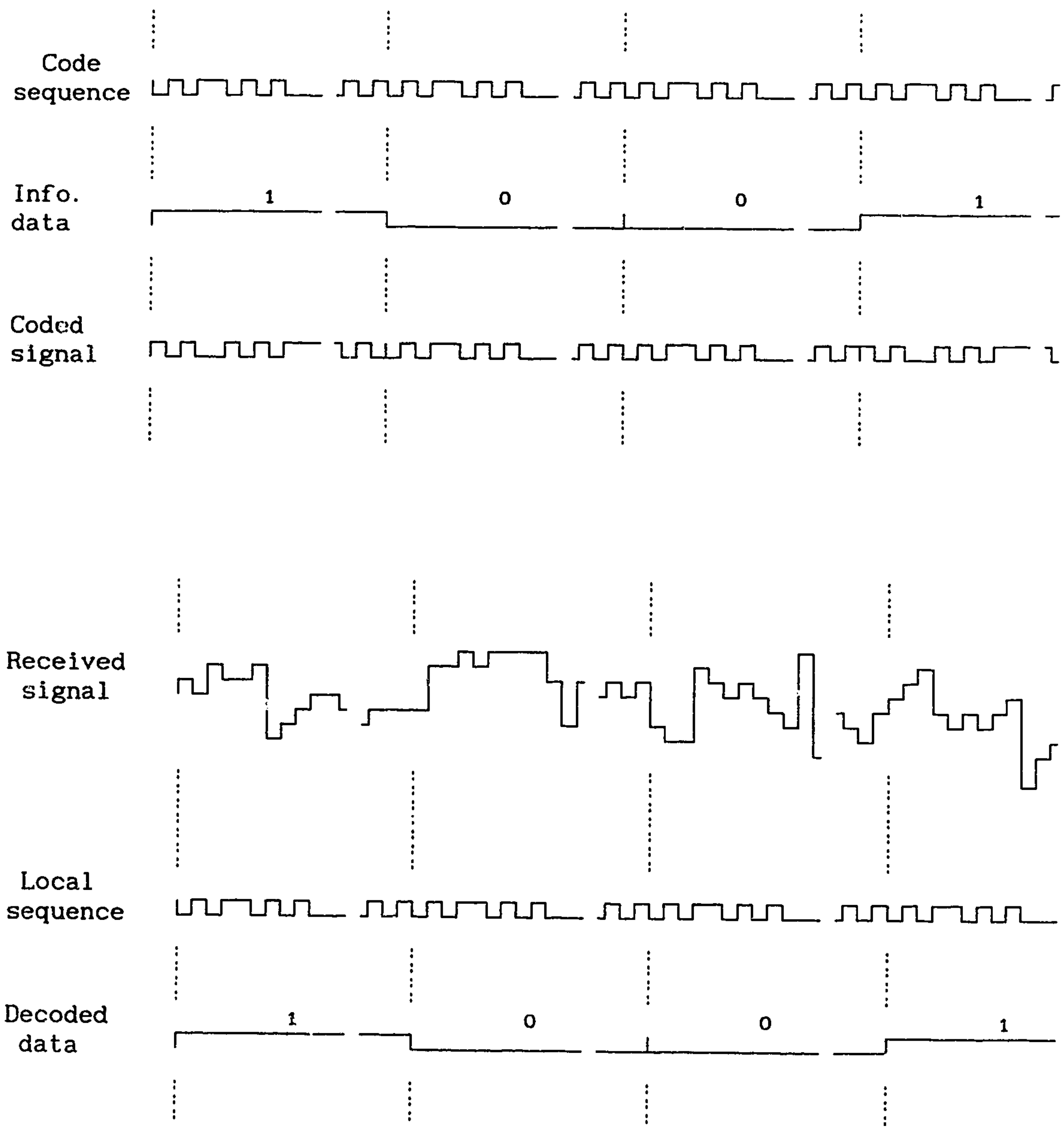

Fig. 2.2 Data encoding and decoding.

meanwhile sending trigger pulses to the receiver to trigger the local code generator.

From (2.1.9), it is obvious that to maximize the correlation of each receiver for the desired message A_j, while rejecting the interference A_i (i = 1, 2, 3, ···, $i \neq j$), two requirements need to be fulfilled:

(1) The coefficients C_{mj} should all be chosen equal to one; i.e., the system should be a power balanced network where signals from different stations arrive at each receiver with the same amount of optical power.

(2) The keywords must have a high auto-correlation $\Phi_{jj}(0)$, as well as a low cross-correlation $\Phi_{ij}(T_l)$.

2.2 Network Configuration for a Power Balanced System

The requirement of a power balanced network places some constraints on the topology of the optical fiber communication system.

In a typical OFC network, k users are geographically separated, and they can be connected with each other by an optical fiber network, such as a ring, bus, or star network. These network topologies are shown in Fig.2.3. When the optical signal is transmitted through the fiber and optical couplers, some optical power is lost due to coupling loss and fiber attenuation. The j^{th} receiver trying to detect the signal sent by the n^{th} transmitter might be much closer physically or connected by fewer couplers to the m^{th} transmitter as compared to the n^{th} transmitter, therefore, the coupling efficiency factor C_{mj} will be larger than C_{nj} in (2.1.9). Assuming that the output optical signal

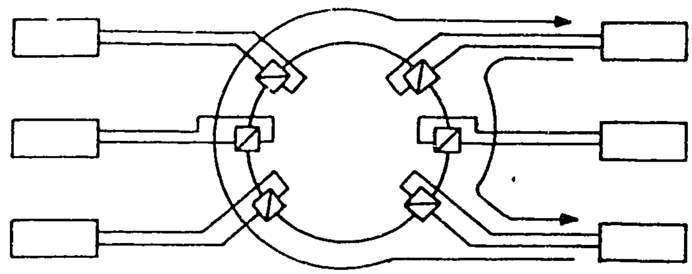

(a)

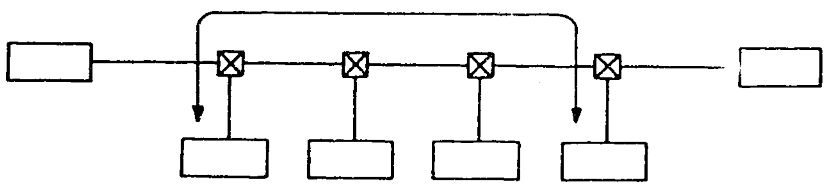

(b)

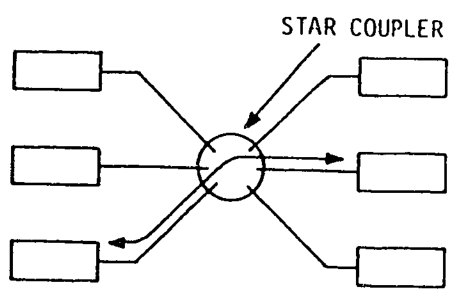

(c)

Fig. 2.3 The network topologies: (a) ring; (b) bus; and (c) star.

------ a station

power from each transmitter is the same, the m^{th} signal will arrive at the receiver j with a stronger power than that of the intended n^{th} signal, i.e. the interference at receiver j due to the m^{th} signal is increased. This decreases the system SNR and increases the error rate, resulting in a decrease in the allowable number of simultaneous users in the network.

This is usually called the "near-far problem" in a radio system using spread spectrum [27]. In an optical fiber local area network, because the fiber loss is only a fraction of 1 dB/km and the distance between users is typically less than 10 km, the "near-far problem " is caused mainly by the difference in the number of optical couplers that a signal passes through, rather than the length of fiber that the signal passes through between the transmitter and receiver.

Because of this, a ring or bus [28, 29] configuration (refer to Fig.2.3) should not be used, unless active couplers are used. A power balanced configuration such as a star network is preferable, where every signal, whether desired or undesired, is received with the same power. In this case $C_{mj} \equiv 1$, where $m = 1, 2, \cdots k$. Then the signal received by station j is

$$R_j = A_j \, \Phi_{jj}(0) + \sum_{i \neq j} A_i \, \Phi_{ij}(T_i) + \bar{n} \qquad (2.2.1)$$

This gives the best average SNR for each station, and hence allows the largest number of simultaneous users.

An N-by-1 star coupler made from a network of 2-by-2 optical couplers can be used to combine optical signals from N stations and feed them into the common optical fiber channel. Such a configuration is show in Fig.2.4. As has been mentioned before, the power loss in the fiber is small in a LAN since the transmission distance is short, but

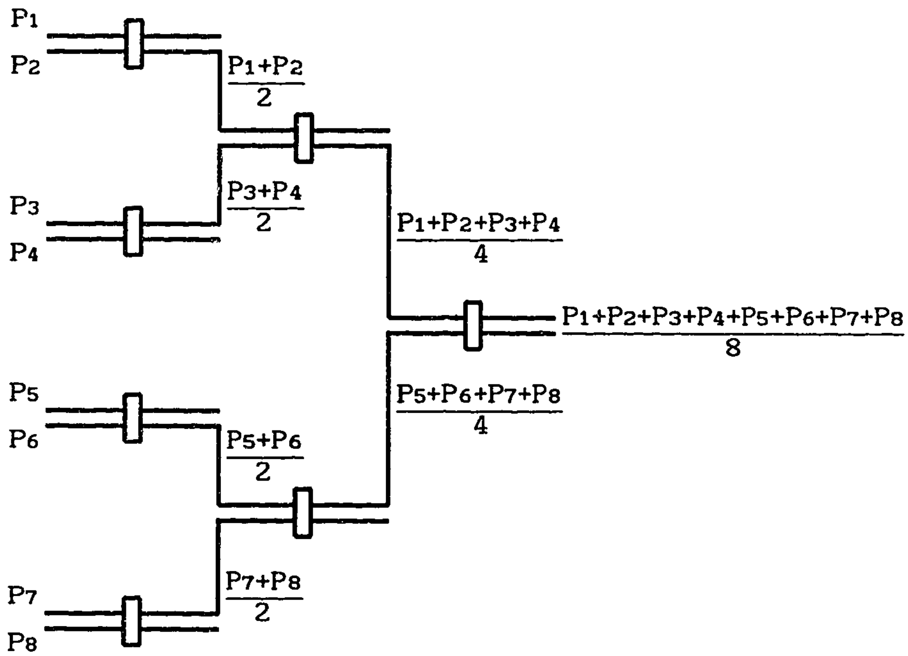

(a) An 8-by-2 star coupler made of a network of 2-by-2 couplers.

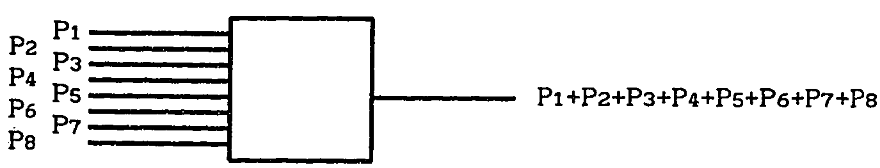

(b) An 8-by-1 star coupler.

Fig. 2.4 Star couplers.

the signal suffers a 3 dB loss when passing through each 3 dB coupler. Therefore, the overall loss depends mainly on the number of couplers the signal passes through. As long as the system power budget allows the use of the N-by-2 star coupler configuration shown in (a), this method is preferable to the commercial N:1 star coupler configuration shown in (b). An N:1 star coupler is usually more expensive and less power balanced due to imperfections in the manufacturing processing.

2.3 Possible Codes for CDMA

To fulfill the second requirement in Section 2.1, the code sequence used for CDMA should have these properties:

(1) be easy to generate,

(2) be statistically pseudo-random,

(3) have high auto-correlation as well as low cross-correlation, and

(4) should be such that it is easy for the receiver to synchronize with the desired signal.

Considerations and discussions about what kind of sequence is best for this project, and the method of sequence generation will be given in the following sections. Among the many codes available, two possible sequences that satisfy some or all of these properties are the M-sequences and Gold sequences.

2.3.1 M-Sequences

Maximal length sequences (often called m-sequences or maximal codes) are, by definition, the longest sequences that can be generated by a shift register, or a delay element, with a given length [30]. An m-sequence of length $N = 2^n-1$ chips is the longest sequence that an n-stage binary linear feedback shift register can generate.

Certain m-sequences will interfere very strongly with each other. Those sequences (a and b) exhibiting the minimum possible cross-correlation peak (bounded by $|\Phi_{ab}| \le 1+2^{(n+1)/2}$, n odd) are referred to as preferred m-sequences [11]. Usually, CDMA requires a large number of assignable addresses. Since there are only a few preferred m-sequences (6 sequences when N = 127), it is not suitable to use a set of different m-sequences (a, b, c, $\cdots$,) for CDMA, when a large number of address sequences are needed.

However, it has been noted that the correlation result for an m-sequence a with its i-chips-shifted sequence $T^i a$, where T is a chip shift operator which shifts the sequence cyclically to the left by one chip (and T^2 by two chips, etc.), is [15, 31]:

$$\Phi_a(i) = \begin{cases} N, & \text{if } i=0 \text{ or } N \\ -1, & \text{otherwise} \end{cases} \tag{2.3.1}$$

Therefore, it is possible to use one m-sequence $a(t_n)$ and its chip-shifted sequences $a(t_n-T_l)$ (ℓ = 1, 2, $\cdots$, N), as address code sequences. From (2.1.9), the correlation result of receiver j is

$$R_j = \sum_n \{ a(t_n-T_j) \Sigma A_i a(t_n-T_i)\}$$

$$= N A_j - \sum_{i\neq j} A_i + n \tag{2.3.2}$$

Such an approach requires correct synchronization between the coded signal and the receiver local keyword, because a one bit shift of the position of the receiver keyword means in fact changing the keyword from $\alpha(t_n-T_j)$ to $\alpha(t_n-T_{j-1})$. This will result in exactly decoding, instead of A_j, the data signal A_{j-1} which was coded by a bit shift $\alpha(t_n-T_{j-1})$ of the code sequence $\alpha(t_n-T_j)$ and was sent to another station. Thus, a correct framing match of the incoming signal and the receiver keyword becomes very important. Unlike other CDMA methods, where wrong synchronization caused by keyword shifting results in getting no data, so that the receiver can shift its local key-sequence until it does decode the data (called re-framing), here, incorrect synchronization results in obtaining data that is intended for another receiver.

In this situation, it is quite difficult to decide how to shift the local key-sequence to make it synchronous with the correct signal. One possible solution to this problem is to send a framing pulse together with the information signal so that the receiver can use this framing information to synchronize correctly.

2.3.2 Prime Codes and Other Codes

Prucnal and others [21, 22, 23] have used the Prime code [32] in some optical processing CDMA networks. MacDonald has proposed the use of the "Alberta Code" for opto-electronic detection processing [24].

Optical signal processing eliminates the limits caused by the speed of electronic signal processors, hence offers a much higher data transmission rate. However, the successful use of this method depends on the development of integrated optical components. Furthermore, there are still many problems with optical processing, such as how to design the optical orthogonal codes, and how to realize and optimize the receiver correlation when using only the positive polarity of the signal.

For this project, because of the many difficulties of using positive signal processing, electrical processing is used in the coder and decoder; thus, the prime code is not suitable.

2.3.3 Multi-Level Sequences

It is possible to utilize multi-level sequences for data encoding in CDMA [33, 34]. This can provide a higher than normal data rate by transmitting the data information using multi-level symbols. It is said that this method may increase the transmission error rate and may need to be investigated further [34].

2.3.4 Gold Sequences

For electrical processing, a set of N-chip Gold Sequences can provide N+2 nearly orthogonal sequences. They can be used as the address codes for a CDMA network and the assignable number of addresses is relatively large (up to N+2).

The addition of two m-sequences, each of length N, produces a sequence of length N which does not belong to the set of maximum length sequences. For each combination of delay between the two m-sequences, the composite sequence is different. Therefore, a pair of m-sequences can generate N non-maximal length binary sequences, each N chips long. If the component m-sequences are properly chosen, the set of composite sequences will have well defined auto-correlation and cross-correlation properties [22, 24].

A Gold sequence is obtained when a pair of preferred m-sequences a and b are combined. By shifting the m-sequence b and combining these shifted sequences (T^1b, T^2b, ···, T^ib, ···, etc.; where T is the chip shift operator as shown in Fig. 2.5) one by one with sequence a, Gold sequences $a \oplus Tb$, $a \oplus T^2b$, ···, $a \oplus T^ib$ are generated.

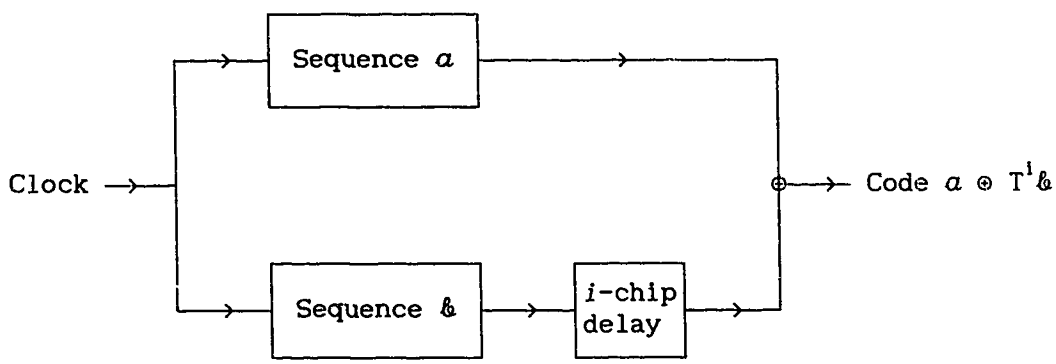

Fig. 2.5 Block diagram of Gold code generator.

For an n-stage register, there are a certain number of m-sequences that can be generated using all the possible linear combinations of the feedback taps. Among these m-sequences, only a few can be used as a preferred pair. Gold has presented a method for choosing the preferred pair of m-sequences [13, 35]. A set of N-chip Gold sequences, comprising N+2 sequences in all, is given by { a, b, $a \oplus b$, $a \oplus Tb$, $a \oplus T^2b$, ···, $a \oplus T^{N-1}b$ }, where $N=2^n-1$.

There are 2^n+1 different Gold sequences in this set. If n is odd, the auto-correlation for each Gold sequence gives

$$\Phi_{ii}(0) = N, \tag{2.3.3}$$

while the in-phase cross-correlation between any pair of sequences (without sequence *b*) is

$$\Phi_{ij}(0) = -1, \tag{2.3.4}$$

For sequence *b*,

$$| \Phi_{bj}(0) | \geq 1, \tag{2.3.5}$$

The out-of-phase cross-correlations, when the sequences are displaced by ℓ chips, are

$$\Phi_{ij}(T_l) = \begin{cases} -1+2^{(n+1)/2} \\ -1 \\ -1-2^{(n+1)/2} \end{cases}, \tag{2.3.6.a}$$

with probability,

$$p\ (\Phi_{ij}(T_l)) = \begin{cases} (2^{n-2}+2^{(n-3)/2})/N \\ (2^{n}-2^{n-1}-1)/N \\ (2^{n-2}+2^{(n-3)/2})/N \end{cases} \tag{2.3.6.b}$$

It is the objective of this project to verify the properties of a CDMA system using Gold codes, both by experiment and by computer simulation, and finally to optimize the system performance.

2.3.5 Generation of M-Sequences and Gold Sequences

An m-sequence generator can be made up of delay lines or even from lengths of coaxial cable; however, it is most commonly made up of digital circuits (flip-flops) in a shift register configuration. This kind of generator consists of a shift register working in conjunction with appropriate logic, which feeds back a logical combination of the state of two or more of its stages to its input. The output of the generator and the contents of its n stages at any time, are functions of the states of the stages fed back at the preceding sample time. Fig.2.6 shows the configuration of the generators for the sequences *[5,3]* and *[5,4,3,2]*, where the numbers in brackets refer to the number of the stages that are fed back to the input in the 5-stage shift register.

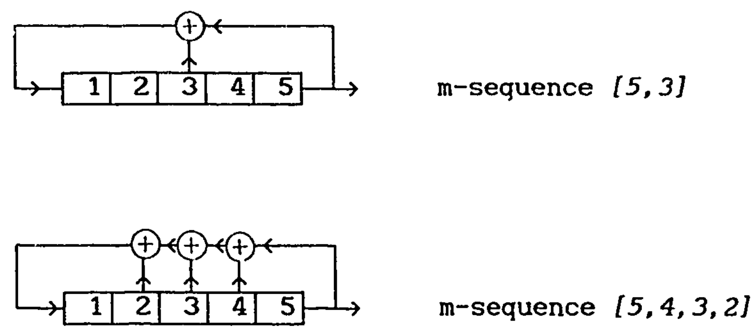

Fig.2.6 Schematic configuration of M-sequence generators.

A set of N-bit Gold sequences can be produced by combining the two N-bit m-sequences with different initial offsets. If N is equal to 31, each of the preferred pairs of 31-bit m-sequences is generated by a 5-stage shift register. The preferred pairs of m-sequences, according to Gold's rule [22, 35], are the *[5,3]* or *[5,2]* code, with the *[5,4,3,2]* code. Since these two possibilities, produced by the different pair combinations, have the same auto-correlation and cross-correlation properties, the pair combination of *[5,3]* and *[5,4,3,2]* have been used. Table 2.1 illustrates the different shift combinations of the pair of m-sequences, i.e., the generation of different Gold codes.

Fig.2.7 shows a schematic diagram of the Gold code generator made of the two m-sequence *[5,3]* and *[5,4,3,2]* generators. It produces a set of Gold sequences including 31 different Gold codes (without codes *[5,3]* and *[5,4,3,2]*), each with a length of 31 chips. Among this set, the i^{th} sequence can be written as $\mathcal{X}_i = [5,3] \oplus T^{i-1}[5,4,3,2]$ (i = 1, 2, $\cdots$, 31). A list of this set of Gold sequences $\{\mathcal{X}_1, \mathcal{X}_2, \cdots, \mathcal{X}_{31}\}$ is given in Table 2.2.

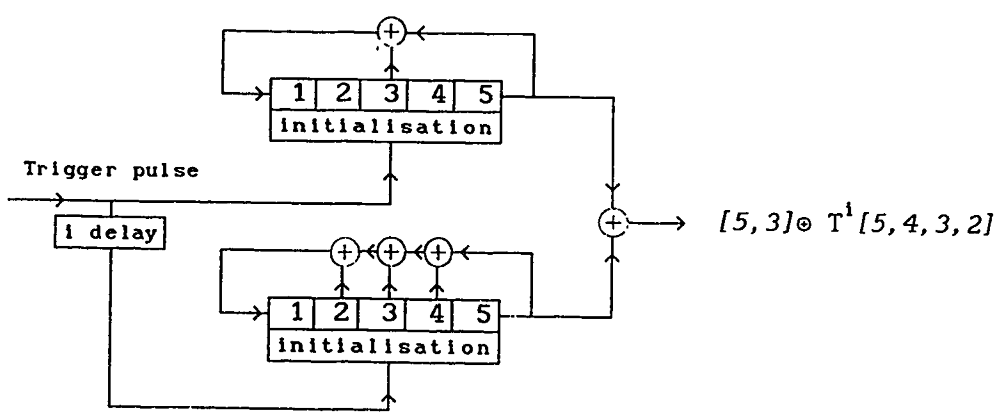

Fig.2.7 Schematic configuration of Gold code generator.

Table 2.1 Generation of Gold Codes.

Zero-shift combination:

a: 1 1 1 1 1 0 0 0 1 1 0 1 1 1 0 1 0 1 0 0 0 0 1 0 0 1 0 1 1 0 0

$T^0 b$: 1 1 1 1 1 0 0 1 0 0 1 1 0 0 0 0 1 0 1 1 0 1 0 1 0 0 0 1 1 1 0

$\mathcal{X}_1$: 0 0 0 0 0 0 0 1 1 1 1 0 1 1 0 1 1 1 1 1 0 1 1 1 0 1 0 0 0 1 0

One-chip-shift combination:

a: 1 1 1 1 1 0 0 0 1 1 0 1 1 1 0 1 0 1 0 0 0 0 1 0 0 1 0 1 1 0 0

$T^1 b$: 1 1 1 1 0 0 1 0 0 1 1 0 0 0 0 1 0 1 1 0 1 0 1 0 0 0 1 1 1 0 1

$\mathcal{X}_2$: 0 0 0 0 1 0 1 0 1 0 1 1 1 1 0 0 0 0 1 0 1 0 0 0 0 1 1 0 0 0 1

...

Five-chip-shift combination:

a: 1 1 1 1 1 0 0 0 1 1 0 1 1 1 0 1 0 1 0 0 0 0 1 0 0 1 0 1 1 0 0

$T^5 b$: 0 0 1 0 0 1 1 0 0 0 0 1 0 1 1 0 1 0 1 0 0 0 1 1 1 0 1 1 1 1 1

$\mathcal{X}_6$: 1 1 0 1 1 1 1 0 1 1 0 0 1 0 1 1 1 1 1 0 0 0 0 1 1 1 1 0 0 1 1

Table 2.2 A list of the set of 31 Gold sequences.

Gold sequences (without a and b) used as address codes: $\mathcal{X}_1$, $\mathcal{X}_2$, $\cdots$ $\mathcal{X}_{31}$ = $a \oplus T^0 b$, $a \oplus T^1 b$, $\cdots a \oplus T^{30} b$ (a result from program OG).

$\mathcal{X}_1$: 0 0 0 0 0 0 0 1 1 1 1 0 1 1 0 1 1 1 1 1 0 1 1 1 0 1 0 0 0 1 x 0

$\mathcal{X}_2$: 0 0 0 0 1 0 1 0 1 0 1 1 1 1 0 0 0 0 1 0 1 0 0 0 0 1 1 0 0 0 x 1

$\mathcal{X}_3$: 0 0 0 1 1 1 0 0 0 0 0 1 1 1 1 1 1 0 0 1 0 1 1 0 0 0 1 0 1 1 x 1

$\mathcal{X}_4$: 0 0 1 1 0 0 0 1 0 1 0 1 1 0 0 0 1 1 1 0 1 0 1 0 1 0 1 1 0 1 x 1

$\mathcal{X}_5$: 0 1 1 0 1 0 1 1 1 1 0 1 0 1 1 0 0 0 0 1 0 0 1 1 1 0 0 0 0 1 x 1

$\mathcal{X}_6$: 1 1 0 1 1 1 1 0 1 1 0 0 1 0 1 1 1 1 1 0 0 0 0 1 1 1 1 0 0 1 x 1

$\mathcal{X}_7$: 1 0 1 1 0 1 0 0 1 1 1 1 0 0 0 0 0 0 0 0 0 1 0 1 0 0 1 0 0 1 x 0

$\mathcal{X}_8$: 0 1 1 0 0 0 0 0 1 0 0 0 0 1 1 1 1 1 0 0 1 1 0 0 1 0 1 0 0 0 x 0

$\mathcal{X}_9$: 1 1 0 0 1 0 0 0 0 1 1 0 1 0 0 0 0 1 0 1 1 1 1 1 1 0 1 0 1 0 x 1

$\mathcal{X}_{10}$: 1 0 0 1 1 0 0 1 1 0 1 1 0 1 1 1 0 1 1 1 1 0 0 1 1 0 1 1 1 1 x 0

$\mathcal{X}_{11}$: 0 0 1 1 1 0 1 0 0 0 0 0 1 0 0 1 0 0 1 1 0 1 0 1 1 0 0 1 0 0 x 0

$\mathcal{X}_{12}$: 0 1 1 1 1 1 0 1 0 1 1 1 0 1 0 1 1 0 1 0 1 1 0 1 1 1 0 0 1 0 x 1

$\mathcal{X}_{13}$: 1 1 1 1 0 0 1 1 1 0 0 0 1 1 0 0 1 0 0 1 1 1 0 1 0 1 1 1 1 1 x 1

$\mathcal{X}_{14}$: 1 1 1 0 1 1 1 0 0 1 1 1 1 1 1 0 1 1 1 1 1 1 0 0 0 0 0 1 0 1 x 0

$\mathcal{X}_{15}$: 1 1 0 1 0 1 0 1 1 0 0 1 1 0 1 0 0 0 1 1 1 1 1 0 1 1 0 0 0 0 x 0

$\mathcal{X}_{16}$: 1 0 1 0 0 0 1 0 0 1 0 1 0 0 1 1 1 0 1 1 1 0 1 1 0 1 1 0 1 0 x 0

$\mathcal{X}_{17}$: 0 1 0 0 1 1 0 1 1 1 0 0 0 0 0 0 1 0 1 1 0 0 0 0 0 0 1 1 1 0 x 0

$\mathcal{X}_{18}$: 1 0 0 1 0 0 1 0 1 1 1 0 0 1 1 0 1 0 1 0 0 1 1 0 1 0 0 1 1 0 x 1

$\mathcal{X}_{19}$: 0 0 1 0 1 1 0 0 1 0 1 0 1 0 1 0 1 0 0 0 1 0 1 1 1 1 0 1 1 1 x 0

$\mathcal{X}_{20}$: 0 1 0 1 0 0 0 0 0 0 1 1 0 0 1 0 1 1 0 1 0 0 0 1 0 1 0 1 0 0 x 1

$\mathcal{X}_{21}$: 1 0 1 0 1 0 0 1 0 0 0 0 0 0 1 0 0 1 1 0 0 1 0 0 0 1 0 0 1 1 x 1

$\mathfrak{X}_{22}$: 0 1 0 1 1 0 1 1 0 1 1 0 0 0 1 1 0 0 0 0 1 1 1 0 0 1 1 1 0 1 x 0

$\mathfrak{X}_{23}$: 1 0 1 1 1 1 1 1 1 0 1 0 0 0 0 1 1 1 0 1 1 0 1 0 0 0 0 0 0 0 x 1

$\mathfrak{X}_{24}$: 0 1 1 1 0 1 1 0 0 0 1 0 0 1 0 0 0 1 1 1 0 0 1 0 1 1 1 0 1 1 x 0

$\mathfrak{X}_{25}$: 1 1 1 0 0 1 0 1 0 0 1 0 1 1 1 1 0 0 1 0 0 0 1 1 0 0 1 1 0 0 x 1

$\mathfrak{X}_{26}$: 1 1 0 0 0 0 1 1 0 0 1 1 1 0 0 1 1 0 0 0 0 0 0 0 1 0 0 0 1 1 x 0

$\mathfrak{X}_{27}$: 1 0 0 0 1 1 1 1 0 0 0 1 0 1 0 0 1 1 0 0 0 1 1 1 1 1 1 1 0 0 x 0

$\mathfrak{X}_{28}$: 0 0 0 1 0 1 1 1 0 1 0 0 1 1 1 0 0 1 0 0 1 0 0 1 0 0 0 0 1 0 x 0

$\mathfrak{X}_{29}$: 0 0 1 0 0 1 1 1 1 1 1 1 1 0 1 1 0 1 0 1 0 1 0 0 1 1 1 1 1 0 x 1

$\mathfrak{X}_{30}$: 0 1 0 0 0 1 1 0 1 0 0 1 0 0 0 1 0 1 1 0 1 1 1 1 0 0 0 1 1 1 x 1

$\mathfrak{X}_{31}$: 1 0 0 0 0 1 0 0 0 1 0 0 0 1 0 1 0 0 0 1 1 0 0 0 1 1 0 1 0 1 x 1

* There is an extra chip for dumping in each sequence. It is indicated by x, which can be either 0 or 1. Adding this extra chip will not change the cross-correlation properties of the Gold codes.

3. COMPUTER SIMULATIONS OF CDMA USING GOLD CODES

This chapter will investigate the properties of the multi-user transmission system using computer simulation. Different transmission patterns and interference from signals intended for other stations are analyzed first, to determine which pattern gives the lowest error probability caused by interference. The noise considered in this chapter is mainly that of signal interference. The additional effect of thermal noise is not discussed. Then, the relation of the system BER with the number of simultaneous users, as well as the length of the code are investigated. Finally, various transmitting conditions are simulated, and waveforms for the data, the coded ignals, the received signals, the correlated signal, and the decoded data, are illustrated.

3.1 Different Transmission Patterns

3.1.1 Asynchronous Data Slot Transmission

Asynchronous data slot transmission is depicted in Fig.3.1. In this kind of transmission, each station transmits its data at the same speed, but different stations access the network asynchronously; their coded signals are synchronous in the sense of chip bits but are asynchronous in the sense of data bits.

In order to receive the signal, the receiver j must maintain synchronization with the first chip in a data slot of the signal transmitted to it (refer to Section 1.3). Then, it is ready to decode the data coded by X_j. Since the receiver j is only synchronized with the signal coded by X_j and not with any of the other signals coded by X_i being sent to station i (i = 1, 2, 3,···, $i \neq j$), the correlation results in an auto-correlation $\Phi_{jj}(0)$ and an ℓ chips out-of-phase cross-correlation $\Phi_{ij}(T_l)$. Assuming that i+1 stations are transmitting and that the channel noise is neglected, the correlator output at the receiver j is, from (2.2.1)

$$R_j = A_j\, \Phi_{jj}(0) + \sum_{i \neq j} A_i\, \Phi_{ij}(T_l) \qquad (3.1.1)$$

where A_j, A_i = +1 or -1.

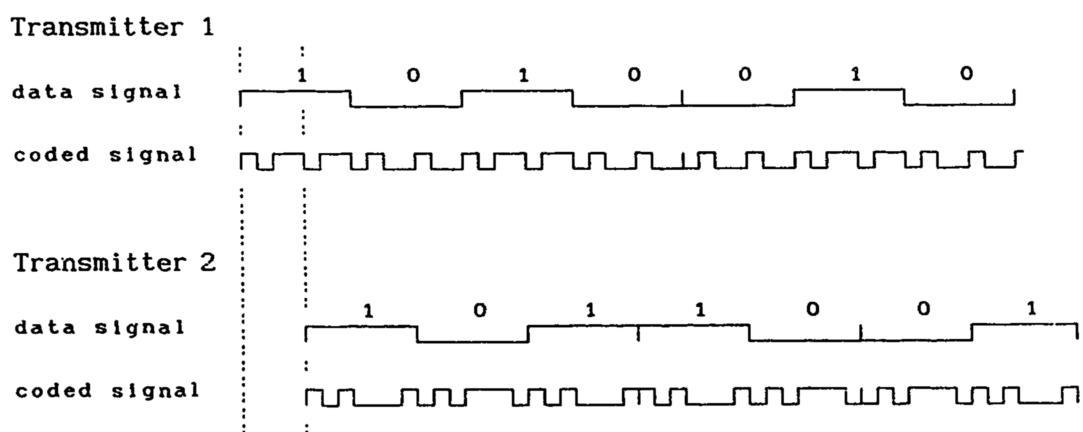

Fig. 3.1 Asynchronous data slot transmission.

3.1.2 Synchronous Data Slot Transmission

In this kind of transmission, stations in the network are synchronized with respect to not only the chip bits but also the data slots. Each station can still access the network at any time, except that it needs to wait until the beginning of each data time slot, so that the transmitted signals are synchronous in the sense of both chip bit and data slot, as [illegible] in Fig. 3.2. When the receiver i maintains synchronization with [illegible] nal coded by its address code X_i in order to receive the data, it is automatically synchronized with other signals coded by different codes and intended to be sent to different receivers. In this case, the correlator output at the receiver j (from (2.2.1)) is

$$R_j = N \cdot A_j + \sum_{i \neq j} A_i \, \Phi_{ij}(0) \tag{3.1.2}$$

where A_j, A_i = +1 or −1.

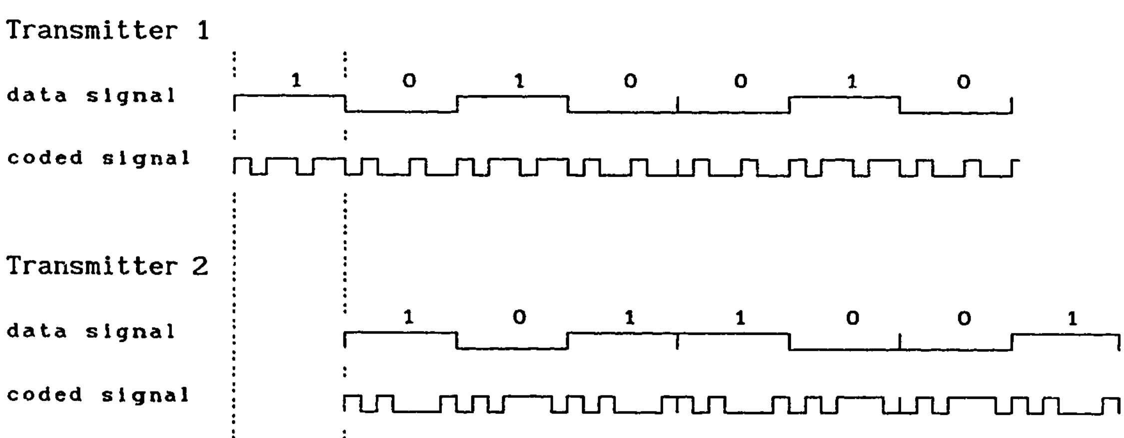

Fig. 3.2 Synchronous data slot transmission.

3.2 Interference and System BER

3.2.1 The Asynchronous Case

In general, for any number of simultaneous users k, calculation of the interference and hence the BER requires consideration of how each station interferes with other stations, using the two different phases (depending on data +1 or -1) of the three possible distributed cross-correlation values (shown in (2.3.6)). It is relatively easy to obtain the average BER versus number of users k by some approximation method, when k is very large or very small.

Referring to the detailed discussion in APPENDIX A, when the number of transmitting stations is sufficiently large, the mean value of the interference term $A_i\ \Phi_{ij}(T_i)$ in (3.1.1) is given by (A.7)

$$\mathbb{E}(\ A_i\ \Phi_{ij}(T_i)\ ) = 0, \tag{3.2.1}$$

with the variance given by (A.9)

$$\sigma^2_{asyn} = \frac{(\ N^2 + N - 1)}{N}, \tag{3.2.2}$$

and the total variance of all the k-1 different interference terms in (3.1.1) is $(k-1)\sigma^2$. For large values of k, according to the Central Limit Theorem [38], the overall interference has an almost Gaussian distribution [36, 37]. The error probability, and hence the system BER, caused by the Gaussian distributed interference with zero mean and variance $(k-1)\sigma^2$, is (refer to (A.13):

$$BER_{asyn} = \frac{1}{2} - \frac{1}{2}\,\mathrm{erf}\left[\sqrt{\frac{N^3}{2(k-1)(N^2+N-1)}}\,\right], \tag{3.2.3}$$

where

$$\mathrm{erf}(x) = \frac{2}{\sqrt{\pi}}\int_0^x e^{-u^2/2}\,du \tag{3.2.4}$$

is the error function [39], and N is the chip length of the Gold Codes.

The BER versus the number of stations k given by (3.2.3), when using different length (N) Gold sequences, are shown in Fig. 3.3. Some of the BER (N, k) values are listed in Table 3.1.

Table 3.1 BER (N, k) for asynchronous case, results of Gaussian approximation

N	k	BER
31	2	2.09×10^{-8}
	3	5.29×10^{-5}
	4	7.74×10^{-4}
	5	3.06×10^{-3}
	6	7.10×10^{-3}
127	8	1.10×10^{-5}
	9	3.61×10^{-5}
511	16	2.76×10^{-9}
	17	8.22×10^{-9}

When k is small, the interference no longer has a Gaussian distribution. Referring to the detailed discussion in APPENDIX B.1, the largest interference occurs when the intended data is $A_j = 1$ while the undesired data being sent to other stations are $A_i \equiv -1$ (i=1, 2, 3, ⋯, $i \neq j$), or $A_j = -1$ while $A_i \equiv 1$. Since the maximum value of the cross-correlation $\Phi_{ij}(T_i)$ is $\pm|1+2^{(n+1)/2}|$, in this case, the

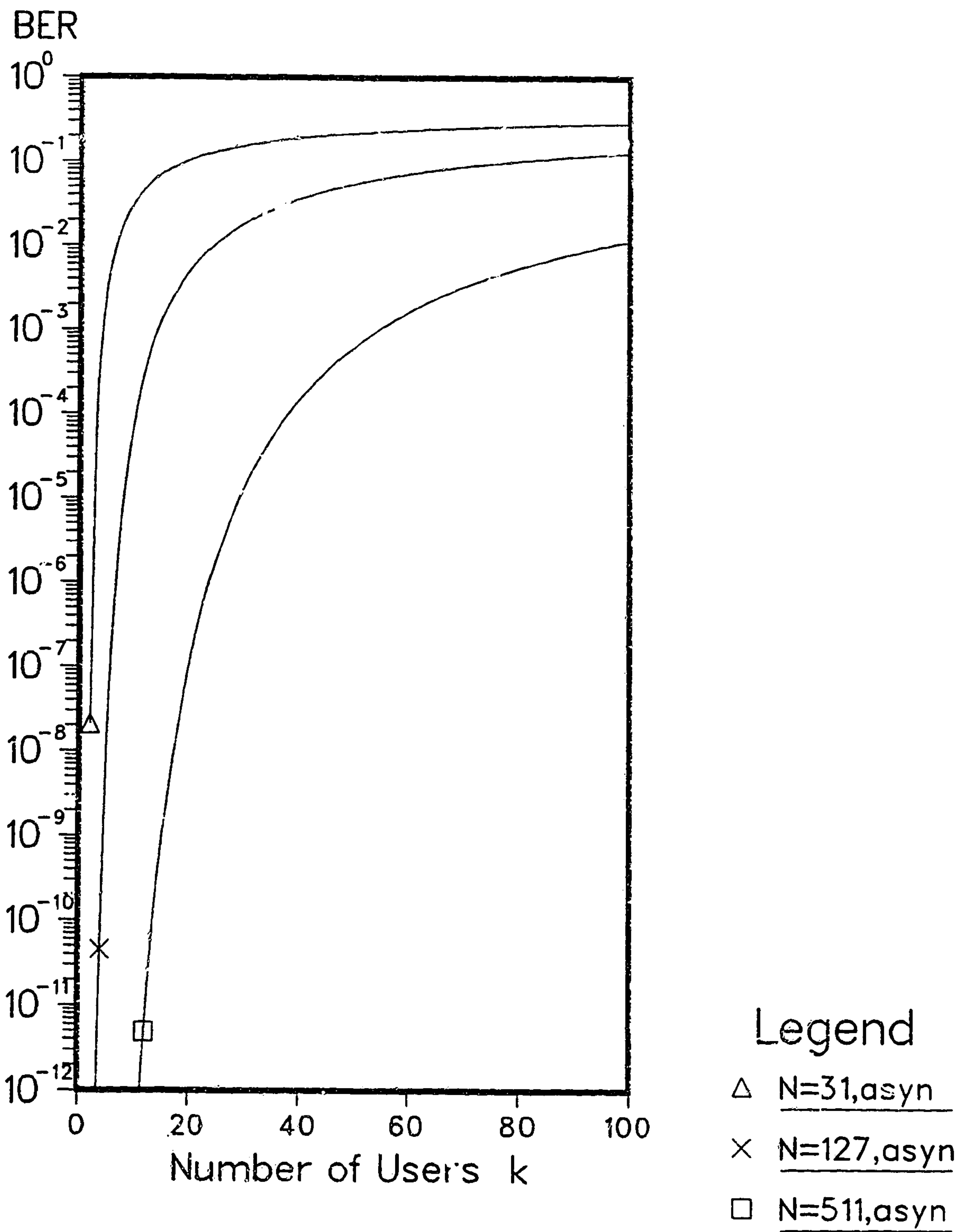

Fig. 3.3 BER (N, k) for asynchronous data slot transmission, Gaussian approximation (good for large k).

correlator output at receiver j is given by (B.1.1):

$$R_j = N + (-1)(k-1)(1+ 2^{(n+1)/2}) \quad (3.2.5)$$

and we have

$$BER_{k<K} = 0 \quad (3.2.6)$$

where

$$K = \frac{2^n + 2^{(n+1)/2}}{1 + 2^{(n+1)/2}} \quad (3.2.7)$$

When k is larger than K, it is still possible to get no error caused by interference. This is due to two reasons. First, $|1+2^{(n+1)/2}|$ is the largest interference among the three possible interference values; it may not occur all the time. Second, interference caused by two or more stations may cancel partly or totally, depending on whether the stations are sending data 1 or data 0, and what the code signal is at that chip. The relationship of BER versus user number k is illustrated in Table 3.2 (refer to APPENDIX B.1). Comparing Tables 3.1 and Table 3.2, it is seen that, as k increases, the result of the accurate calculation agrees more and more closely with the result from the Gaussian approximation; at k = 6 (N=31), the BER calculated by the two method are almost the same. This indicates that for k > 6, the Gaussian approximation is sufficiently accurate.

It is reasonable to assume that the BER versus k curve is continuous and smooth, so that, using the BER (k) results of (3.2.3) for large k and the BER (k) results of Table 3.2 for small k, the BER versus k curves over the whole range of k can be obtained. These BER versus k curves are shown in Fig.3.4. The BER increases quite rapidly as more users (k) are transmitting in the system. By increasing the length (N) of the Gold codes, the system capacity can be increased under the same amount of BER, or alternatively the BER can be improved if the number of users is kept same.

Table 3.2 BER (N, k) for asynchronous case, results of accurate calculation

N	k	BER
31	1 to 4	0
	5	2.14×10^{-3}
	6	6.41×10^{-3}
127	1 to 8	0
	9	2.82×10^{-6}
511	1 to 16	0
	17	6.86×10^{-11}

3.2.2 The Synchronous Case

In this case, for any number of simultaneous users k, the interference and hence the BER can be calculated by considering that each station gives a cross-correlation of +1 or -1 as interference to any other station. For this case, it is relatively easy to obtain BER versus k, for either large or small k using some approximation method.

When k, the number of transmitting stations, is sufficiently large, the average value of the interference term is (refer to (A.7))

$$\mathbb{E}(A_i \, \Phi_{ij}(0)) = 0 \qquad (3.2.8)$$

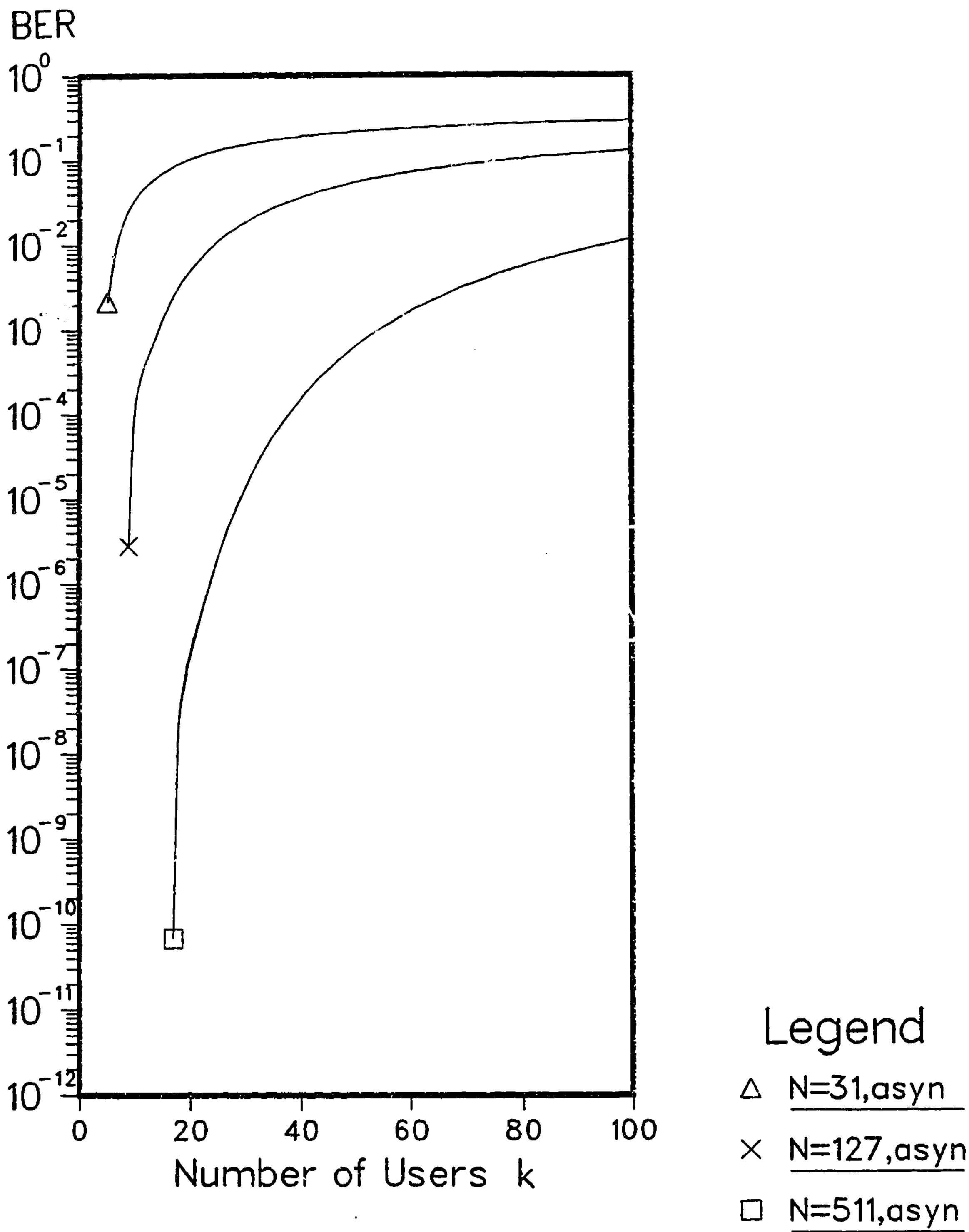

Fig. 3.4 BER(N,k) for asynchronous data slot transmission.

$$\sigma^2_{syn} = 1 \ , \tag{3.2.9}$$

and the total variance for all the k-1 different interference terms in (3.1.2) is $(k-1)\sigma^2$. Since k is large, the overall interference is Gaussian distributed [35, 36], according to the Central Limit Theorem [38]. Thus, the error probability or BER caused by the interference is (refer to (A.14)),

$$BER_{syn} = \frac{1}{2} - \frac{1}{2} \text{ erf} \left[\frac{N}{\sqrt{2(k-1)}} \right]. \tag{3.2.10}$$

Where erf(x) is the error function given in (3.2.4). The BER (N, k) curves are shown in Fig. 3.5. Some BER (N, k) are listed in Table 3.3.

Table 3.3 BER (N, k) for asynchronous case, results of the Gaussian approximation

N	k	BER
31	31	7.58×10^{-9}
	32	1.29×10^{-8}
	33	2.13×10^{-8}
	34	3.40×10^{-8}
	35	5.29×10^{-8}
	36	8.03×10^{-8}
127	127	can be ignored (6×10^{-30})
	128	can be ignored (9×10^{-30})

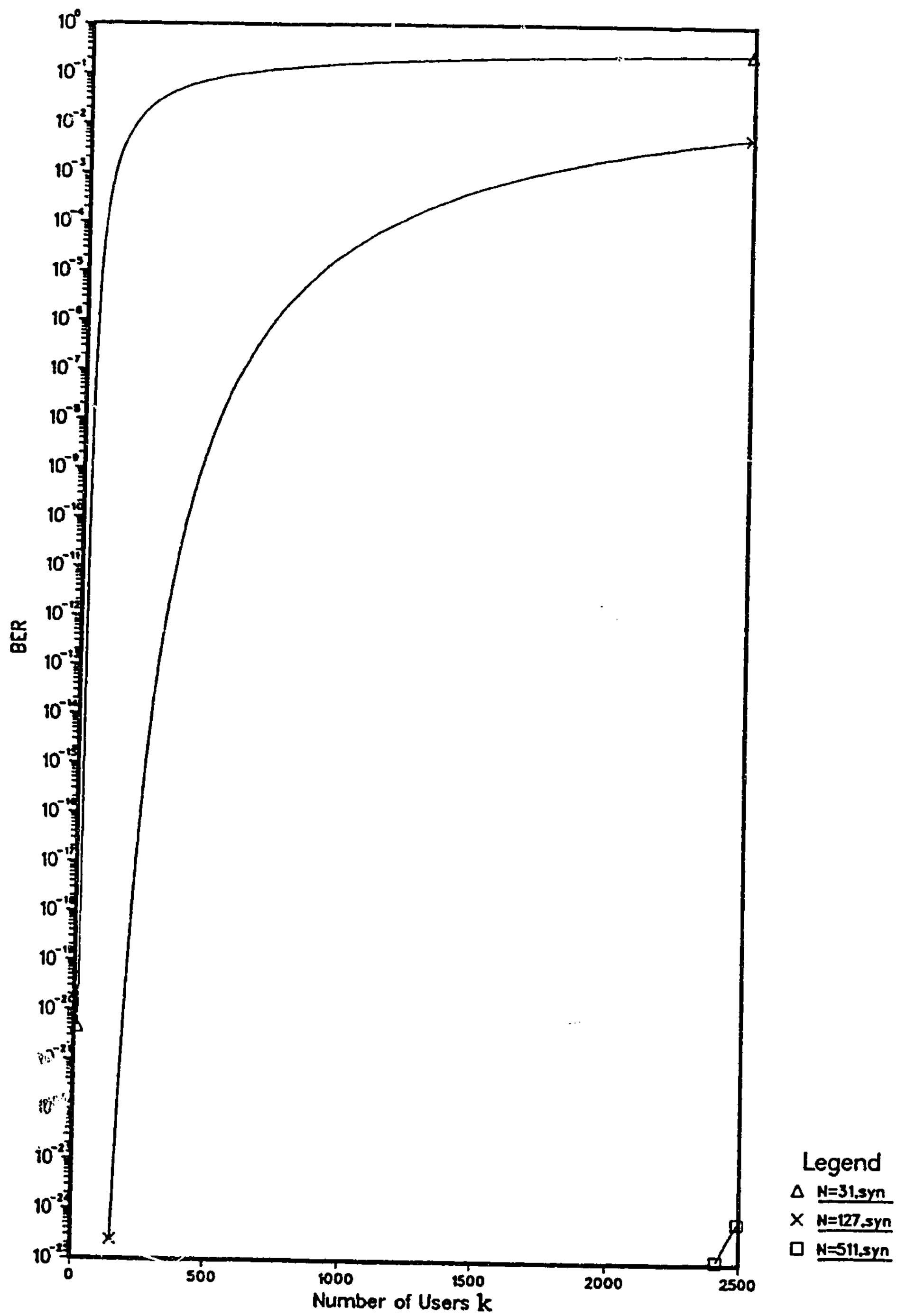

Fig. 3.5 BER (N,k) for synchronous data slot transmission, Gaussian approximation (good for large k).

more. Referring to APPENDIX B.2, the largest interference occurs when the intended data signal is $A_j = 1$ while all the other stations are sending data $A_i \equiv 1$ ($i = 1, 2, 3, \cdots, i \neq j$), or $A_j = -1$ while all other $A_i \equiv -1$. In this case, the correlator output at the receiver j is given by (B.2.2):

$$R_j = N A_j - (k-1) A_i = N - (k-1) . \quad (3.2.11)$$

If R is greater than zero when $A_j = 1$ is transmitting, or R is less than zero when $A_j = -1$ is transmitting, then there will be no error caused by interference, and we have

$$BER_{k<K} = 0 , \quad (3.2.12)$$

where

$$k < K = N+1 , \quad (3.2.13)$$

When k is larger than K, it is still possible to get no error caused by interference. The relationship of BER and the number of users, k, when k is relatively small, may be calculated as detailed in APPENDIX B.2; the results are illustrated in Table 3.4.

Comparing Table 3.3 and Table 3.4, it is seen that the approximate and exact BER values become closer as k increases, however, even at k = 36 (N=31), the BER values are still not close enough. This indicates that for up to 36 users, the Gaussian approximation is still not accurate enough. In addition, when using 127- or 511-chip Gold codes, with more than one hundred users, the interference is very small, so that the BER will be virtually zero.

As for the asynchronous case discussed in Section 3.1.1, it can be assumed that the BER versus k curves vary continuously and smoothly as k changes, hence, using the BER (k) results of (3.2.9) for large k and the BER (k) in Table 3.4 for small k, the BER versus k for the whole range of k can be obtained. The BER versus k curves are shown in Fig.3.6. As can be seen, the BER increases as k increases, but more slowly than for the asynchronous case.

Table 3.4 BER (N, k) for synchronous cast, results from accurate calculation

N	k	BER
31	1 to 31	0
	32	2.33×10^{-10}
	33	2.33×10^{-10}
	34	2.04×10^{-9}
	35	2.04×10^{-9}
	36	8.69×10^{-9}
127	1 to 127	0
	128 to 130	can be ignored (10^{-38})

3.2.3 Comparison of Asynchronous and Synchronous Transmissions

Fig.3.7 illustrates the BER(k) for the case of synchronous and asynchronous data slot transmissions. It is clear that for the same BER, and using the same set of 31-chip Gold codes, synchronous data slot transmission can support many more users than asynchronous transmission.

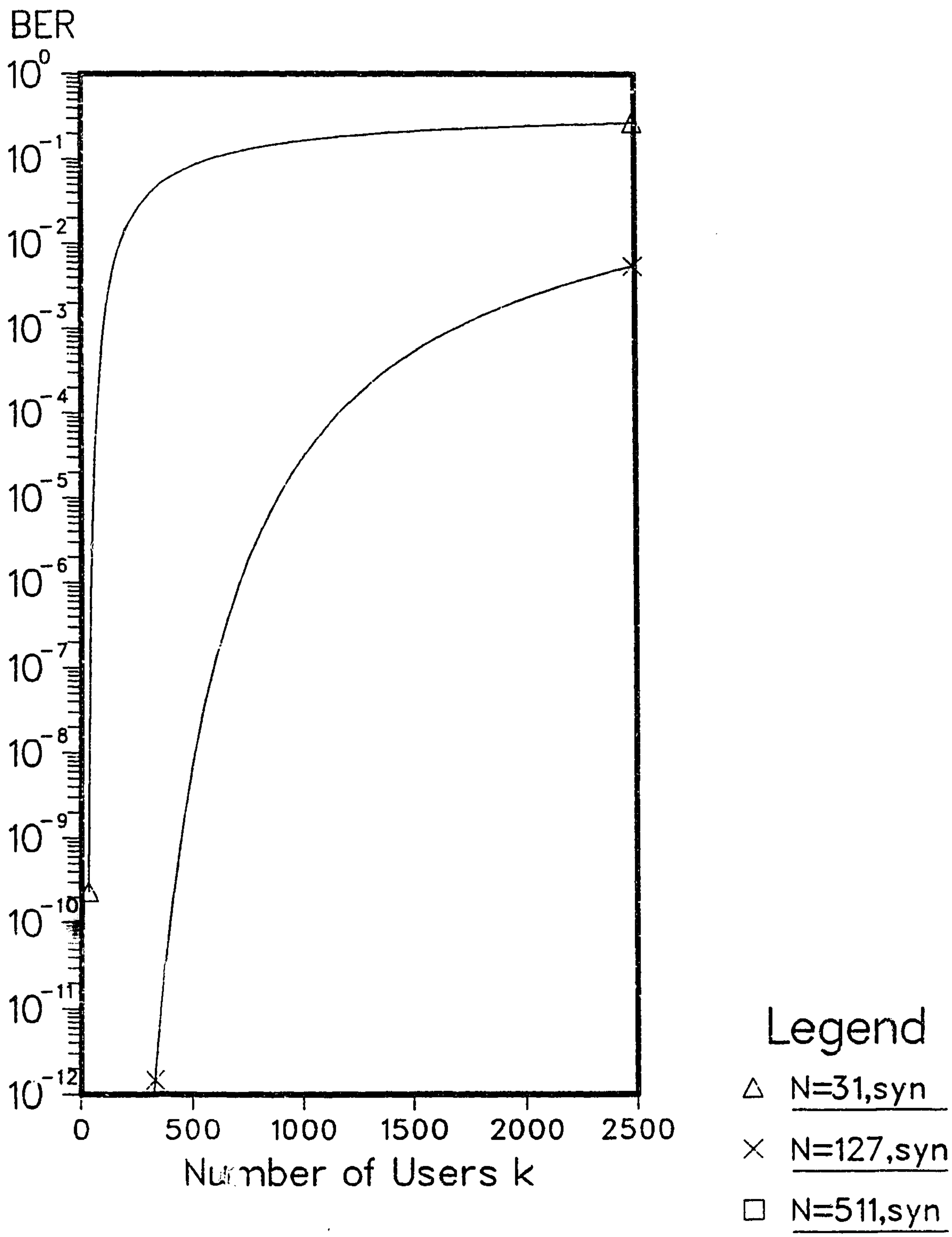

Fig. 3.6 BER (N,k) for synchronous data slot transmission.

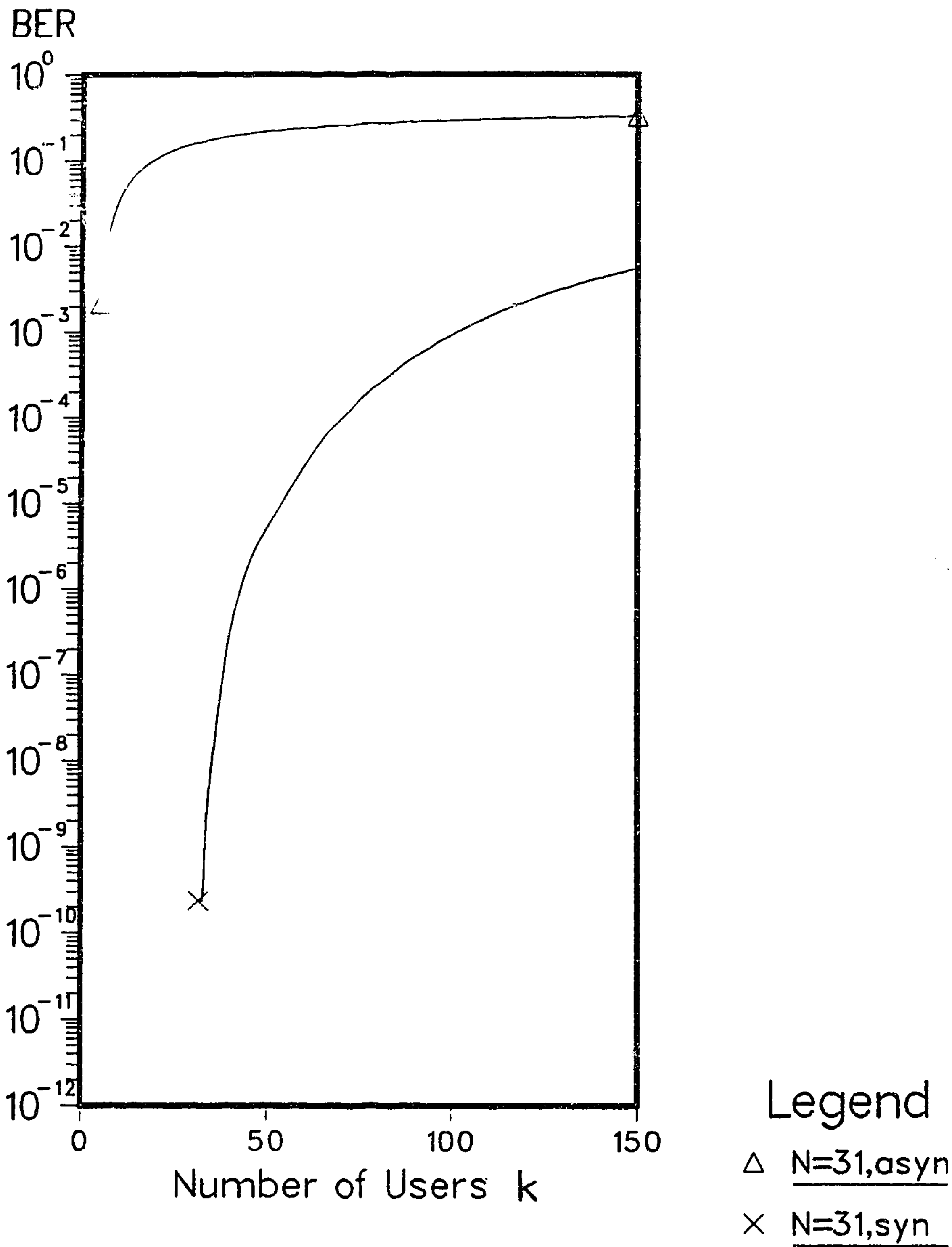

Fig.3.7 BER (N,k) for asynchronous and synchronous transmissions.

system capacity significantly in the case of synchronous transmission, compared with the case of asynchronous transmission, as shown in Figs. 3.4 and 3.6.

3.3 Simulations for Different Transmission Conditions

Real data transmission situations, using a set of N = 31 Gold sequences as address keywords for different stations, have been simulated using the computer. These computer simulations show the effectiveness of a CDMA system when accessed by many users [40].

Data signal is encoded in each transmitter and the binary optical signal is fed onto the common channel (see Fig. 3.8). If there is one station transmitting, the optical signal transmitted in the common channel, as well as the signal arriving at the receivers, is only the one encoded signal (see Fig. 3.9 (a)). The desired receiver uses its keyword to correlate the received electrical signal, and then obtains an output using an integrate-and-dump filter. Therefore, the filter output waveform is a distinct ramp, which attains the peak positive value +31 or peak negative value -31 at the end of each data slot when data 1 or 0 is sent, respectively. This is shown in Fig. 3.9 (b). After that, a decision circuit is used and the value at the end of each data slot is compared with a threshold level 0 volts. The decision that a data 1 or 0 was transmitted will be made, corresponding to the final output value is larger than 0 or smaller than 0 (see Fig. 3.9 (c)).

When two stations are transmitting simultaneously, the signal in the common channel as well as the received signal contain three levels

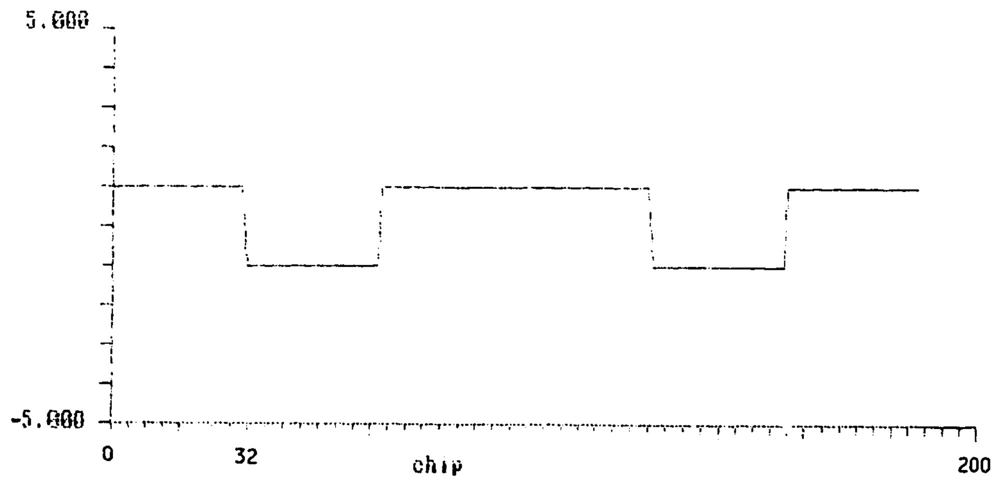

(a) Transmitted data.

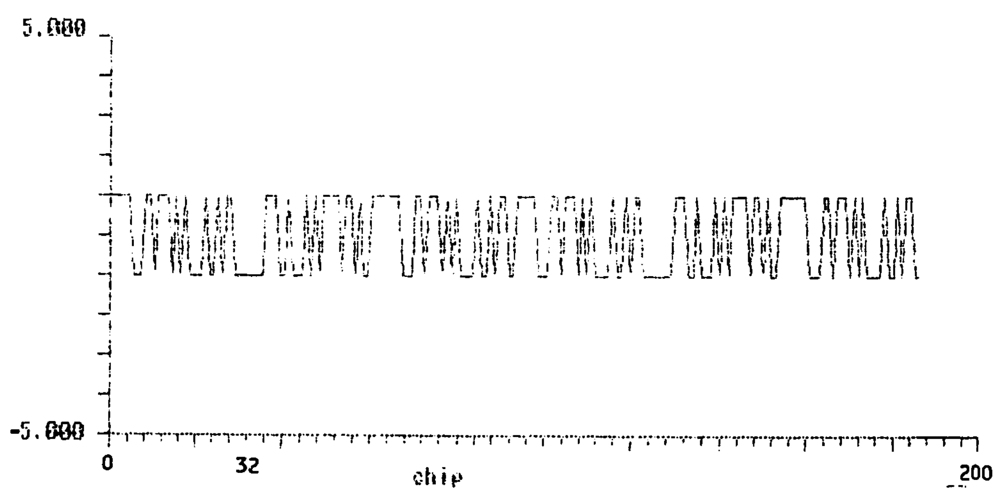

(b) Encoded signal.

Fig. 3.8 Transmitted data and encoded signal.

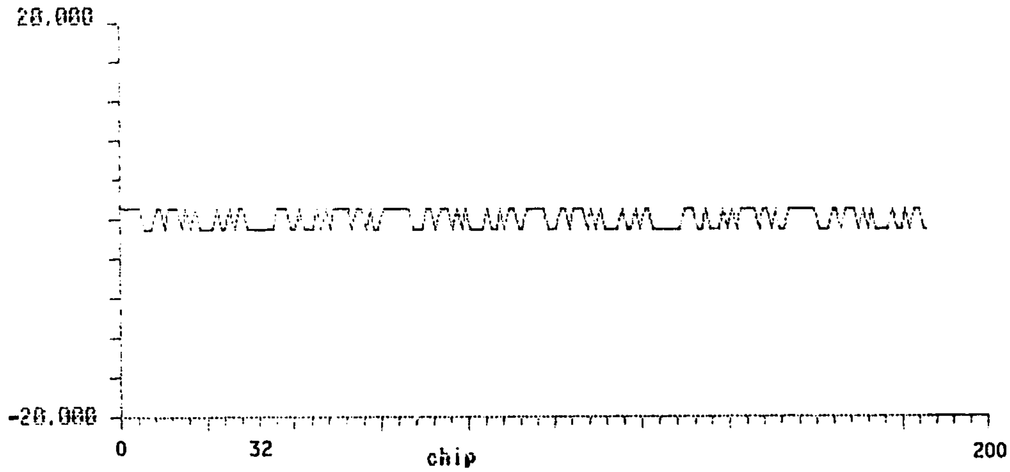

(a) Received signal.

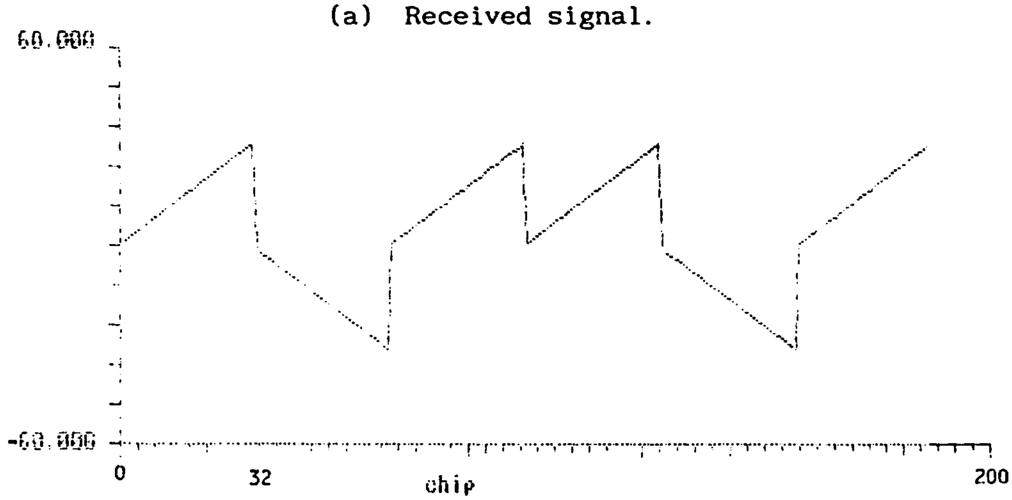

(b) Integrate-and-dump output signal.

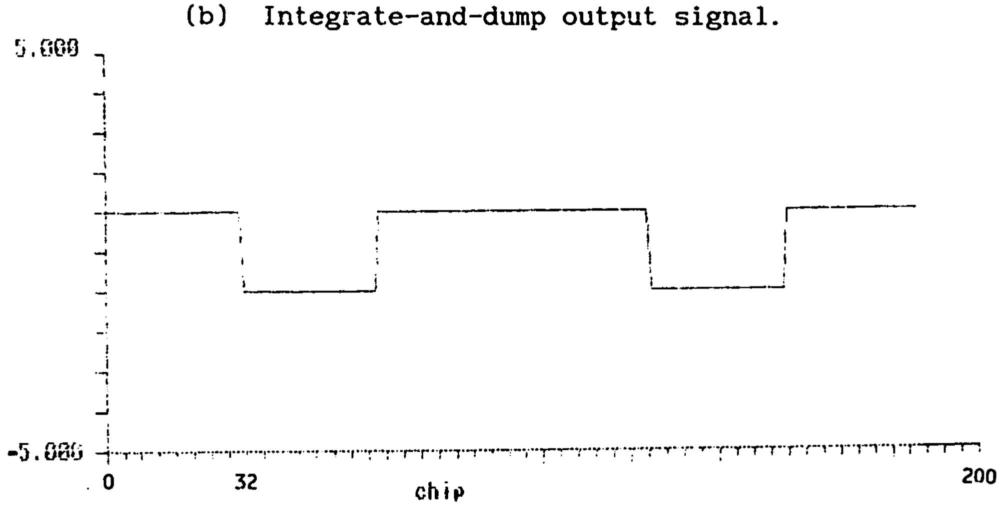

(c) Data decoded.

Fig. 3.9 One station transmitting.

from each station at the passive optical coupler. The output waveform becomes less perfect and, in general, it cannot always reach the previous peak value, because of the interference given to the receiver by the undesired signal.

As the number of stations increases, the received signal waveform contains an increasing number of levels and the integrate-and-dump filter output waveform becomes progressively less distinct. However, as long as the value at the end of each data slot remains positive or negative correctly, the right decision can be made. Figs 3.10 - 3.14 show situations for 3, 10, or 31 stations transmitting simultaneously.

Synchronous transmission can always support a larger number of users than asynchronous transmission under the same BER restriction, as concluded in Section 3.2. This conclusion is verified by the waveforms in Figs. 3.10 - 3.14. It is shown in these figures, that synchronous transmission always provides a more distinct ramp waveform at the I-D filter and gives a larger peak output at the end of each data slot than asynchronous transmission does. Thus, assuming the same number of users, synchronous data slot transmission will give less errors.

For example, for 10 stations transmitting asynchronously (refer to Fig. 3.13), there is an unacceptable decoding error caused by the incorrect output voltage (polarity) at the end of the second data slot. For synchronous transmission with 10 stations, the waveform is still quite distinct as is the accumulated output value, and hence the decoded data is correct (see Fig. 3.13). Fig. 3.14 shows that, with synchronous transmission, 31 stations can transmit simultaneously without error, as was already been proved in Section 3.2.

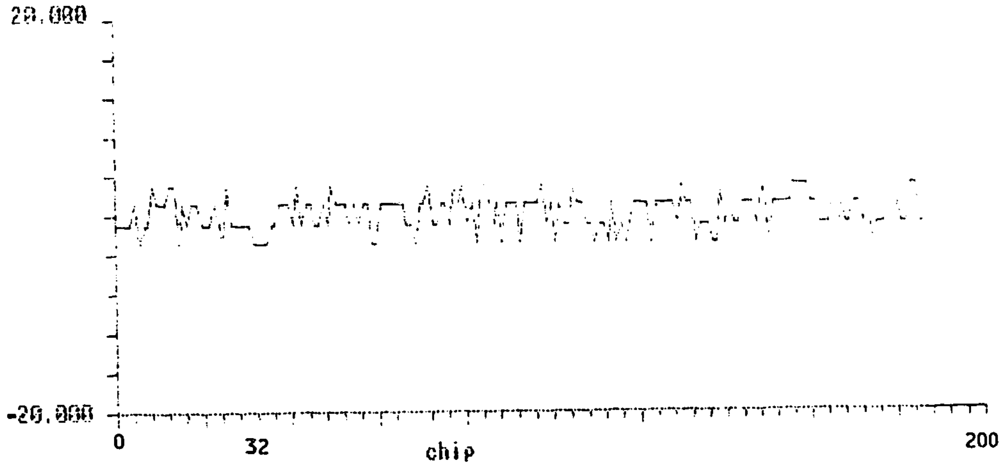

(a) Received signal.

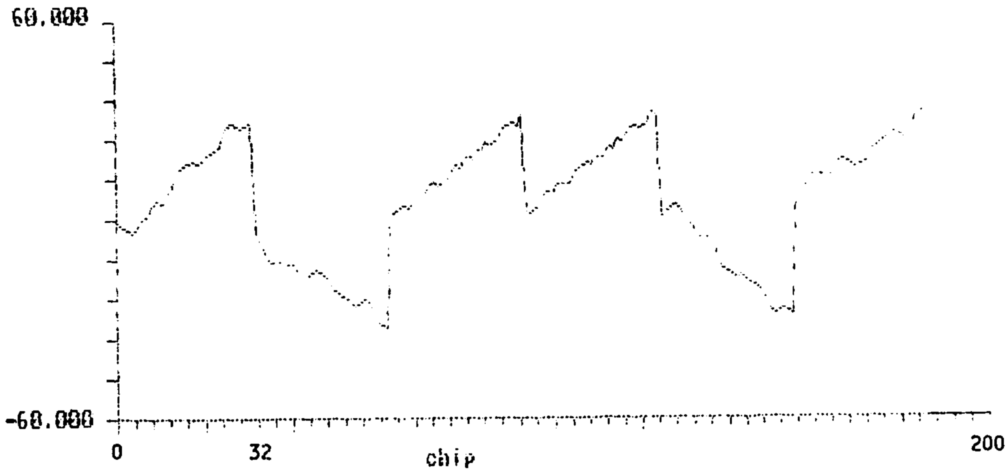

(b) Integrate-and-dump output signal.

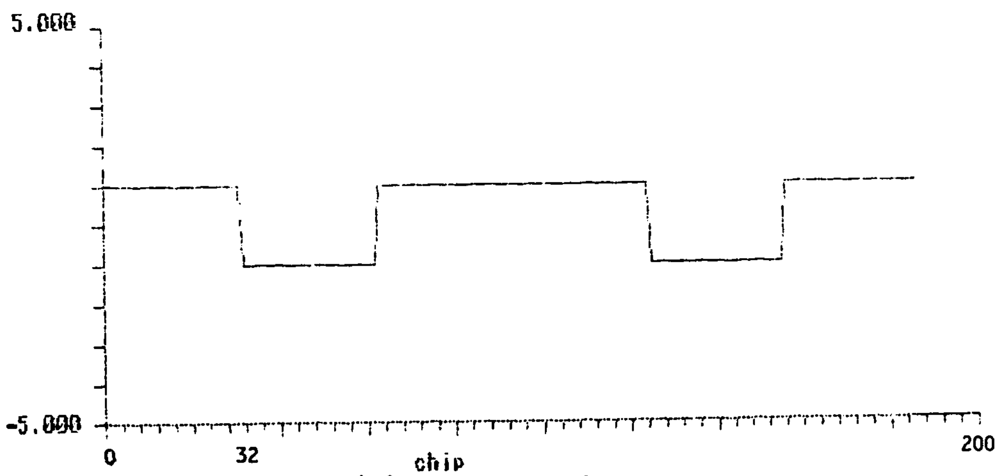

(c) Data decoded.

Fig. 3.10 Three synchronous stations transmitting.

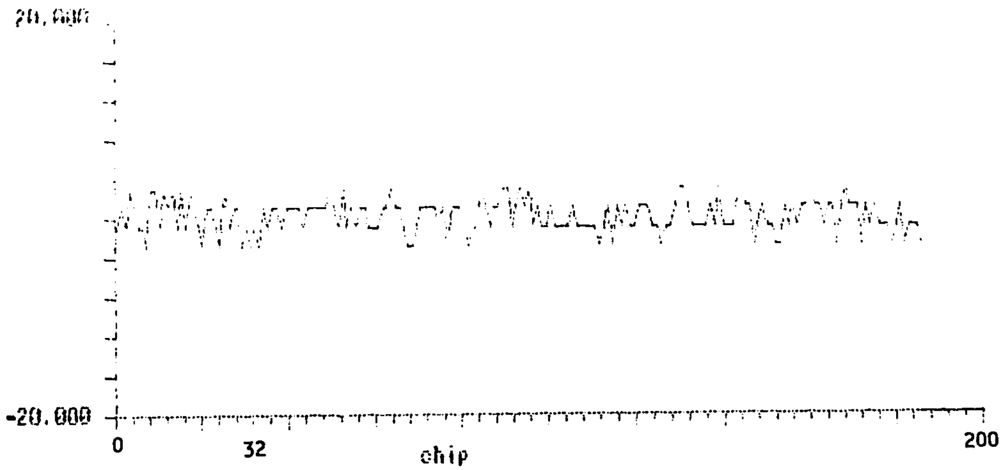

(a) Received signal.

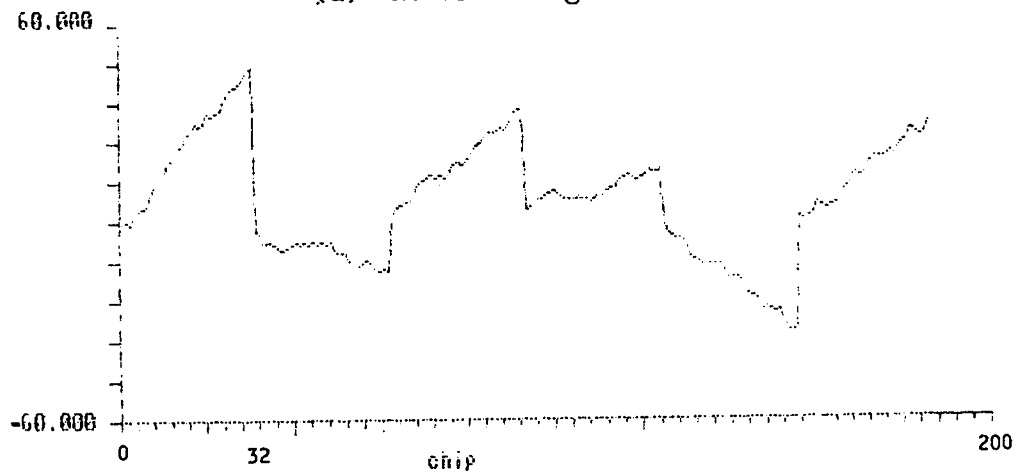

(b) Integrate-and-dump output signal.

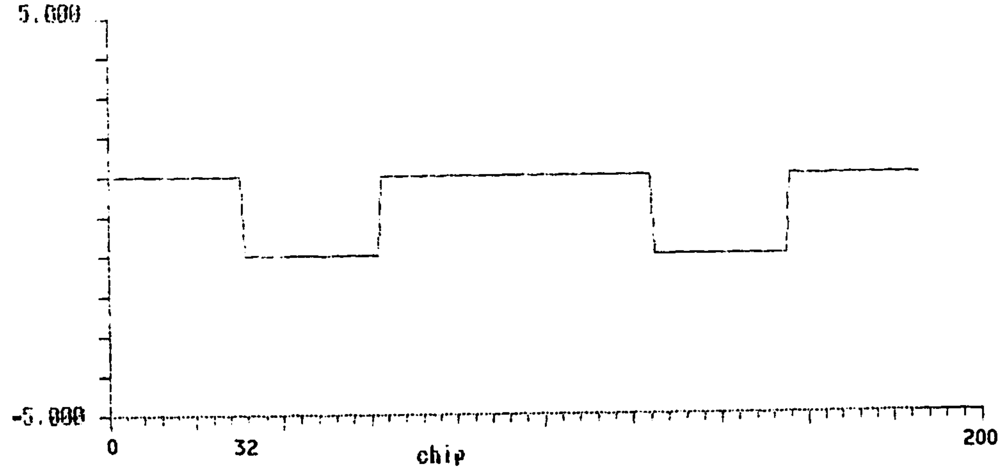

(c) Data decoded.

Fig. 3.11 Three asynchronous stations transmitting.

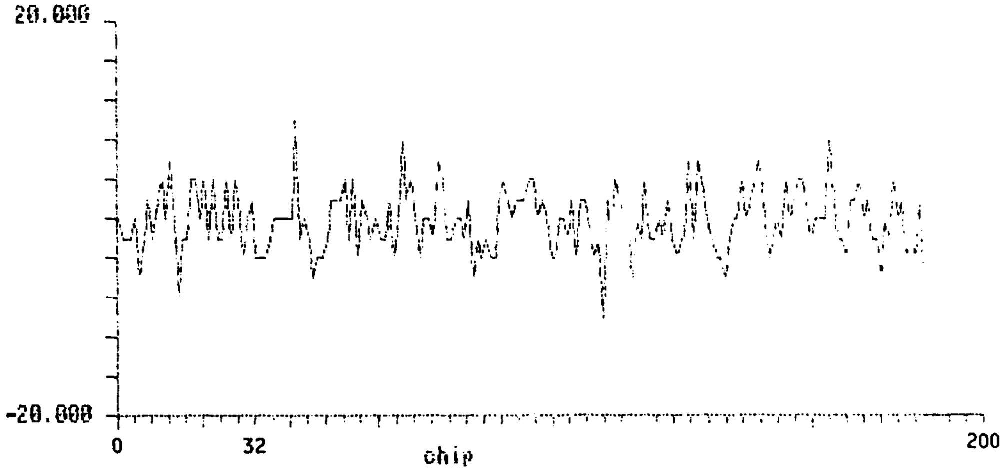

(a) Received signal.

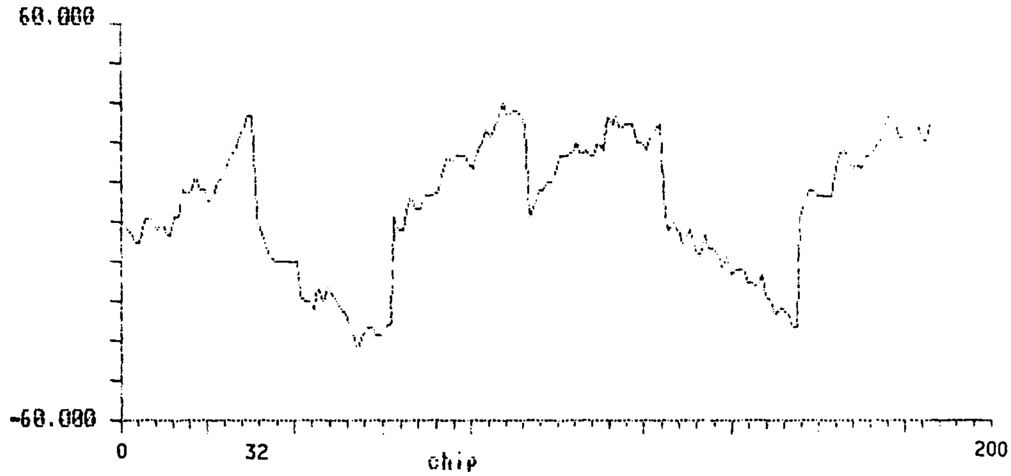

(b) Integrate-and-dump output signal.

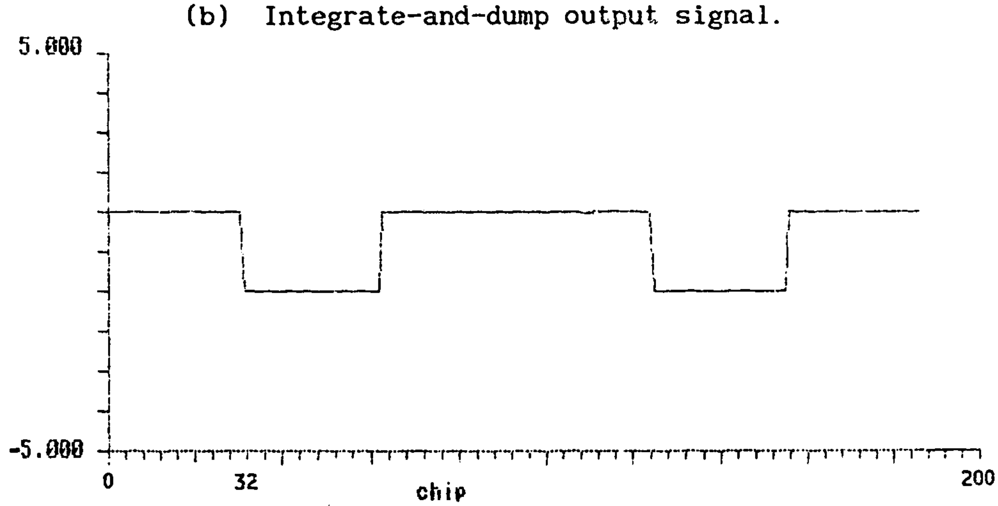

(c) Data decoded.

Fig. 3.12 Ten synchronous stations transmitting.

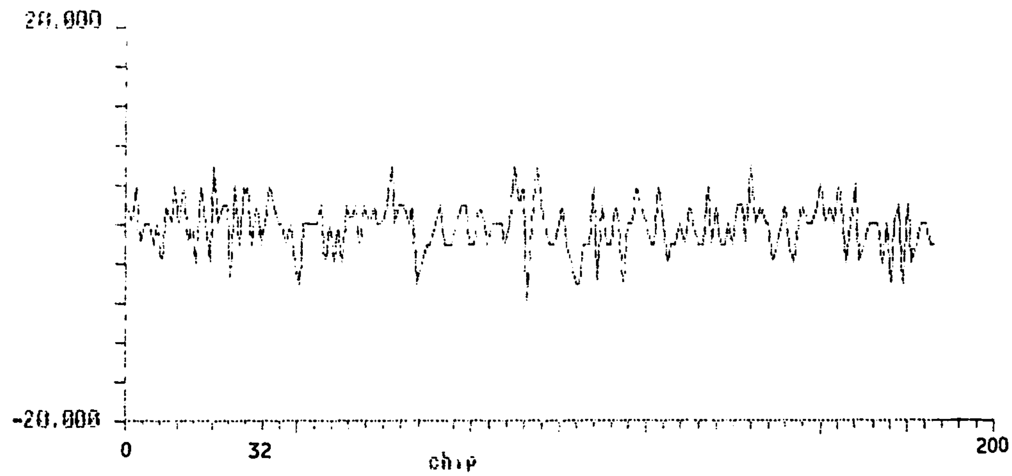

(a) Received signal.

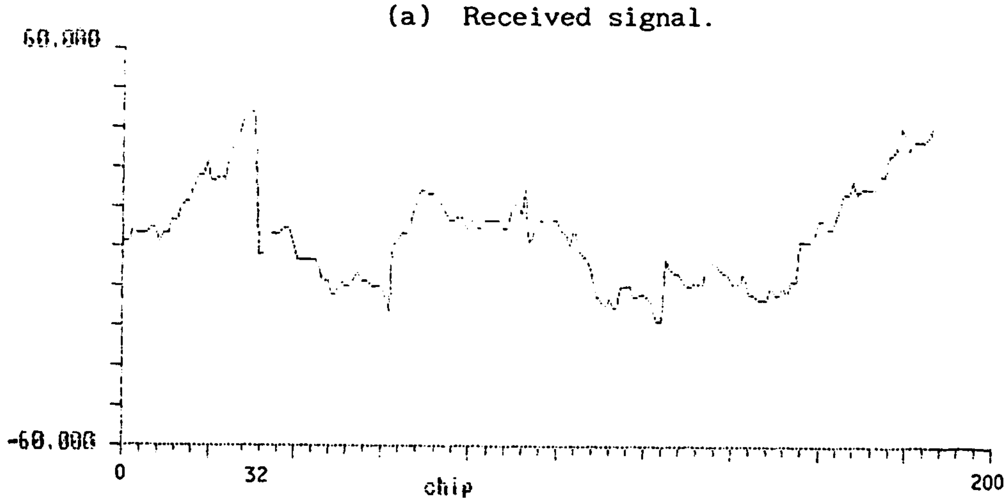

(b) Integrate-and-dump output signal.

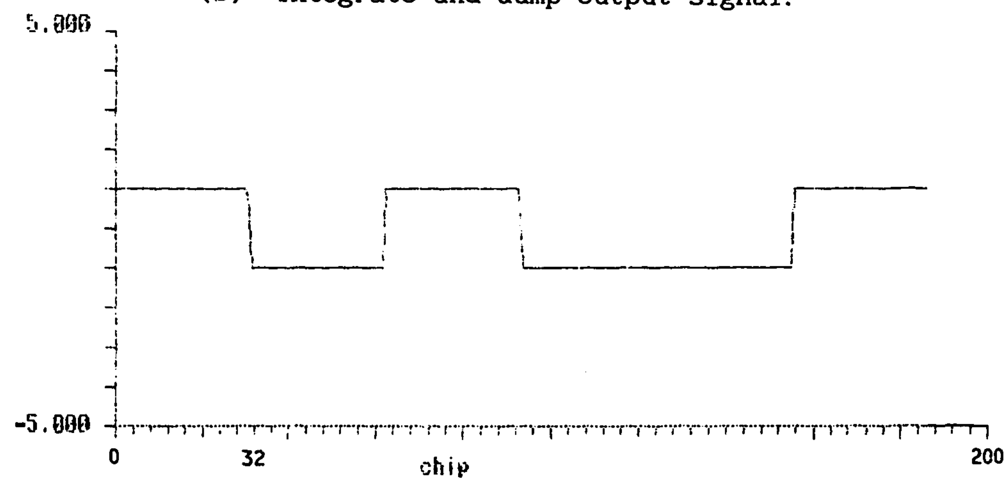

(c) Data decoded.

Fig. 3. 13 Ten asynchronous stations transmitting.

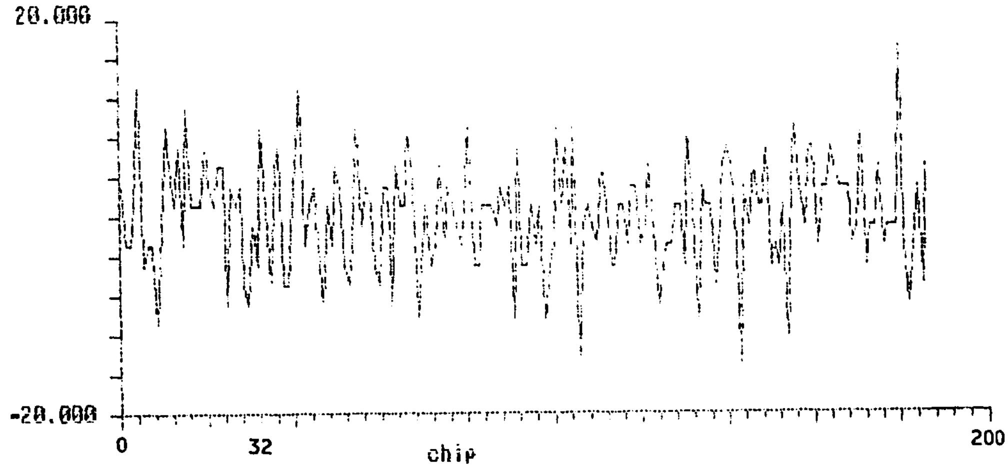

(a) Received signal.

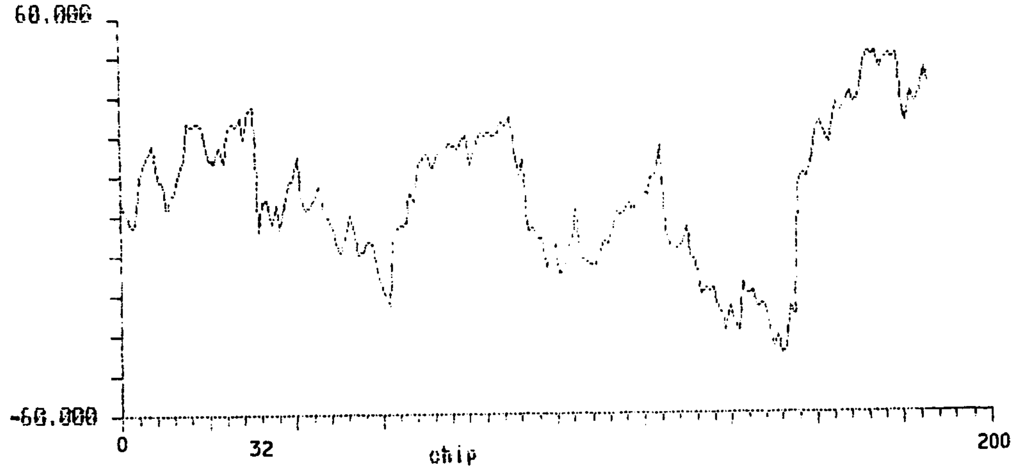

(b) Integrate-and-dump output signal.

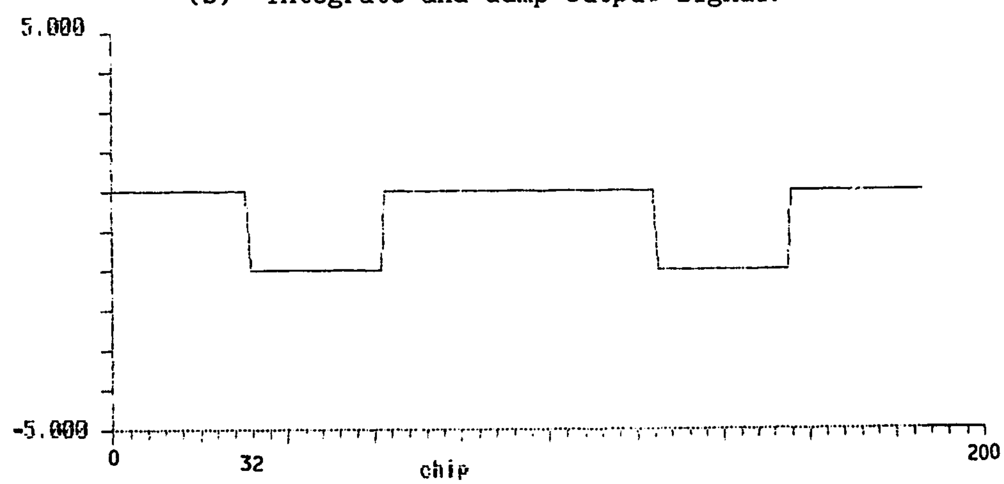

(c) Data decoded.

Fig. 3.14 Thirty-one synchronous stations transmitting.

neglected, synchronous transmission using 32 Gold sequences: a, $a \oplus b$, $a \oplus Tb$, $a \oplus T^2 b$, $\cdots$, $a \oplus T^{30} b$ (each of them has a length N = 31); allows 31 simultaneous users; while for the asynchronous case only 3 users can transmit simultaneously without any chance of error caused by interference from other users.

4. EXPERIMENTAL SYSTEM

4.1 Introduction

An experimental optical fiber multi-user system employing the CDMA technique was set up. Fig.4.1 shows the overall experimental system. It consists of two transmitting stations, a 3 dB optical coupler, an optical fiber common channel, and a receiving station capable of representing any one of the possible 31 different receiving stations. The data is generated by a data generator (HP-3764A) at the transmitter end and the system bit error rate (BER) is measured by an error detector (HP-3763A) at the receiver.

Each transmitting station comprises a Gold code generator, an encoder and a laser transmitter (E/O converter). The receiving station consists of a PIN detector with a preamplifier, a main amplifier, a Gold code generator and a decoder.

The operation of the system may be described as follows. Assume that the encoder of transmitting station 1 intends to send data to the n^{th} station. The encoder uses the n^{th} Gold code among the set of 31 Gold sequences (which is chosen by setting a switch to number n-1), thus encoding the incoming data at 1.40 Mb/s and producing a coded 44.736 Mb/s (DS-3 rate) NRZ signal. The coded signal modulates the laser diode, producing an intensity modulated optical digital signal of 44.736 Mb/s at a wavelength of 1.3 μm. Meanwhile, the other transmitting station trying to send data to the m^{th} station uses the m^{th} Gold code to encode its data and finally generates an optical signal at a speed of 44.736 Mb/s and at a wavelength of 1.3 μm. The two

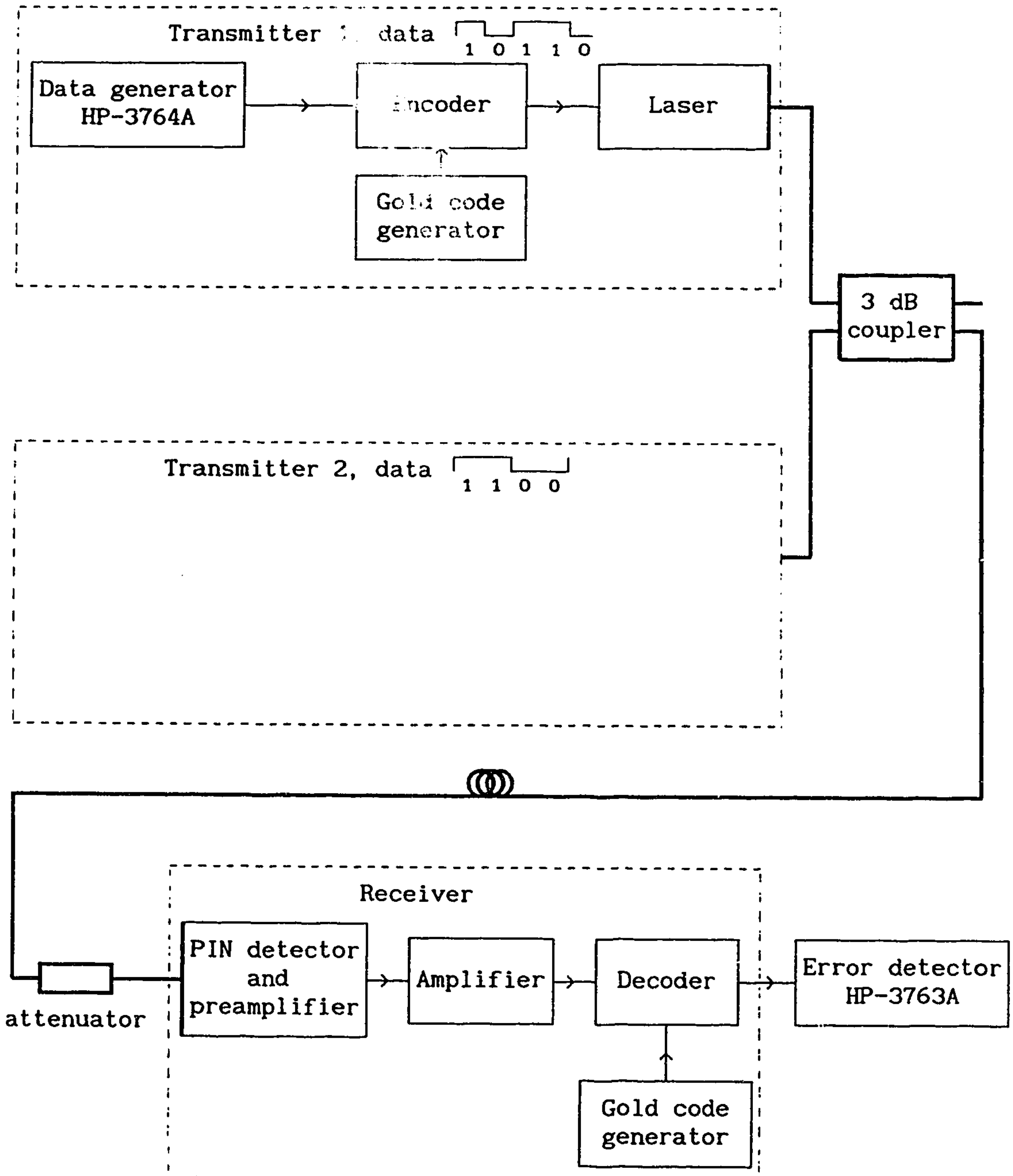

Fig. 4.1 The experimental transmission system.

stations are transmitting in synchronization so that, at the receiver, the code words from the two transmitter stations begin at the same time (we refer to this as synchronous data slot transmission).

The optical signals from the two transmitting stations are fed into a 3 dB optical coupler (1.3 μm) which sums the two binary optical signals into a three-level optical intensity modulated signal. This signal is then passed through the optical fiber transmission line.

At the receiving station, the optical signal is first converted into an electrical AC signal by a PIN detector with a preamplifier, followed by a main amplifier. The output of the main amplifier is fed into the decoder. The Gold code sequence assigned to the receiver is produced by a local code generator, and is also fed into the decoder. After the correlation and the decision making process, the NRZ binary data signal transmitted to the station is decoded. At each receiver, because of the correlation property of the codes, signals intended to be received by other stations behave like interference. Usually, the interference is small enough that the decision as to what data was transmitted can be made correctly.

The decoded data is fed into an error detector which compares the data received with the data sent; the bit error rate may thus be measured for a variety of data test patterns.

The design and construction of the experimental components and circuits are described in detail in this chapter.

4.2 Transmitter

4.2.1 Data Source

An HP-3764A data generator which generates a TTL compatible non-return-to-zero (NRZ) signal, is used as the data source. It can produce a pseudo-random binary sequence (PRBS) pattern of length $2^{10}-1$, $2^{15}-1$, or $2^{23}-1$ bits. It can also be programmed to produce any 10 or 16 bit word pattern. The data rate in our system is 1.40 Mb/s.

4.2.2 Gold Code Generator

A generator capable of producing a set of 31 Gold sequences, each with a length of N=31 chips, was designed and constructed on standard printed circuit boards using TTL and ECL chip components. Fig.4.2 is a block diagram of the Gold sequence generator. The generator consists of generators for m-sequences a and b, which are driven by a common clock at 44.736 Mb/s, a decimal counter which provides certain fixed delays in order to obtain different a and $T^i b$ combinations, and a modulo-2 adder which combines a and $T^i b$. The binary NRZ code sequences $\{a \oplus b$, $a \oplus Tb$, $a \oplus T^2 b$, $\cdots$, $a \oplus T^{31} b\}$, which can be written as $\{X_1, X_2, \cdots, X_{31}\}$, are generated at a chip speed of 44.736 Mb/s.

Fig 4.3 illustrates the schematic circuit of the Gold sequence generator used in the transmitter. A mechanical switch S1 is used to reset the two D flip-flops D1 and D2, which provide a trigger pulse (rising edge) to the system. A 44.736 Mb/s common clock is distributed by several 74F04 (B1 to B4) chips.

A 32 chip counter which functions as a 0 chip counter, and an i chip counter, are both triggered by the rising edge at the D2 output, and produce the 0^{th} and i^{th} trigger pulses. In the counter, counting up

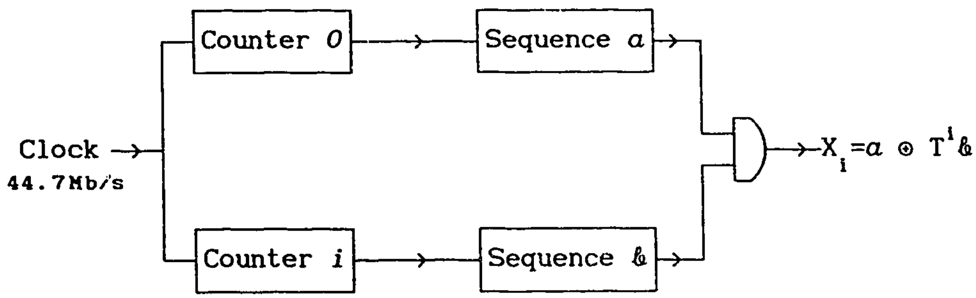

Fig. 4.2 Block diagram of the Gold sequence generator.

to a larger number produces more delay than counting up to a smaller number. To avoid the delay error and to get the 0^{th} and i^{th} trigger pulses at exactly the right rising edge position, the pulses are resynchronized with the clock rising edge by D3 and D4.

The ICs B5, B6, B7, A1, B10 and B11 produce a clock which is the same as the 44.736 Mb/s common clock except that the 0^{th}, 32^{nd}, $(32\cdot2)^{th}$ ···, $(32\cdot n)^{th}$, ···, chips in the clock sequence are dumped (refer to Fig. 4.4).

This dumped clock is then converted into an ECL signal by a MC10124 IC and functions as a clock for the a and $T^i b$ 31 chip m-sequence generators. The 0^{th} and i^{th} pulses are also converted into an ECL signal and are used to trigger the a and $T^i b$ m-sequence generators, respectively.

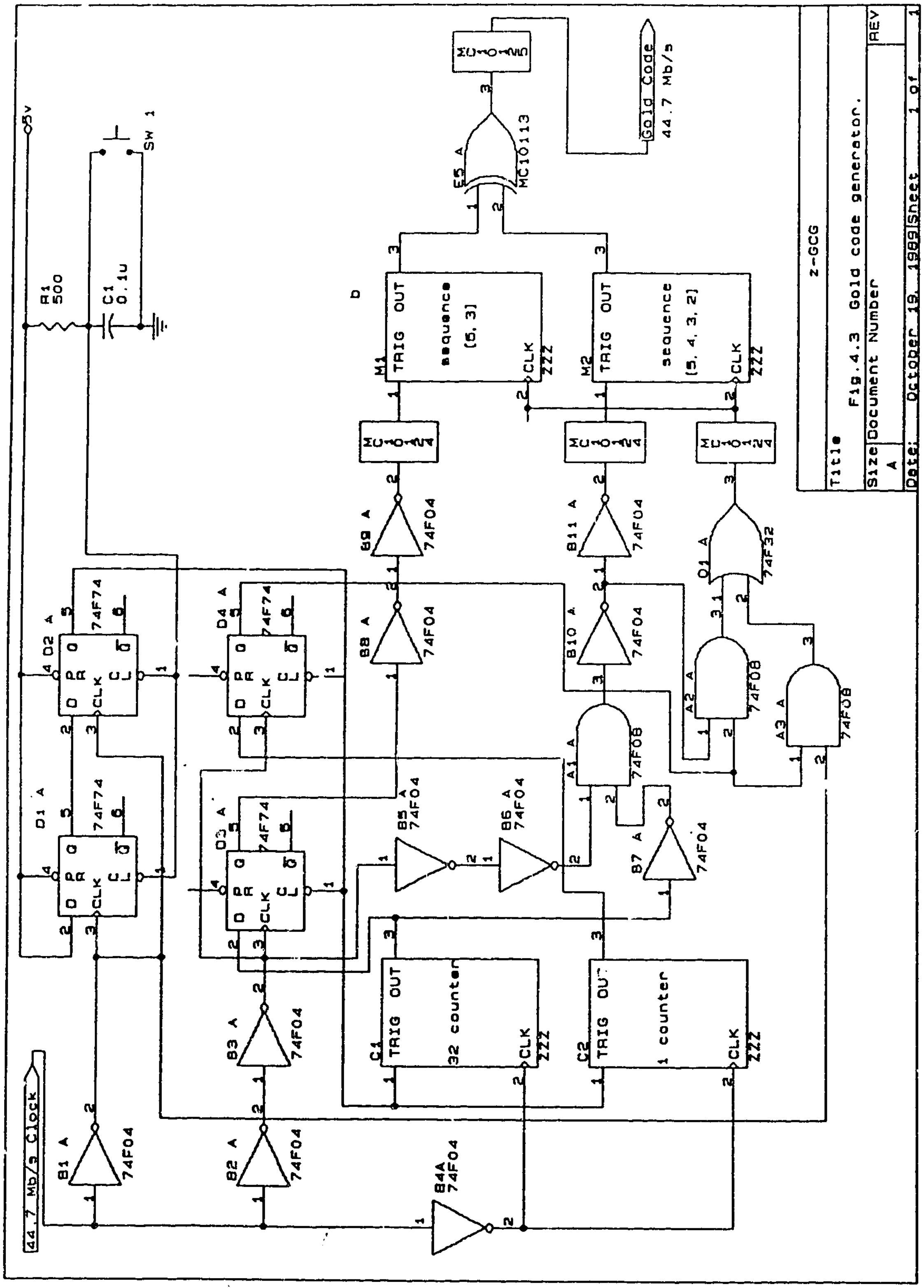
44.7 Mb/s Clock
5v
R1 500
C1 0.1u
Sw 1
D1 A 74F74
D2 A 74F74
D3 A 74F74
D4 A 74F74
B1 A 74F04
B2 A 74F04
B3 A 74F04
B4A 74F04
B5 A 74F04
B6 A 74F04
B7 A 74F04
B8 A 74F04
B9 A 74F04
B10 A 74F04
B11 A 74F04
A1 A 74F08
A2 A 74F08
A3 A 74F08
O1 A 74F32
C1 TRIG OUT 32 counter CLK ZZZ
C2 TRIG OUT 1 counter CLK ZZZ
M1 TRIG OUT sequence [5, 3] CLK ZZZ
M2 TRIG OUT sequence [5, 4, 3, 2] CLK ZZZ
MC10124
MC10125
E5 A MC10113
Gold Code 44.7 Mb/s
z-GCG
Title Fig.4.3 Gold code generator.
Size A
Document Number
REV
Date: October 19, 1989 Sheet 1 of 1

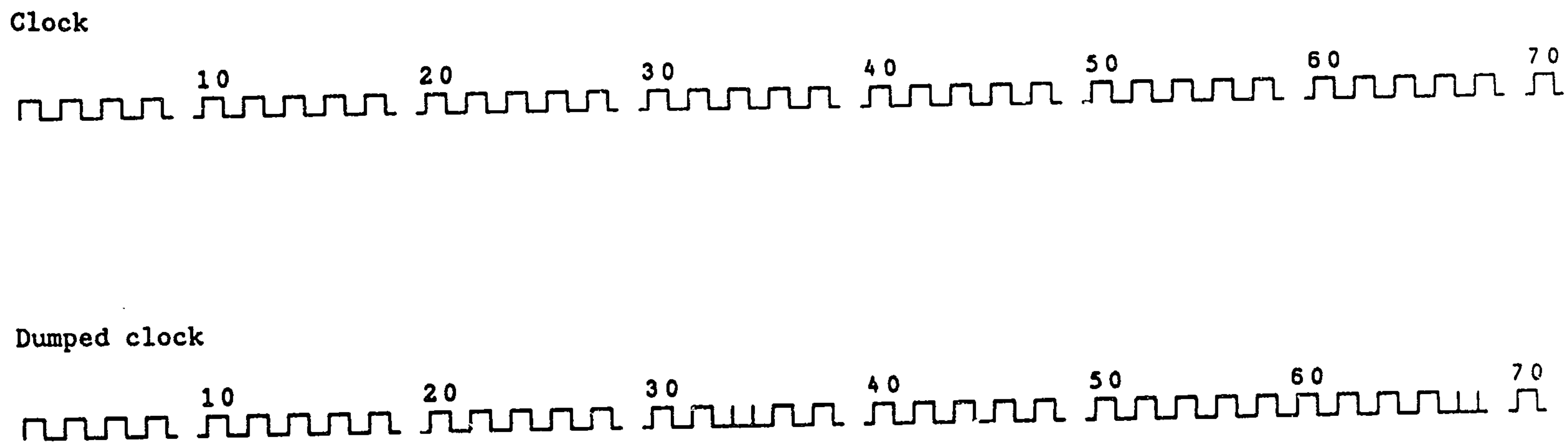

Fig.4.4 The clock and dumped clock signals.

As discussed in Chapter 2, according to Gold's method, sequence a is a *[5,3]* sequence and b is a *[5,4,3,2]*. Each of these sequences is produced by a shift register with a particular feedback layout, which has already been shown in Fig.2.6 (page 30). The circuit diagram is illustrated in Fig.4.5. The generator for a is composed of the U1 and U2 5-bit shift register and a modulo-2 adder E1. The sequence b is generated by the U3 and U4 shift registers and three modulo-2 adders (E2 to E4). The reason for using ECL chips to generate the m-sequences is that in the b sequence generator, the accumulated delay given by three TTL modulo-2 adders is so large [41] that the shift register cannot produce a cyclical sequence b, whereas an ECL chip gives much less delay, so that it can produce this sequence [42, 43]. The i-chip shift of sequence b is decided by the i^{th} trigger pulse sent by the i counter . The output a and $T^i b$ sequences are combined chip by chip in a modulo-2 adder E5, and then converted into a TTL signal by an MC10125. Codes a, $T^i b$ and $a \oplus T^i b$ are all the same length (31 chips).

The counter circuit is illustrated in Fig.4.6. The generated Gold sequence $a \oplus T^i b$ is chosen by a 5-bit binary switch S2 which shows the order number i (from 0 to 31) for the intended receiver i+1. This switch then controls a counter comprising U7 and U8, the latter providing the i^{th} trigger pulse which is delayed by i (any number between 0 to 31) chips to the generator of sequence b. Another counter, which comprises U5 and U6, always produces the 0^{th} chip trigger pulse (the same as the 32^{nd} chip trigger pulse) to the generator of sequence a. Therefore, the phase difference between a and b, or the delay i in $T^i b$, is i chips (refer to the timing diagram shown in Fig.4.7), and their combination produces the i+1^{th} Gold sequence $a \oplus T^i b$.

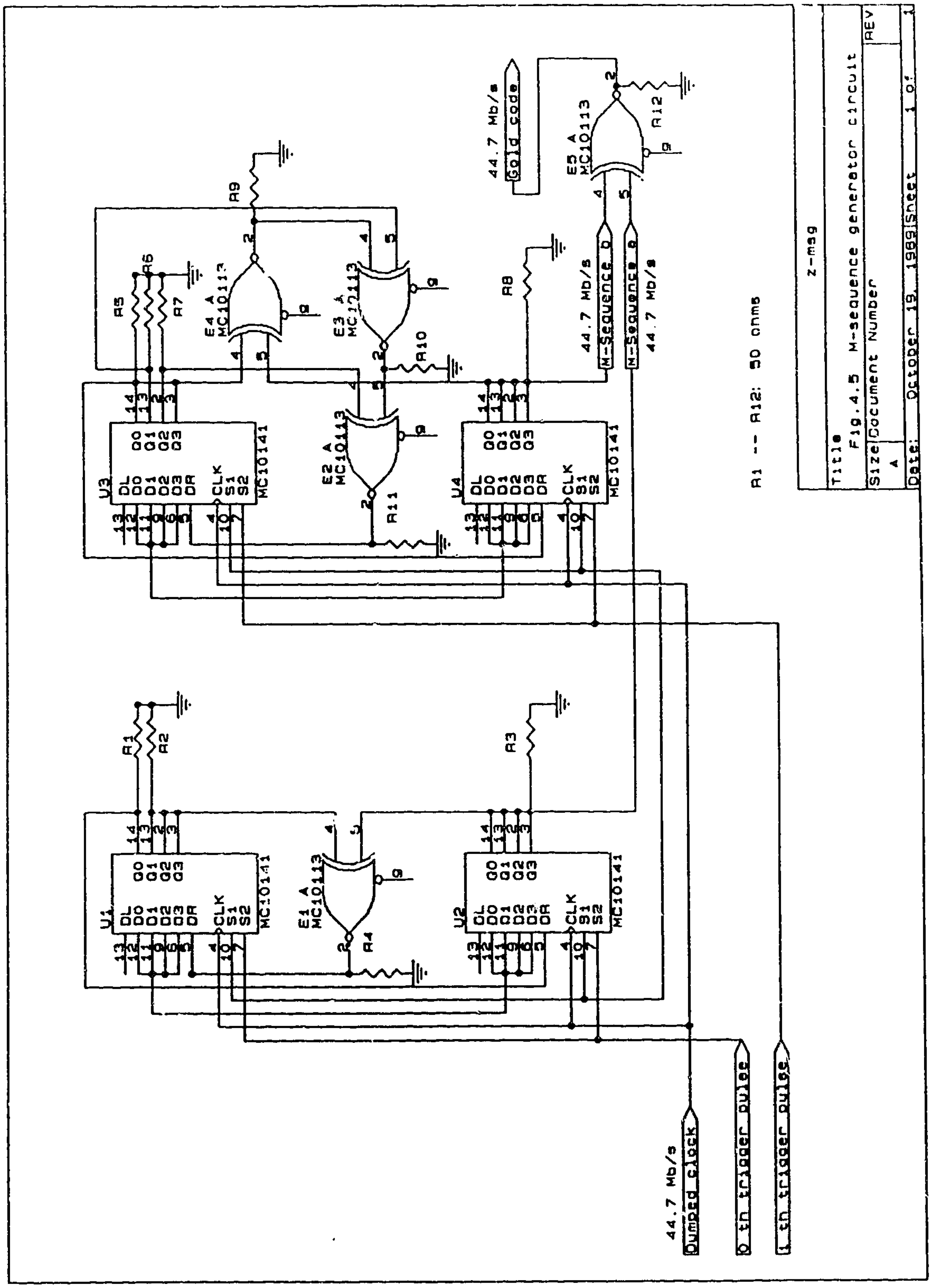
44.7 Mb/s
Gold code
E5 A
MC10113
R12
E4 A
MC10113
E3 A
MC10113
E2 A
MC10113
E1 A
MC10113
R1
R2
R3
R4
R5
R6
R7
R8
R9
R10
R11
U1
U2
U3
U4
MC10141
DL
D0
D1
D2
D3
DR
CLK
S1
S2
Q0
Q1
Q2
Q3
44.7 Mb/s
M-Sequence p
M-Sequence q
44.7 Mb/s
R1 -- R12: 50 ohms
44.7 Mb/s
Dumped clock
0 th trigger pulse
1 th trigger pulse
z-msg
Title
Fig.4.5 M-sequence generator circuit
Size
A
Document Number
REV
Date: October 19, 1989
Sheet 1 of 1

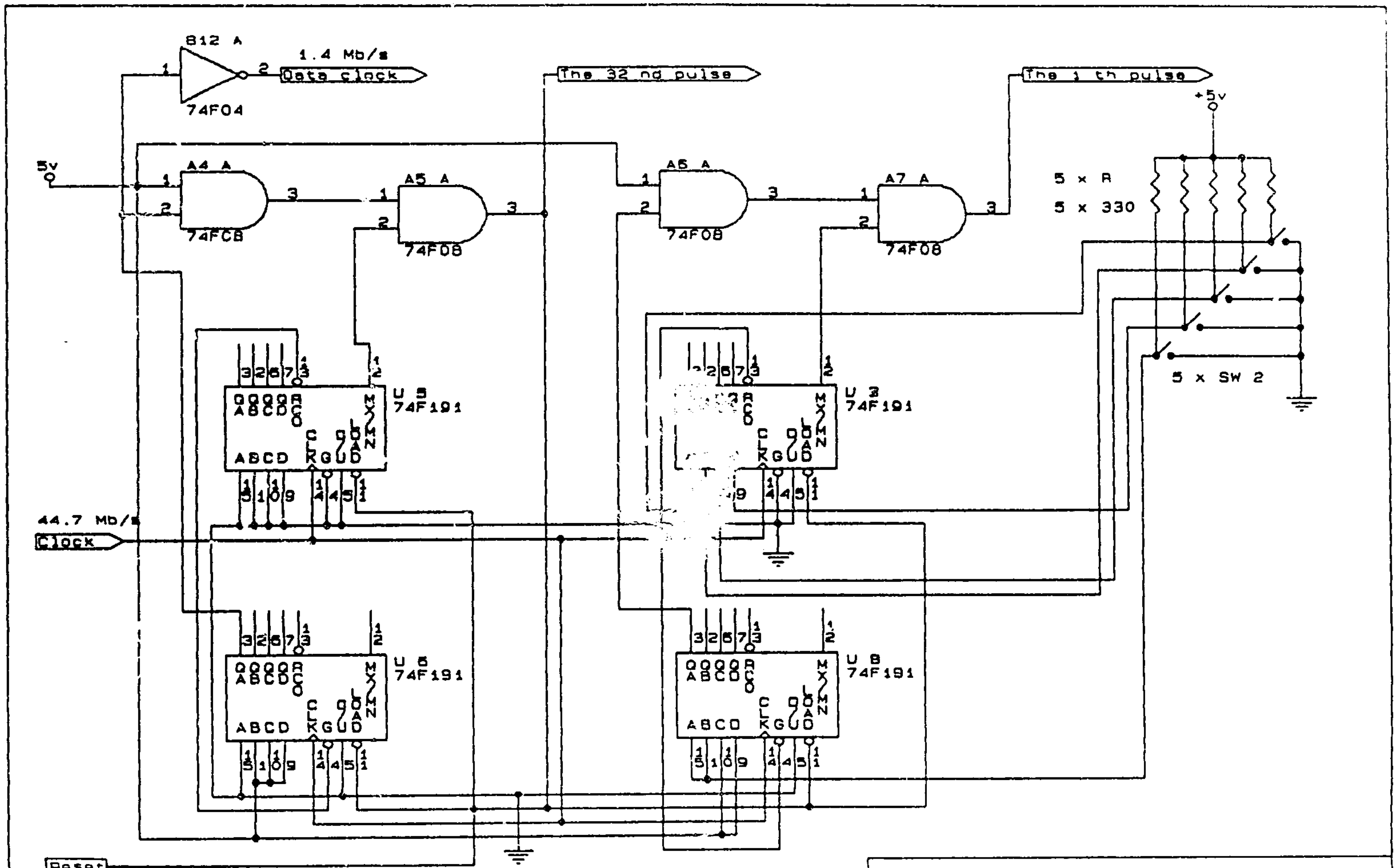

z-count		
Title Fig.4.6 The counter circuit		
Size A	Document Number	REV
Date: October 19, 1989	Sheet 1 of 1	

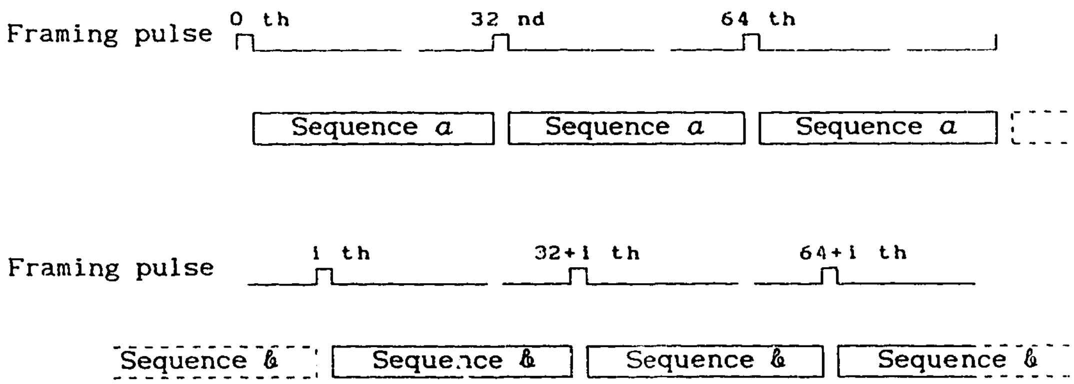

Fig.4.7 Timing diagram of sequences a and $T^i b$.

4.2.3 Encoder

Fig.4.8 shows a diagram of the encoder, in which the data signal is combined with the Gold sequence by a modulo-2 adder E6. D6, D7 and A8 are used here to avoid the delay introduced in the chip components, so that the coded signal is synchronized chip by chip with the 44.736 Mb/s clock. The coded signal is then sent to modulate the laser diode.

4.2.4 Laser Diode and Its Modulator

Two packaged lasers, each of which includes a laser diode (LD) chip, a thermo-electric (TE) cooler, a thermistor, a monitor photo diode, and confocal coupling to a fiber pigtail, are used in the transmission system. A Northern Telecom. PBH 4317-32 LD is used by the first station. It has a threshold current of 40 mA and can provide a fiber output power of 0.6 to 0.9 mW. A HITACHI HL1321DL LD is used by

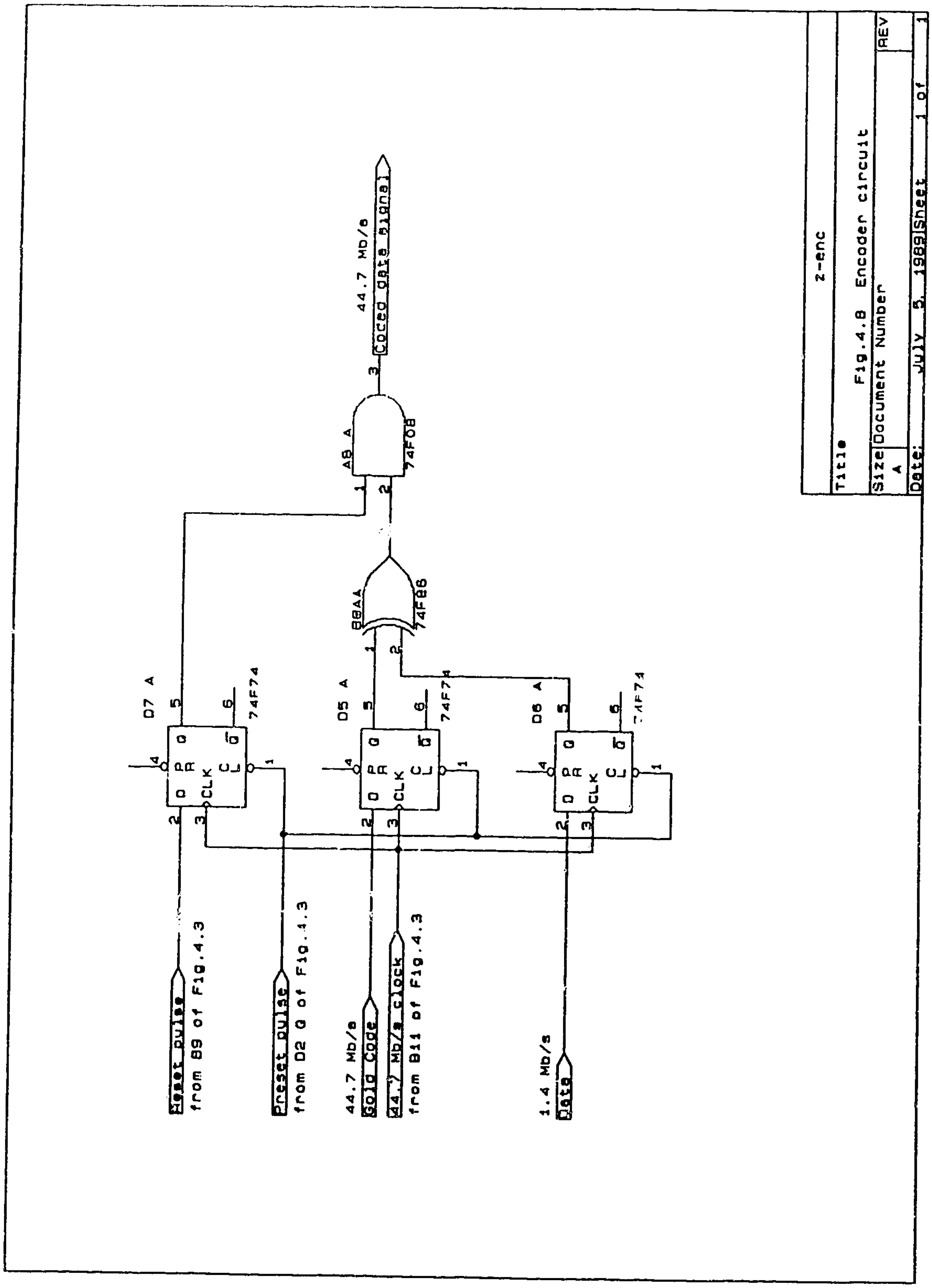
z-enc
Title
Fig.4.8 Encoder circuit
Size
A
Document Number
REV
Date: July 5, 1989
Sheet 1 of 1
44.7 Mb/s
Coded data signal
A8 A
74F08
74F86
D7 A
74F74
D5 A
74F74
D6 A
74F74
Reset pulse
from B9 of Fig.4.3
Preset pulse
from D2 Q of Fig.4.3
44.7 Mb/s
Gold Code
44.7 Mb/s clock
from B11 of Fig.4.3
1.4 Mb/s
Data

the second station. It requires a threshold current of 30 mA and can produce a fiber output power of 0.6 to 1.2 mW. Both LDs produce optical power with a wavelength ranging from 1290 nm to 1310 nm; they can be modulated up to a signal speed of 800 Mb/s.

The LD temperature control circuit is shown in Fig.4.9. When the bridge circuit (R3 to R7) is balanced, the two input voltages (V2 and V3) of U1 are equal. As the laser heats up, the thermistor resistance R4 decreases, causing the bridge to become unbalanced. The differential amplifier amplifies the difference between V2 and V3, and its output V6 drives a power transistor Q2 whose current varies with V6. This voltage controlled current source delivers a current I_c through the TE cooler, which cools the laser and the thermistor. This cooling causes an increase in the thermistor resistance, thus increasing the voltage V_2, and decreasing V_o and I_c. Therefore, by setting the potentiometer R6 to permit enough current I_c to flow through the cooler, the laser can be controlled to a proper temperature of about 20 °C.

Each of the two LDs is intensity modulated by the 44.736 Mb/s coded NRZ signal at each station. Great care must be taken to ensure that the instantaneous LD drive current never exceeds the maximum safe current, even if the modulator is overdriven or breaks into oscillation [44]. The LD modulation circuits shown in Fig.4.10 (a) and (b) are designed to limit the maximum possible drive current to a safe value, thus fulfilling the above requirement.

The LD modulation circuit comprises a differential amplifier utilizing Widlar current sources [45], which allow precise control of the bias current and the modulation depth of the LD. Neglecting the base currents, since each transistor has a β greater than 100, and

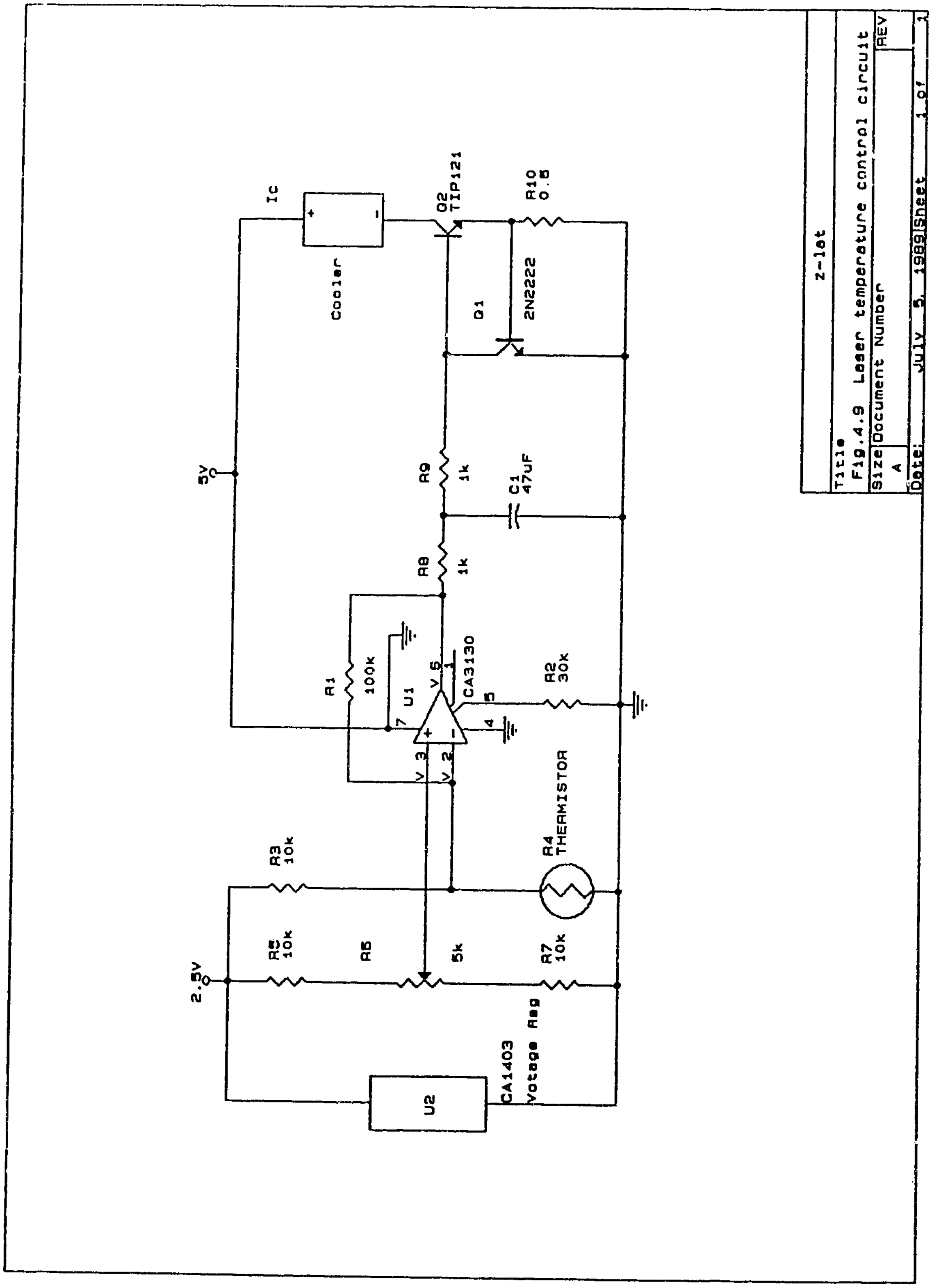

z-lat
Title
Fig.4.9 Laser temperature control circuit
Size A
Document Number
REV
Date: July 5, 1989
Sheet 1 of 1
Cooler
Ic
Q2 TIP121
R10 0.5
Q1 2N2222
5V
R9 1k
C1 47uF
R8 1k
R1 100k
U1 CA3130
R2 30k
R4 THERMISTOR
R3 10k
R5 10k
R6 5k
R7 10k
2.5V
U2
CA1403 Votage Reg

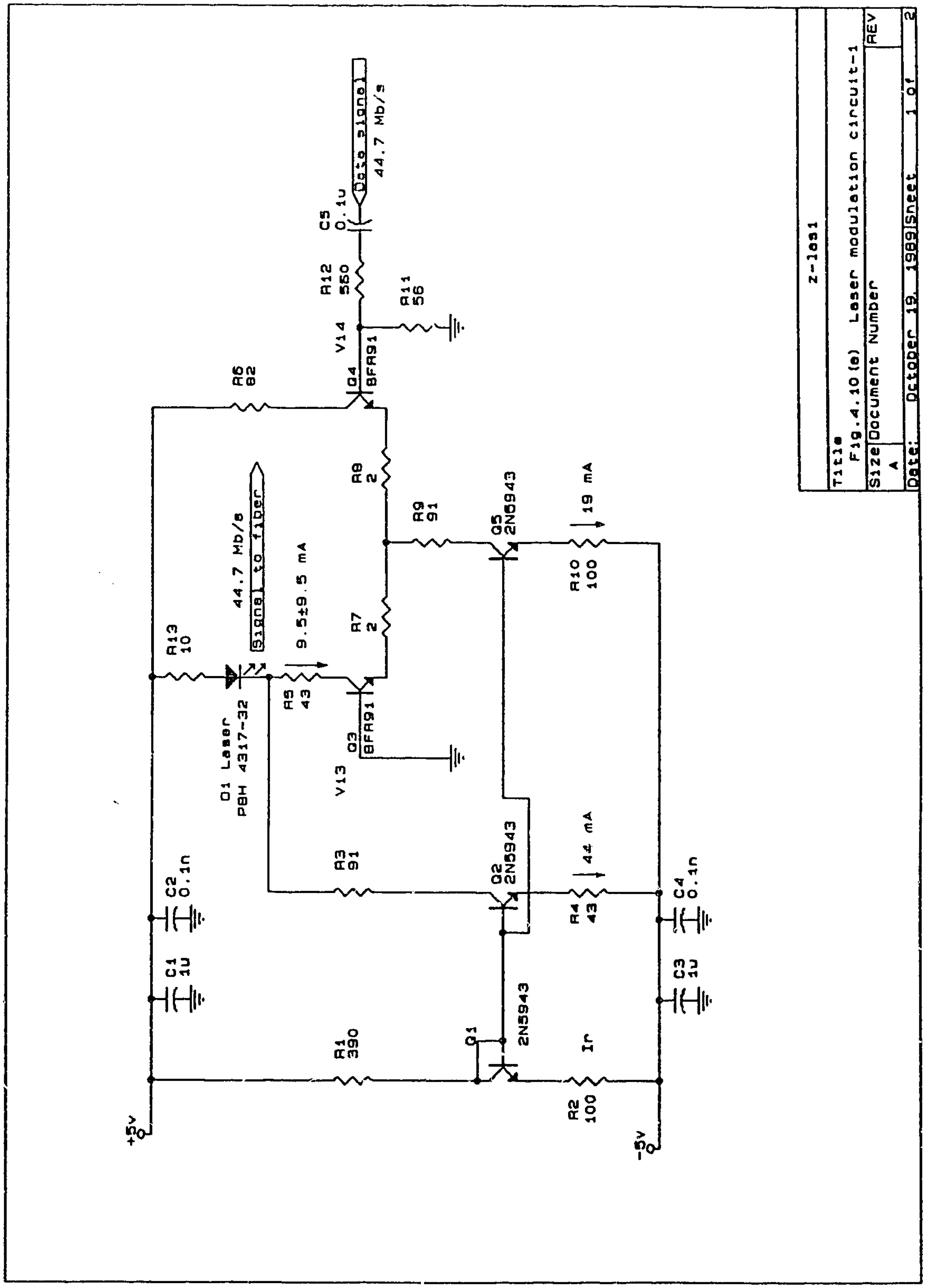
Data signal
44.7 Mb/s
C5
0.1u
R12
550
R11
56
V14
Q4
BFR91
R6
82
R8
2
R9
91
Q5
2N5943
19 mA
R10
100
R7
2
44.7 Mb/s
Signal to fiber
9.5±9.5 mA
R13
10
R5
43
Q3
BFR91
V13
D1 Laser
PBH 4317-32
R3
91
Q2
2N5943
44 mA
R4
43
C4
0.1n
C3
1u
C2
0.1n
C1
1u
R1
390
Q1
2N5943
Ir
R2
100
+5v
-5v
z-las1
Title
Fig.4.10(e) Laser modulation circuit-1
Size
A
Document Number
REV
Date: October 19, 1989
Sheet 1 of 2

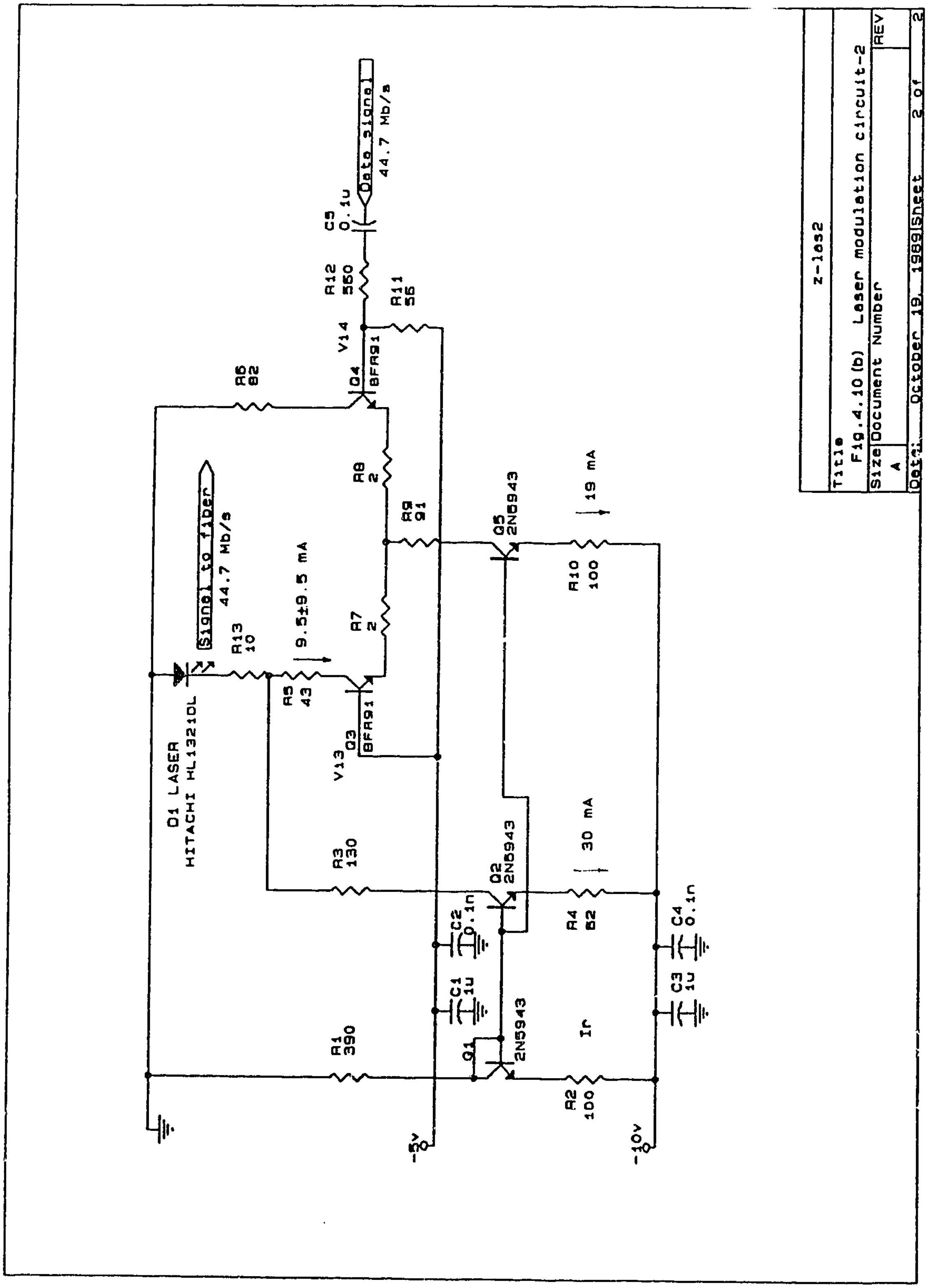
D1 LASER
HITACHI HL1321DL
Signal to fiber
44.7 Mb/s
Data signal
44.7 Mb/s
C5
0.1u
R12
550
R11
55
V14
R6
82
Q4
BFR91
R8
2
R9
91
Q5
2N5943
19 mA
R10
100
R7
2
9.5±9.5 mA
R13
10
R5
43
Q3
BFR91
V13
R3
130
Q2
2N5943
30 mA
R4
82
C2
0.1n
C4
0.1n
C1
1u
C3
1u
R1
390
Q1
2N5943
Ir
R2
100
-5v
-10v
z-las2
Title
Fig.4.10(b) Laser modulation circuit-2
Size Document Number REV
A
Date: October 19, 1989 Sheet 2 of 2

taking the base-emitter voltages to be 0.65V, then the reference current, I_r, is determined by the collector and emitter resistors (R_1, R_2) of Q_1:

$$I_r = (V_c - V_e - V_{be1}) / (R_1 + R_2)$$
$$= (5-0.65) / (390+100)$$
$$= 8.88 \text{ mA} \quad (4.1)$$

Transistors Q_2 and Q_5 are Widlar current sources. The collector currents of Q_2, and Q_5, are given by

$$I_{2C} \cong I_r R_2 / R_4 \quad (4.2)$$

$$I_{5C} \cong I_r R_2 / R_{10} \quad (4.3)$$

Therefore, Q_2 draws a constant current of I_{2C} through the LD, and Q_5 draws a constant current of I_{5C} through the differential pair Q_3 and Q_4.

Under quiescent conditions ($V_{i3} = V_{i4} = 0$), the collector currents of both Q_3 and Q_4 are equal to $I_{5C}/2$, since Q_3 and Q_4 are a matched pair. When an input signal, no matter how large, is applied to V_{i4}, the peak-to-peak current modulation of the LD is always less than or equal to I_{5C}.

The collector resistors of Q_2, Q_3, Q_4 and Q_5 are used to reduce the collector-emitter voltages, and hence to reduce the power dissipated in these transistors to a permissible level. Their values are such that none of the transistors is driven into saturation, even under conditions of maximum modulation of the differential amplifier The emitter resistors (R_7, R_8) of Q_3 and Q_4 improve the distortion performance of the LD transmitter.

The emitter resistors of Q_2 and Q_5 control the LD bias and modulation current, respectively. When R_1 and R_2 are fixed, changing R_4

can change the LD's bias current, while R_{10} is used to control the modulation current. Therefore, the output optical power of the LD can be adjusted. Usually, R_4 and R_{10} are chosen so that each LD produces the same amount of output power. Because the two LDs have a different threshold current and maximum modulation current, their modulation circuits are slightly different, as shown in Fig. 4.10 (a) and (b).

4.3 Optical Coupler, Fiber Link and Fiber Connections

4.3.1 Optical Coupler and Optical Fiber

The 2-by-2 optical coupler used here is a GOULD S/N 1300-BA-100036 3 dB coupler with a coupling ratio of 50% at 1309 nm and an excess loss of 0.74 dB. It was made of AT&T single mode fiber working in the range 1290 nm to 1330 nm.

The optical fiber used as the common channel is 1.3 μm single mode step index fiber with a length about 1 km; this was the maximum length available. Since single mode fiber has a loss of about 0.2 dB/km, and the system power budget allows a channel loss of 12 dB - 4 dB (coupling loss) = 8 dB, the maximum fiber length might be 40 km.

4.3.2 Fiber Connections

When making the fiber connections in a system, the main concern is to obtain the smallest optical power loss and signal distortion. The usual method for connecting optical fibers has been to use simple butt-joint connections. Other techniques, such as graded index rod lenses, ball lenses and holographic methods have been suggested, but the butt-joint configuration is certainly much simpler and also gives a very low coupling loss (down to 0.2 dB).

For single mode fiber butt-joint connections (splices or connectors), there are two kinds of loss; extrinsic loss and intrinsic loss [46]. Extrinsic loss is caused by the quality of the connection (extrinsic parameters), while intrinsic loss is caused by differences in the two pieces of fiber being connected (intrinsic parameters). Extrinsic loss can be minimized by proper connection design and construction, including fiber end preparation and alignment, as well as cleanliness, degree of index matching in the connection, and core deformation (fusion splices). The loss due to the differences in the intrinsic parameters, such as the width of the Gaussian beam (mode field radius), outer diameter variations, circularity and core concentricity, cannot be easily eliminated.

Three methods are often used for butt-joint coupling: fusion splice, micro-positioner joining, and v-groove joining. Usually, a fusion splice provides the smallest insertion loss (0.2 dB) and the most stable coupling. Mechanical connection using a micro-positioner can result in the best alignment for a joint, hence causing quite small loss which is even compatible with a fusion splice. However, this method requires an optical table as well as accurate and frequent adjustment. Mechanical connection using a V groove causes a bigger loss. Nevertheless, proper end face preparation, good alignment and using index matching fluid between the two fiber ends can greatly reduce the insertion loss (down to less than 2 dB) [47]. In this project, fusion splices have been used wherever possible.

Fig 4.11 illustrates the different fiber connections used in the experimental system. At points A and B, the LDs output pigtail fibers are connected to the fiber from the coupler by biconic connectors, where the two fiber ends are butt joined via a mechanical V groove splice using glycerin index matching fluid. The insertion loss was about 2 dB.

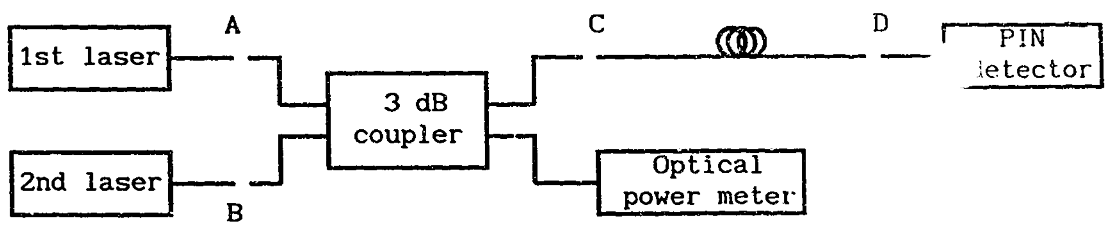

A, B: V-groove mechanical splice.

C, D: Fusion splice.

Fig. 4.11 Fiber connections in the experimental system.

One reason for using butt-coupling for the source is that this makes it easy to connect and disconnect the LD from the system if it is required for other purposes or for checking LD operation, etc., while the larger insertion loss (compared to that introduced by a fusion splice) introduced by a butt-joint is not a problem for the system because the power output of the source is relatively high.

The optical connections at points C and D in Fig. 4.11 use fusion splices, which gives an insertion loss of about 0.1 to 0.2 dB. The splices were made at the Alberta Telecommunication Research Centre (ATRC) using their arc fusion machine; an insertion loss of 0.3 to 0.5 dB (per splice) was obtained.

4.3.3 Optical Power Attenuator

Because the fiber used here is not very long, the optical power loss is very small. It was shown in the experiment that the received power caused saturation of the PIN detector and its built in preamplifier. To avoid the PIN detector from being saturated by receiving too much power, and also to simulate a real system with a longer fiber, an optical attenuator was used. Because no commercial attenuator operating at 1.3 μm was available, power attenuation was introduced by winding a short length of fiber around a 0.9 cm diameter cylinder for four turns, as shown in Fig.4.12 (refer to [48] for bending loss). In this way, an optical power attenuation of 8.5 dB was obtained.

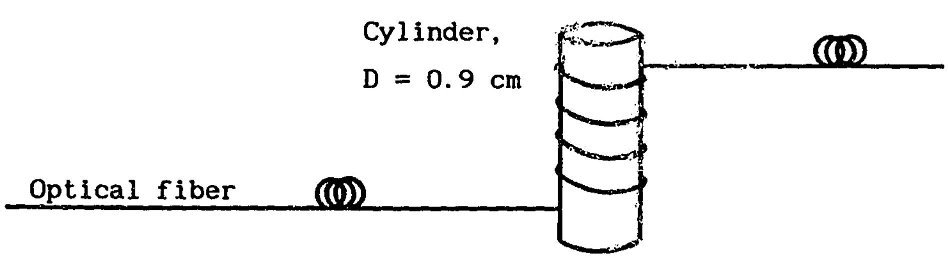

Fig.4.12 Configuration of the optical power attenuator.

4.4 Receiver

4.4.1 Optical Detector and Preamplifier

After transmission over the single mode fiber, the multi-level optical signal is detected by a PIN optical detector (RCA type C30986-150 QC-02). It is an Indium Gallium Arsenide photo-diode with an integrated hybrid preamplifier, supplied in a hermetically-sealed 14 pin dual in-line package. The multi-level electrical output is AC (capacitively) coupled to a 500 ohm termination.

The detector has a system bandwidth of 150 MHz and a responsivity of 18 kV/W. Its sensitivity at a BER of 10^{-9} is -38 dBm, and the noise equivalent power (NEP) is 1.89 pW/(Hz)$^{1/2}$.

4.4.2 Main Amplifier

The output AC signal from the detector preamplifier is amplified by a Keithley 105 Pulse Amplifier, which has a bandwidth of 500 MHz. The voltage gain can be set to either 10 or 100.

4.4.3 The Generation of Receiver Address Codes

The receiver local Gold sequence generator with the delay circuit is shown in Fig 4.13. The address sequence can be set manually to generate any sequence. This enables the one receiver used in the experiment to function as any one of the possible 31 different receiver stations, by producing its particular address sequence.

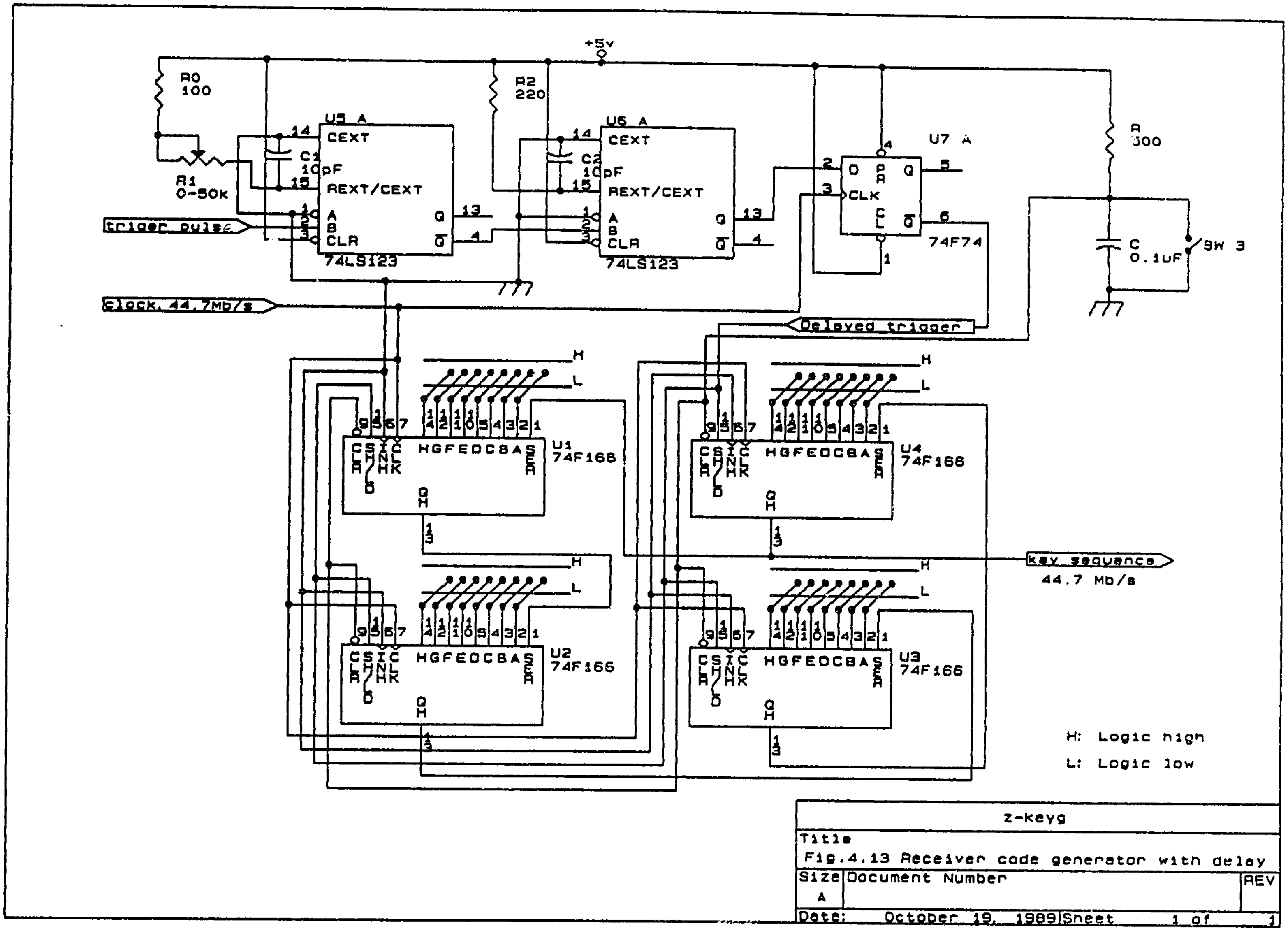

Fig.4.13 Receiver code generator with delay

In order to decode data, the local key sequence must be synchronized with the transmitted signal. This is usually done via a clock recovery and framing tracing technique. In this project, because verification of the code properties and operation of the decoding method are our main goals, the receiver synchronization with the received signal was obtained by using a delayed framing pulse from the transmitter to trigger the local code generator at the receiver.

The delay circuit is made up of mono-stable multivibrators U5 and U6 as shown in Fig.4.13. This circuit delays the trigger pulse, which is transmitted via an extra line from the transmitter to the receiver local sequence generator, by the same amount of time that the information signal takes to arrive at the receiver. The delay was set experimentally by adjusting the resistance R_1, so that the delayed framing pulse triggers the local generator at the correct time. Therefore, receiver decoder synchronism is obtained with the received signal.

4.4.4 Analog Decoder

The received signal is multi-level, due to the combination of the coded signals that are being sent to different stations. To obtain the binary data signal sent to a certain station, the electrical signal must be correlated with the keyword for the particular station and, depending on the output of the correlator, a decision must be made as to whether a 1 or 0 has been received. The decoder schematic diagram is shown in Fig.4.14.

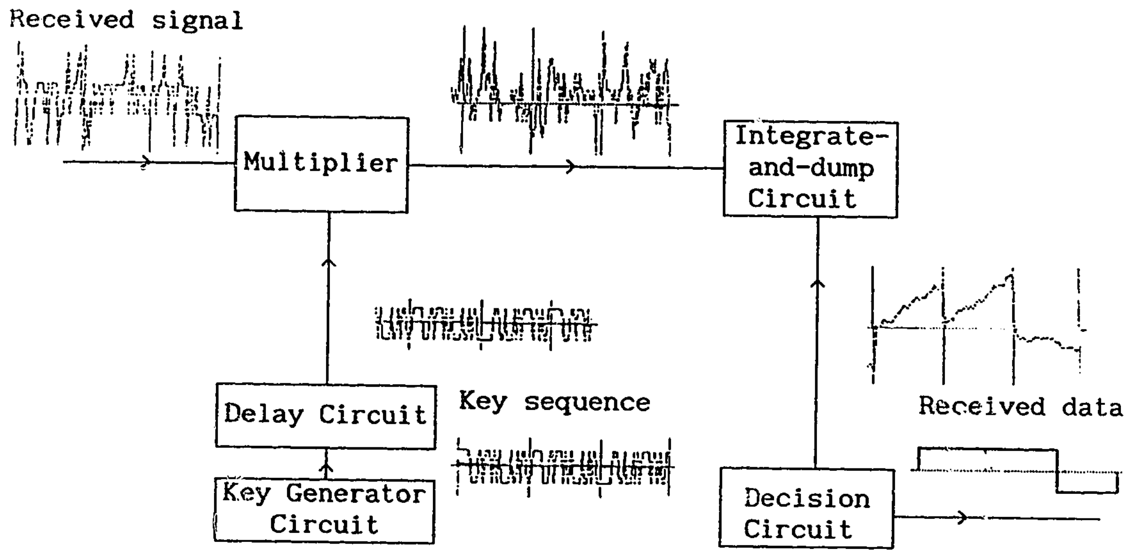

Fig. 4. 14 Schematic diagram of decoder.

The signal is multiplied in a correlator with the address sequence (key word) of the receiver. The correlator can utilize surface-acoustic-wave (SAW) devices, charge-coupled devices (CCD), or a tapped delay line [49]. However, SAW devices are comparatively expensive; charge coupled devices have been used by some researchers [20], but they are somewhat slow and hence limit the system data rate.

The Gold sequence correlator used in this thesis consists of a high-speed analog 4-quadrant multiplier (MC12002) followed by an integrate-and-dump filter, as illustrated in Fig. 4. 15. The multiplier is a high frequency analog mixer which changes the phase of the input signal by 0° or 180° according to the logical high or low of each chip of the local keyword.

The differential output of the multiplier is converted to a single

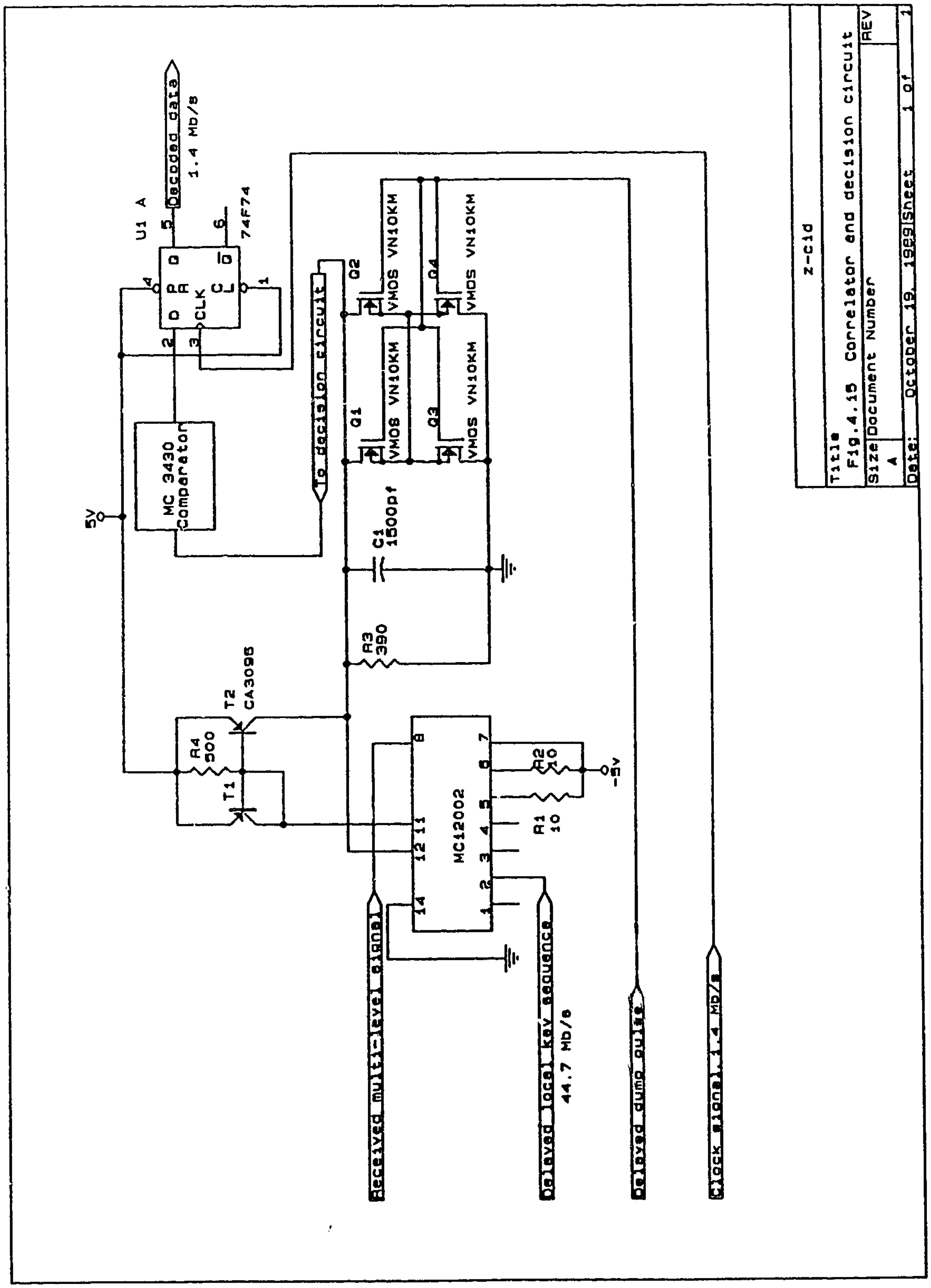

Fig.4.15 Correlator and decision circuit

ended output using the current mirror formed by T1 and T2. This output is filtered by an integrate-and-dump (I-D) circuit comprising the capacitor C1 and a high-speed switch VMOSFET (VN10KM) for discharging (dumping) the capacitor voltage [50]. At the end of each 32 chip period, a very short pulse switches the FET on so that the drain-source resistance becomes very small and the capacitor is discharged. Thus, the voltage across the capacitor at the beginning of each data period is set to zero.

It is desired to complete the discharge of the capacitor at least within a chip time interval, and the shorter the discharge time or the smaller the RC constant, the shorter the reset time will be. Because of this, the basic requirements of the filter are a slow integration time and a quick dumping time (less than a few nanoseconds). To obtain a low "on resistance", two FETs are used in parallel, which gives an R_{on} of 2.5 ohm. The two groups of FETs Q1-Q2 and Q3-Q4 are connected back-to-back in series, so that they make up a switch, which operates for both positive and negative input / output voltages. To completely discharge the capacitor, a dump time of nearly 30 ns is necessary. This was achieved by using a mono-stable multivibrator, which controls the pulse width of the delayed 0^{th} pulse. An increase of the pulse width from 22 ns to 30 ns was obtained in this way.

In the decision circuit (also shown in Fig.4.15), the output voltage of the filter is first compared with a threshold (*0* Volts) by a comparator (MC3430). Corresponding to a positive or negative input, a TTL compatible output of 1 or 0 is achieved. Following this is, a D flip-flop samples the TTL output at the end of each data period (at the time slot corresponding to the 32^{nd} chip). According to whether this voltage is 1 or 0, the output of the D flip-flop is held to 1 or 0 for the duration of the next data period (32 chips). Thus, the decision of a data bit of 1 or 0 is made and the transmitted data signal is regenerated.

When errors are made, the regenerated waveform differs from the one originally transmitted. This can be measured by the error detector.

4.4.5 Error Detector

The decoded data is fed into an HP 3763A Error Detector, which compares the received data with the original transmitted data pattern. In this project, 10-bit words were used to test the system operation, and 16 bit word as well as pseudo-random sequences were used in the BER measurements. The error detector and the data generator were driven by a common clock at a speed of 1.40 Mb/s. This detector can be set at "displaying BER when over 10 errors are measured" (10 error pattern), or at "displaying BER when over 100 errors are measured" (100 error pattern). Because of the very low bit error rate, it usually takes hours to get a single BER measurement when the 100 error pattern is used. Over such a long period, the system might be changed by occasional interference and the measured results might be meaningless. To avoid this, the 10 error pattern was used throughout the BER measurements, even though it is statistically desirable to use a pattern with a large number of errors [51].

5. EXPERIMENTAL RESULTS

Using the experimental system described in the previous chapter, various measurements were made to verify the properties of the CDMA method using Gold codes, and the capability of this method for supporting simultaneous users.

This chapter presents and discusses the experimental results. Firstly, the performance of the encoder, laser, optical receiver, and decoder are presented. Secondly, the experimental relation between the BER and various parameters, such as the power of the received signal, the power of the other interfering station, the number of stations, and the noise power, are given. Next, the power spectra are illustrated and discussed. Finally, the possible sources of BER are investigated.

5.1 System Topology

Fig.5.1 illustrates the whole experimental system. A Wavetek model 178 50 MHz Programmable Waveform Synthesizer generates a TTL compatible clock signal at 44.736 Mb/s. This provides the clock signal for the Gold code generator and, by means of a frequency divider, it gives a 1.40 Mb/s clock which drives the HP 3762A Data Generator. The data signal enters the encoder and is processed according to the Gold coding rules; the encoded signal then modulates the laser transmitter. Light signals from the two LDs are coupled to a 1 km length of fiber using a 3 dB coupler. The other output port of the 3 dB coupler is used to monitor the output power from the LDs using an Optikon 22XLA Fiber Optic Multi-meter, which displays the same power level as that coupled

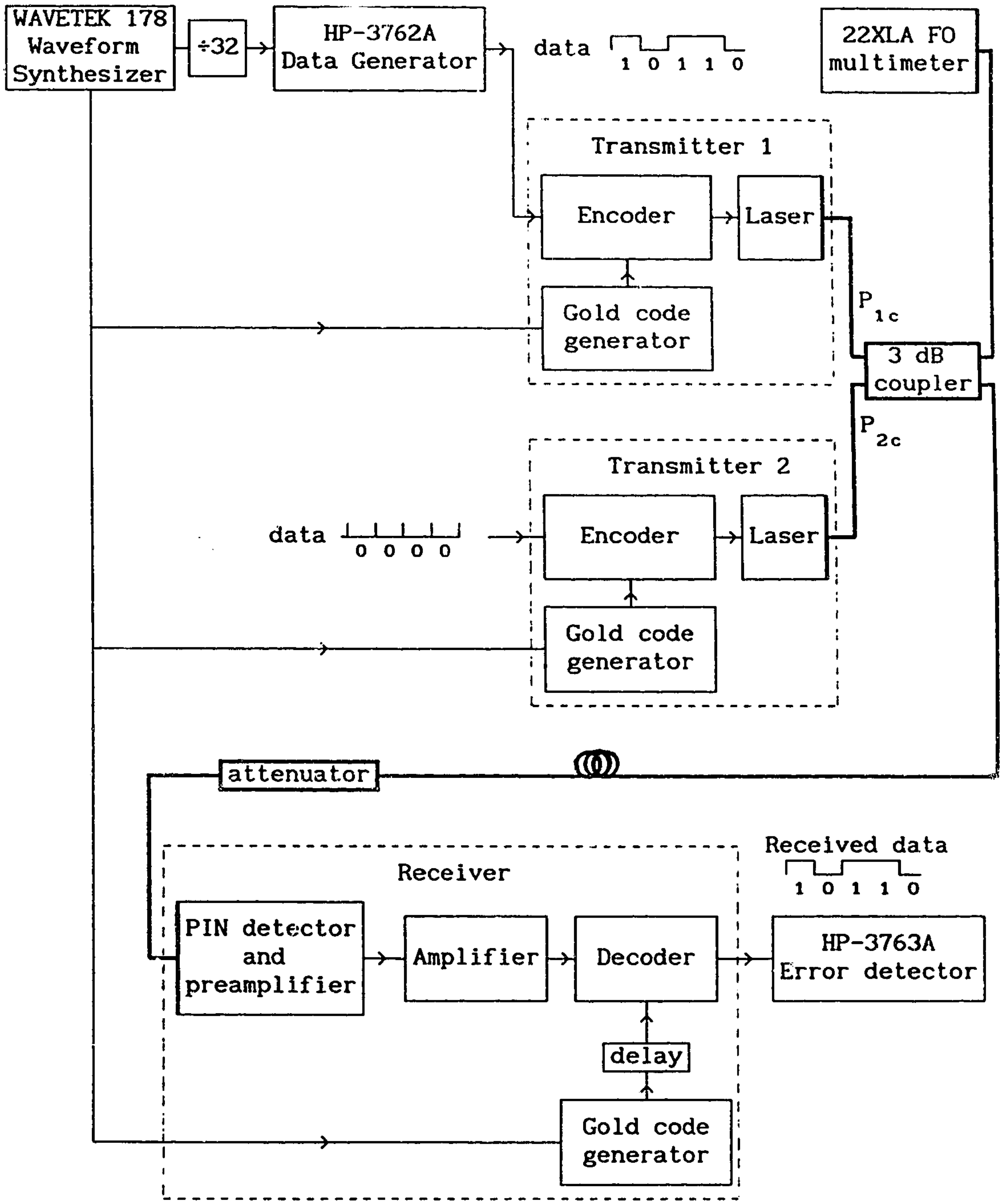

Fig. 5.1 Experimental and measurement system.

into the fiber channel.

At the receiver, a PIN photo detector with a preamplifier converts the optical signal into an electrical signal, which is then passed through a Keithley model 105 Pulse Amplifier to the decoder. The clock used by the decoder local address sequence generator would normally have to be obtained from the received signal using a clock recovery circuit. In this work, however, the receiver clock signals were taken directly from the transmitter. The framing pulses for receiver local keyword synchronization were also taken from the transmitter. Since the transmitted signal is delayed by the fiber transmission line, the framing pulse needs to be delayed by the same amount of time in order to obtain synchronization between the received signal and the local keyword. This was achieved by using two mono-stable multi-vibrators, which provide delays to the framing pulse. By adjusting the delay, the local keyword can be synchronized with the desired signal. The decoder correlates the received signal with the local sequence using a multiplier followed by an integrate-and-dump filter, then a sample-and-hold circuit regenerates the data. This data signal is then sent to the HP 3763A Error Detector, which display the system BER.

The experimental waveforms were obtained using a Tektronix 2465 300 MHz Oscilloscope; the power spectra are measured by a HP 8557A Spectrum Analyzer.

5.2 System Performance and Output Waveforms

5.2.1 Gold Code Generator and Encoder

In each of the two stations, there is a Gold code generator which produces code sequences corresponding to the address sequence of the intended receiver. Two difference sequences $\mathcal{X}_1$ and $\mathcal{X}_2$ are shown in Fig.5.2 (a) and (b).

For each data bit (0 or 1) at the input, the encoder generates the 31 chip code sequence $\mathcal{X}$ or $\overline{\mathcal{X}}$ corresponding to the address code. Since there is an extra chip for dumping in the integrate-and-dump processing, the code is actually 32 chips long. Therefore, the data at a rate of 1.40 Mb/s gives a chip rate of 44.736 Mb/s (the standard T3 transmission rate).

Figs.5.3 (a) and (b) demonstrate the operation of the Gold encoder for two different 10 bit words as the input data. Fig.5.4 shows the situation for a $2^{15}-1$ PRBS data input. As can be seen, the encoder output is a waveform with a symmetrical and almost perfectly opened eye pattern. This indicates that the waveform at the encoder output is a train of almost rectangular pulses with very small amplitude variations (noise) and time variations (jitter).

5.2.2 Laser Modulation, Optical Coupler Combining and Optical Detection

Fig 5.5 shows the modulation current (corresponding to the encoded data) in the LD. Since this is obtained by measuring the voltage across a 1 ohm resistor which is connected in series with the LD, it is

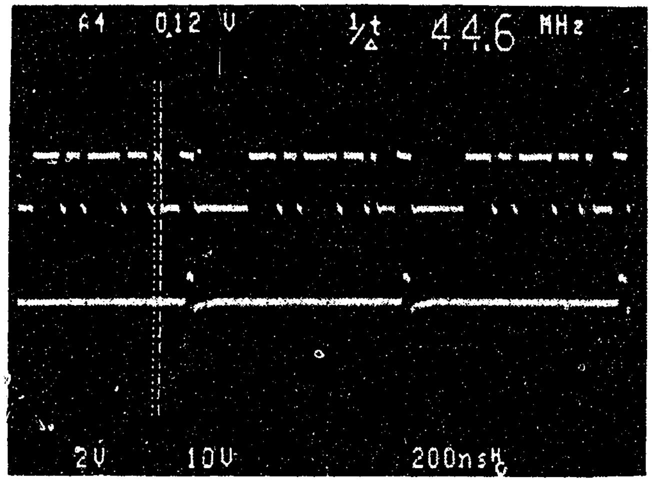

Code sequence

Framing pulse

(a)

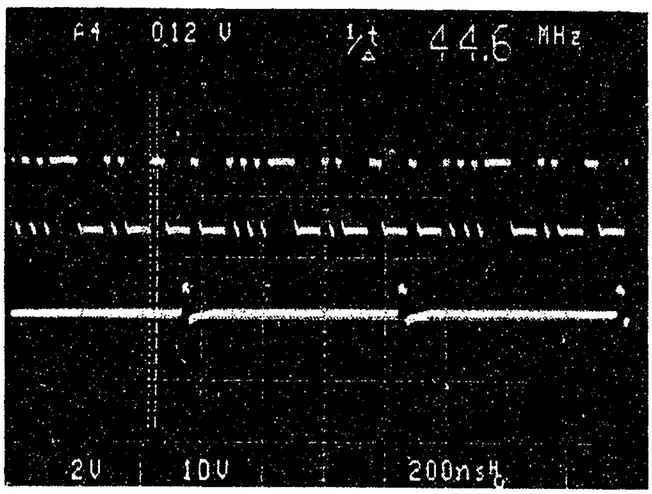

Code sequence

Framing pulse

(b)

Fig. 5.2 The Gold Code Sequences and the 32^{nd} Framing Pulses.

a) $\mathcal{X}_1$, Gold code for the 1st station

b) $\mathcal{X}_2$, Gold code for the 2nd station

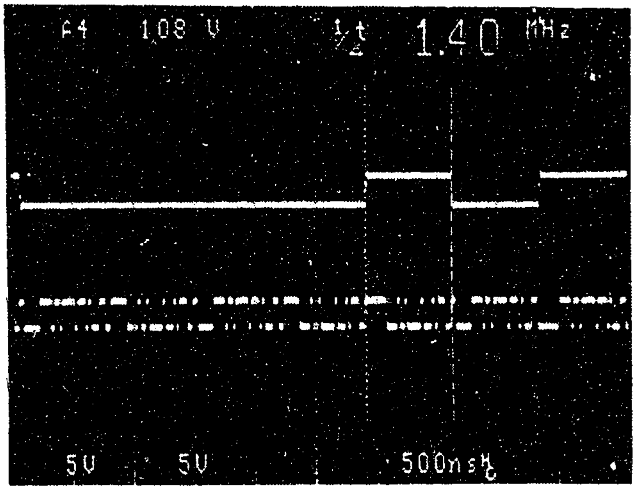

(a)

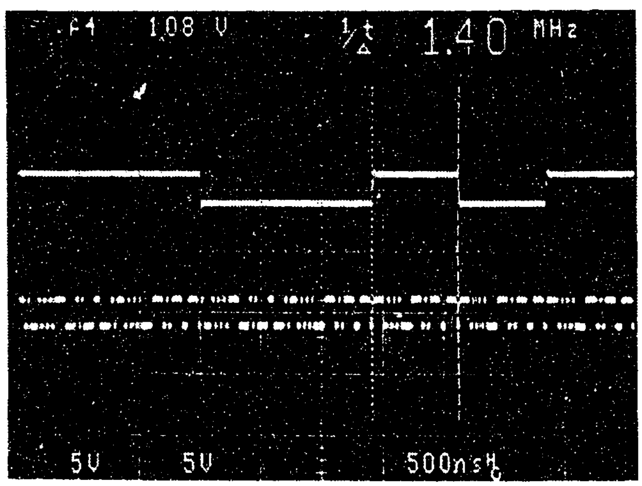

(b)

Fig. 5.3 Encoder operations for 10 bit word data signal.

(a) Signal sending to the 1st station

(b) signal sending to the 2nd station

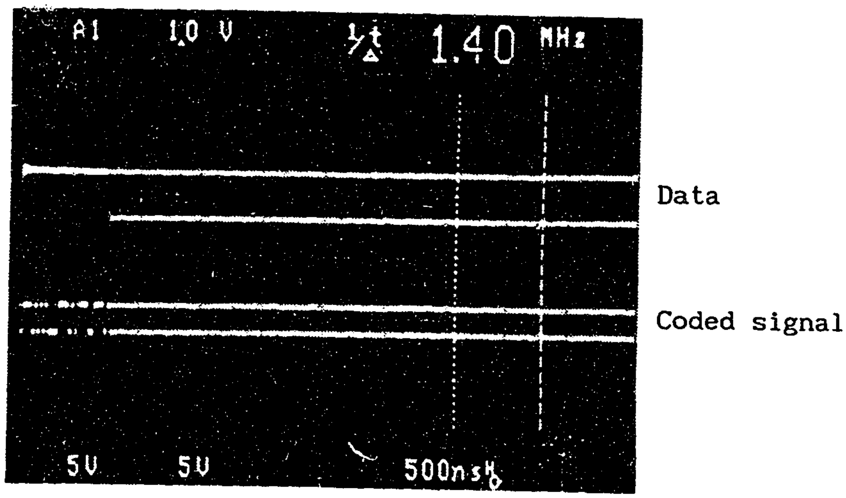

Fig. 5.4 The encoder operation for 2^{15}-1 PRBS data signal.

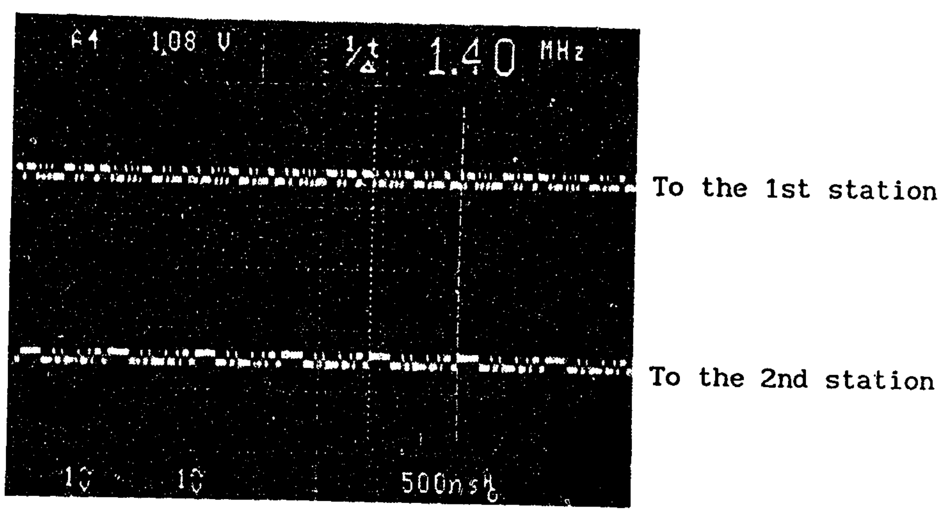

Fig. 5.5 Modulation signals at the LDs.

proportional to the modulation current going through the LD. Therefore, the noise shown here is mainly the circuit's thermal noise; additional noise may be present in the LD output signal.

The 1 km fiber used here is a single mode fiber with an attenuation of about 0.2 dB/km at 1.3 μm. Since the dispersion of single mode fiber is small and the length of the fiber used in a LAN is fairly short (a few meters to ten kilometer), the dispersion of the fiber transmission line could be ignored.

It was found during the experiment that the received power caused saturation of the PIN detector and preamplifier. To reduce the received power so that the receiver would operate in its linear region, an optical power attenuator was employed. The attenuation inserted was about 8.5 dB, equivalent to the attenuation caused by a length of about 42 km fiber; however, it does not give the same dispersion as is caused by 42 km of fiber.

Figs. 5.6 (a) and (b) show the received signal at the PIN preamplifier output when either of the two stations is transmitting, and (c) shows the output when the two stations are transmitting simultaneously. The transmitted signal and the received signal are identical with the exception of a time delay and the noise spikes on the received signal.

The delay is due to the system transmission time. The spikes are caused by the 44.736 Mb/s clock, which is a return to zero (RZ) signal. As is shown in Fig. 5.2, there is a small fluctuation of 44.736 frequency noise on top of the 44.736 Mb/s non-return-to-zero (NRZ) coded signal; in Fig. 5.6, there is a larger fluctuation of the same noise on top of the received 44.736 Mb/s NRZ signal at the output

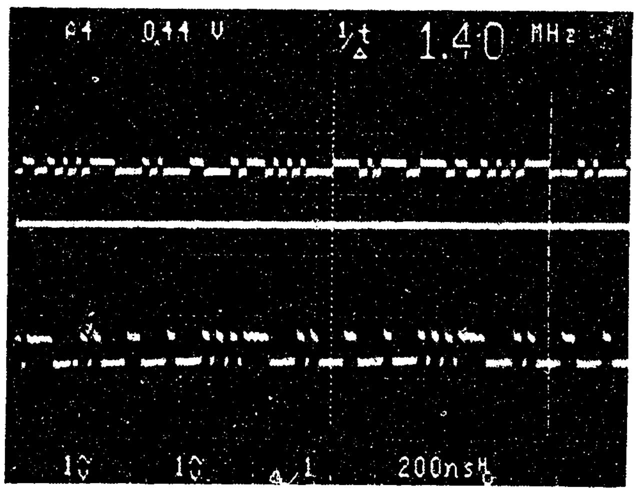

The 1st laser

The 2nd laser

PIN preamplifier

(a)

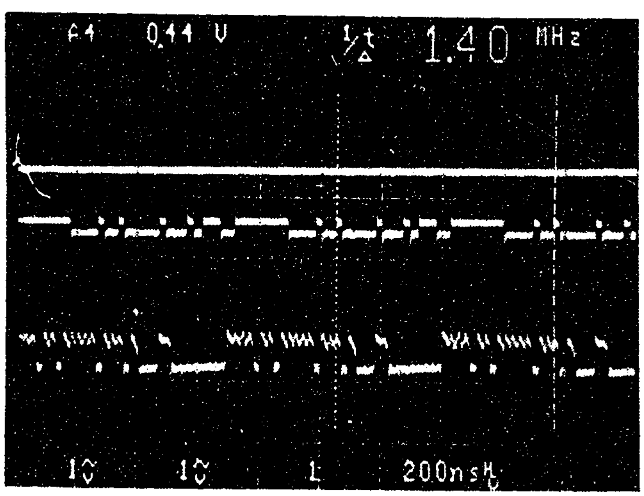

The 1st laser

The 2nd laser

PIN preamplifier

(b)

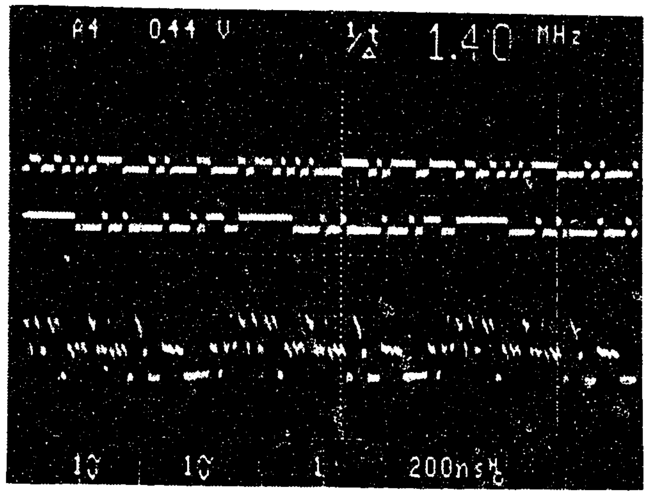

(C)

Fig. 5.6 Laser modulation signal and PIN received signal.

(a) One station transmitting

(b) Another station transmitting

(c) Two stations transmitting simultaneously

of the preamplifier. This clock noise may be picked up, mainly by the detector and preamplifier and partially by the encoder, due to insufficient power supply decoupling of the encoder circuit, and due to insufficient isolation and shielding between various parts of the system. There is also random noise in the preamplifier output, which is primarily contributed by the PIN detector noise and the preamplifier noise. The LD modulation circuit noise and the LD source noise are very small, because the LD is operated at a relatively high power level. The channel noise is also very small, since the optical fiber is virtually noiseless. Usually, a BER of less than 10^{-9} was obtained, which indicates that the overall system noise was not large enough to cause any data decoding problems.

5.2.3 Generation of Local Address Sequence with Variable Delay

Fig.5.7 shows a local key sequence generated with a variable delay pulse set by a delay circuit.

To simplify the receiver circuit design and construction, the receiver synchronization with the received signal was obtained by sending a framing pulse directly from the transmitter to the receiver through a variable delay circuit. Thus, the local code generator was triggered at the correct time, so that the local code was synchronized with the received signal.

5.2.4 Decoder Correlation

In the decoder, the received multi-level signal is correlated with the local key sequence in order to decode the signal. Figs.5.8 (a) and (b) display the output waveform of the integrate-and-dump filter.

For the case of only one station transmitting (see Fig.5.8 (a)), the output closely approximates a linear ramp, which agrees with the computer simulation results. When the other transmitter is also operating (see Fig.5.8 (b)), the waveform becomes distorted, due to the interference.

It is observed in Fig.5.8 that, for a 1 1 data sequence, the

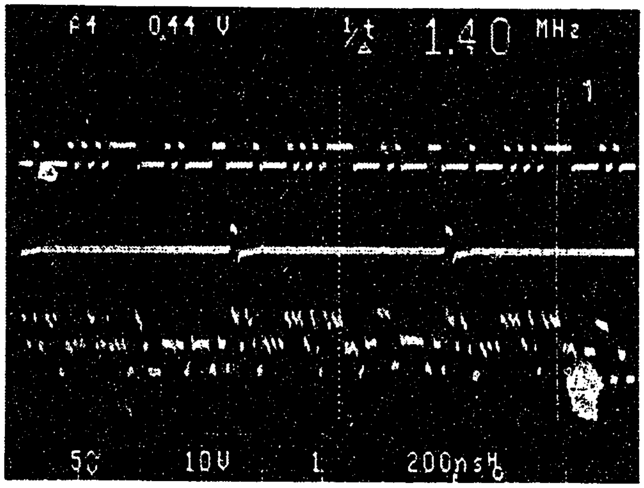

Local code

Framing pulse

without delay

Received signal

(a)

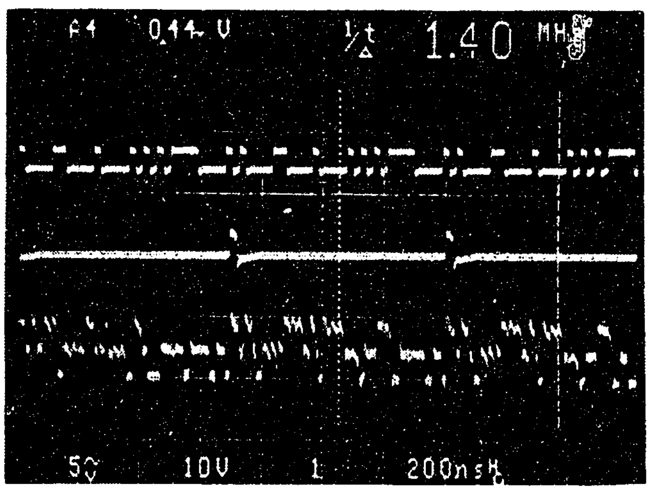

Local code

Framing pulse

without delay

Received signal

(b)

Fig. 5.7 The local address sequence with different delay in a receiver.

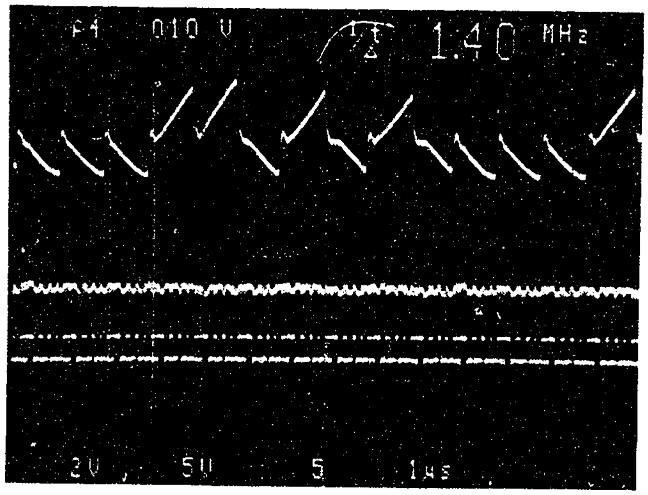

(a)

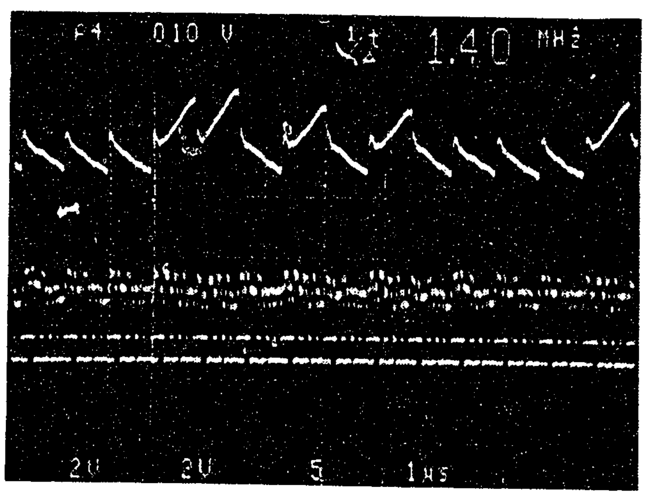

(b)

Fig. 5.8 Integrate-and-dump waveforms at a receiver.

(a) One station transmitting

(b) Two station transmitting to different stations integrate-and-dump filter output waveform is exactly as described; however, for 0 0, 0 1, or 1 0 data sequences, there is a slight negative fluctuation at the beginning of the 2nd data slot correlation. This imperfect correlation is probably due to the turn-off characteristic of the FET switch in the decoder; it may be the charged voltages in the FET channel flow back into the capacitor at the beginning of the next data slot, causing a negative voltage. This imperfect correlation may cause a data transmission error when the SNR is low (such as when the desired signal power is low, or when the undesired signal power is high).

5.2.5 Decoder Decision Circuit

Using the system for direct electrical signal transmission, that is, the transmitter and receiver operating back-to-back without the optical channel, the data was decoded with a BER of less than 1×10^{-9}. This was reported in a conference paper [52]. The following describes the measurements carried out on the complete system, i.e. including the optical channel. The optical signal output power coupled into the fiber from the first station is P_{1c}, and the power from the second LD is P_{2c} (refer to Fig.5.1 on page 89).

Fig.5.9 shows the operation of the sample and hold circuits, when only the 1st station is transmitting. The second trace is the received signal. The third trace shows the integrate-and-dump filter output waveform, which is also the input waveform of the sample and hold circuit. In the sample and hold circuit, the input was compared with a threshold 0, sampled at the 32^{nd} clock time slot, and then held for a

32 clock period (i.e., one data time slot period). The output regenerated data is shown in the first trace.

If P_{1c} decreases, the signal to noise ratio (SNR) is decreased. This situation is illustrated in Fig.5.10: the second trace shows the decreased P_{1c} signal, and the third trace shown the integrate-and-dump waveform. When P_{1c} is in the range from 3.3 dBμ to -3.9 dBμ, the system BER is less than 1×10^{-9}. If P_{1c} is less than -3.9 dBμ, the BER increases rapidly; this will be discussed in Section 5.3.2.

The transmitted and received data under different synchronization conditions are shown in Figs. 5.11 (a) and (b). When the local key sequence is synchronized with the received signal, the integrate and dump waveform is seen to be ideal (Fig.5.11 (a)). When synchronization with the received signal is not obtained, the integrate and dump waveform is very irregular and the decoded data contains many errors (see Fig.5.11 (b)).

Fig.5.11 (c) demonstrates the situation when sequence $\mathcal{X}_3$ is used to decode the incoming signal, while data was intended to be transmitted to the 2^{nd} station (coded by address sequence $\mathcal{X}_2$; refer to Appendix A for the address sequences). There is no data received, and the error detector shows synchronization loss.

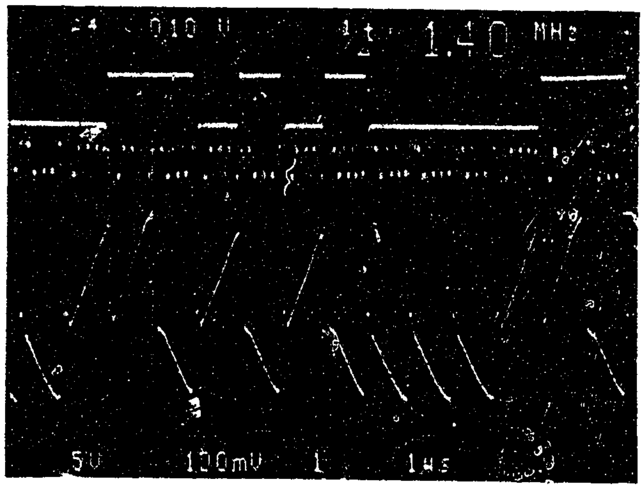

Fig.5.9 Operation of the sample and hold circuit when $P_{1c} = 3.1$ dBμ.

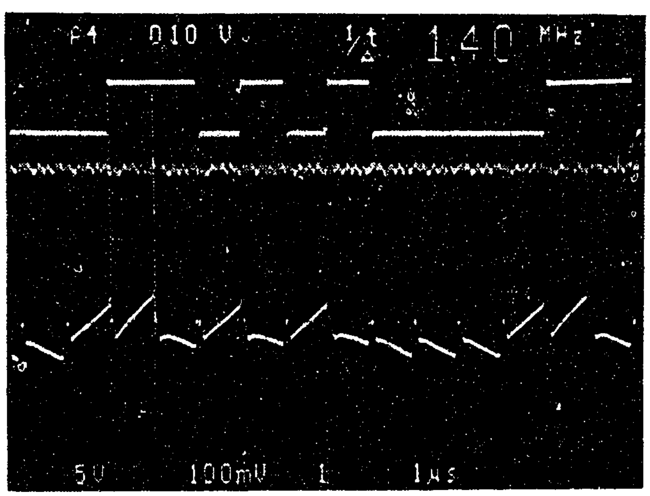

Fig.5.10 Operation of the sample and hold circuit when $P_{1c} = -4.2$ dBμ.

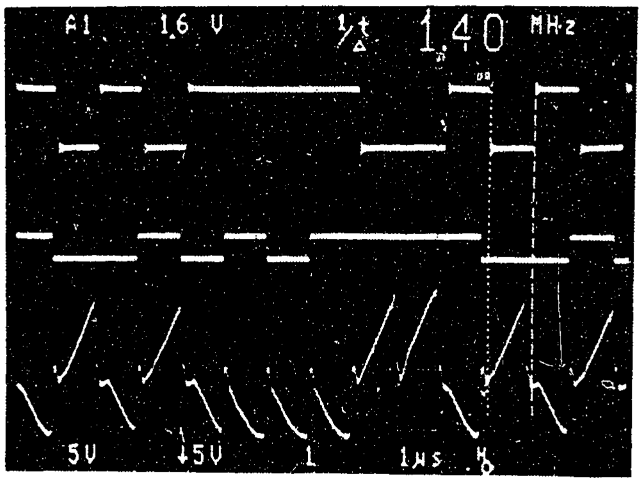

Transmitted data

Received data

Integrate-and-dump waveform

(a)

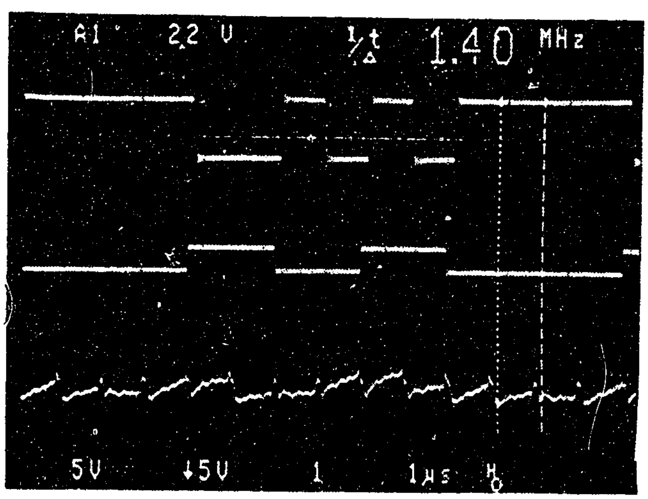

Transmitted data

Received data

Integrate-and-dump waveform

(b)

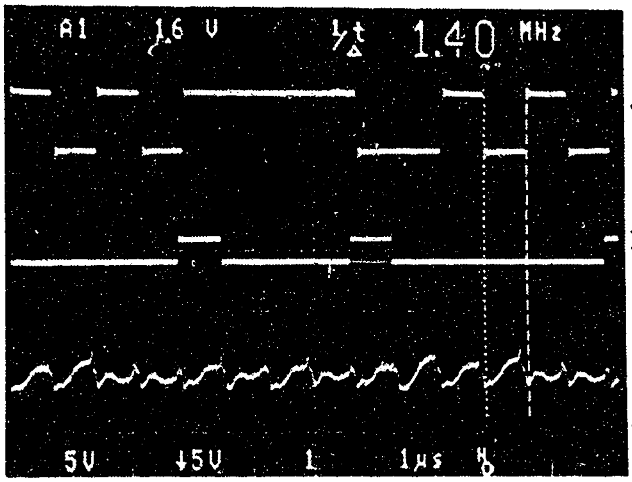

Transmitted data

Received data

Integrate-and-dump waveform

(c)

Fig. 5.11 Transmitted and received data signal.

(a) The desired receiver is synchronized with received signal

(b) The desired receiver is not synchronized with received signal

(c) At the undesired receiver

5.3 Bit Error Rate Measurements

5.3 ' umbe: of Simultaneous Users

. luded from the theoretical discussion and the computer simulatio n Chapter 3 that, with a set of 32 31-chip Gold sequences as the address codes, 31 simultaneous stations can be supported with error free transmission. It was not possible in our experiment to set up a transmission with all these stations. With two LDs available, the test of the circuit had to be limited to two stations. There is the possibility of adding many electrical signals from several stations, and applying the total voltage to one of the LDs, so as to simulate the interference from other users. This would be a good test of the receiver and the correlation; however, this was beyond the scope of this work.

5.3.2 The Transmitted Signal Power

The first LD coupled a maximum optical power of 3.3 dBμ to the fiber. The actual LD output optical power is estimated to be nearly 6 dB more than this. The loss in the 3 dB coupler and the loss in the connection (including a 2 dB connection loss between the LD pigtail and the fiber, and a 0.7 dB coupler excess loss) were measured to be about 5.7 dB.

Fig.5.12 shows the BER curve versus received optical power. Curve A is obtained when only one station is transmitting. The maximum coupled power from the first station is 3.3 dBμ. As long as this power P_{1c} is larger than -3.9 dBμ, the BER is less than 1×10^{-9}. Reducing the power of P_{1c} decreases the SNR of the optical signal, thus increases the BER.

With two stations transmitting, the BER obtained for the desired signal depends on the power transmitted from each station. In general, the BER will increase as the power from the desired station decreases or the power from the interfering station increases. Curve B in Fig.5.12 shows the effect of the power variation of the desired signal P_{1c} on the system BER, while the power of the undesired signal P_{2c}

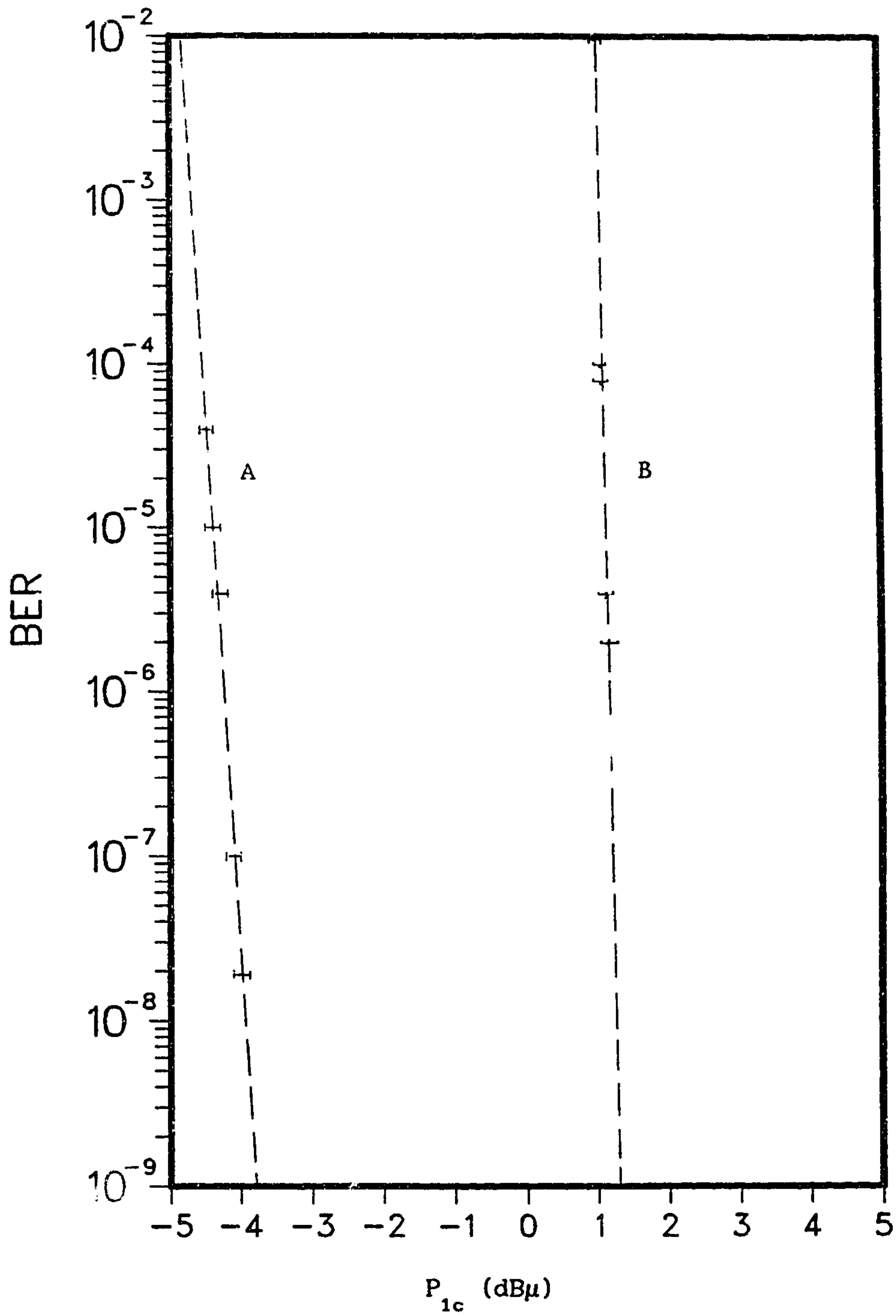

Fig. 5.12 Dependence of the system BER on the optical power of the desired signal (P_{1c}).

Curve A: one station is transmitting

Curve B: two stations are transmitting, P_{2c} = 3.3 dBμ remained at 3.3 dBμ. As long as P_{1c} was larger than 1.3 dBμ, the BER was less than 1×10^{-9}.

Fig.5.13 shows the BER when P_{1c} was kept at 3.3 dBμ while P_{2c}, the power from the other station was increased. This increases the interference. As long as P_{2c} was less than 6.3 dBμ, the BER for the desired signal was less than 1×10^{-9}. It is observed that the BER — Power curve when P_{2c} remains constant and P_{1c} is decreasing (curve B in Fig.5.12), is symmetric with the curve for the case when P_{1c} remains constant and P_{2c} is increasing (Fig.5.13). This is to be expected, because the two situations are the same in the sense of reducing the system SNR, as the noise coming from the LD, detector and amplifier circuits remains approximately constant (although the noise coming from the PIN may vary a little with the received power).

5.4 Power Spectra

The power spectrum of the 1.40 Mb/s data signal is shown in Fig.5.14. Because the data is an NRZ signal, the first harmonic occurs at 0.70 MHz. The peak slopes of the first, third, fifth, ···, harmonics at 0.70 MHz, 2.10 MHz, 3.50 MHz, ···, are illustrated clearly. Fig.5.15 displays the spectrum of the received data. Comparing it with Fig.5.14 (b), it is seen that the spectra of the transmitted and received data are almost the same, as expected.

5.5 Possible Sources of Error

As discussed in Section 3.2.2, the interference from a signal

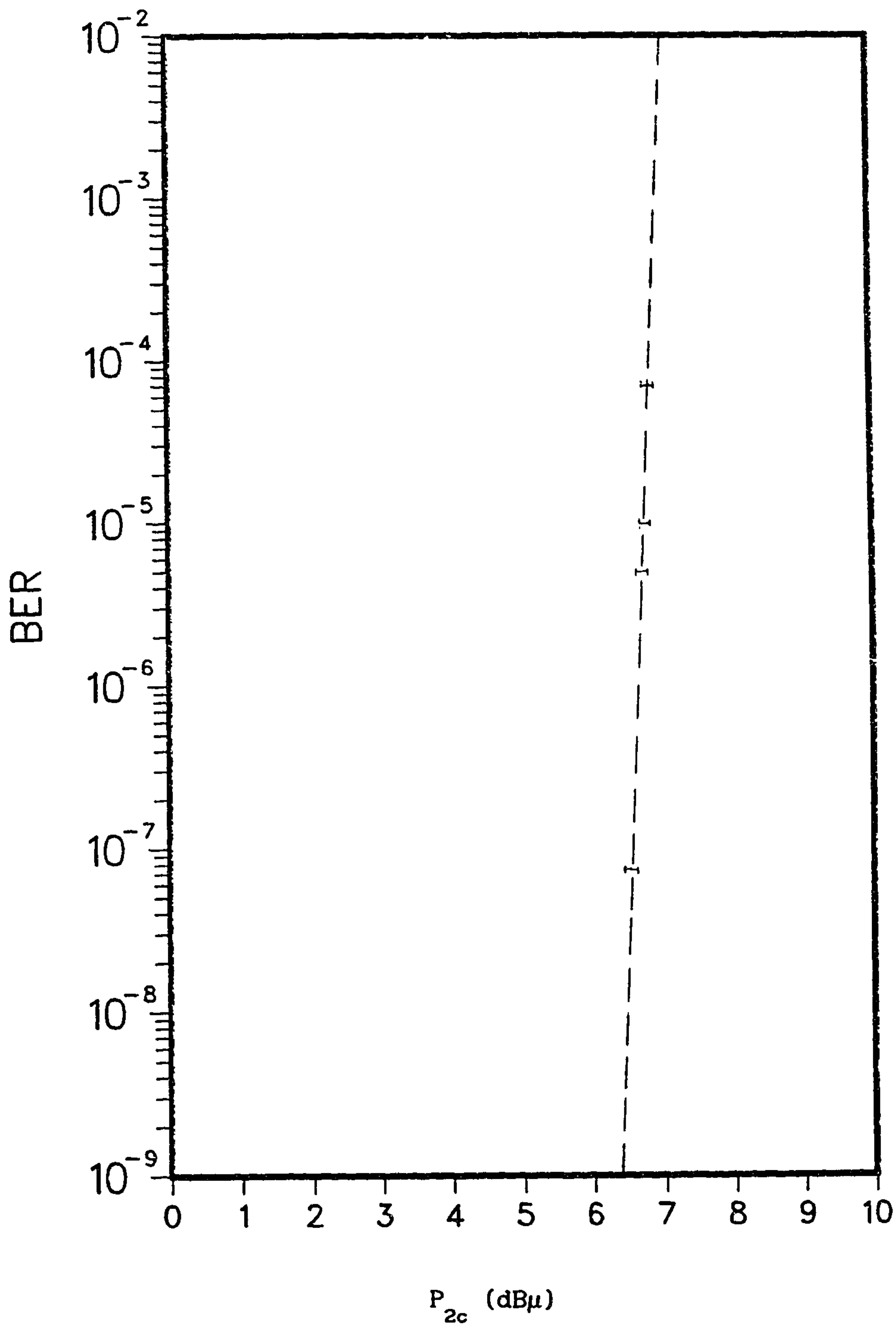

Fig.5.13 Dependence of the system BER on the optical power of the undesired signal (P_{2c}) when two station are transmitting and P_{1c}= 3.3 dBμ.

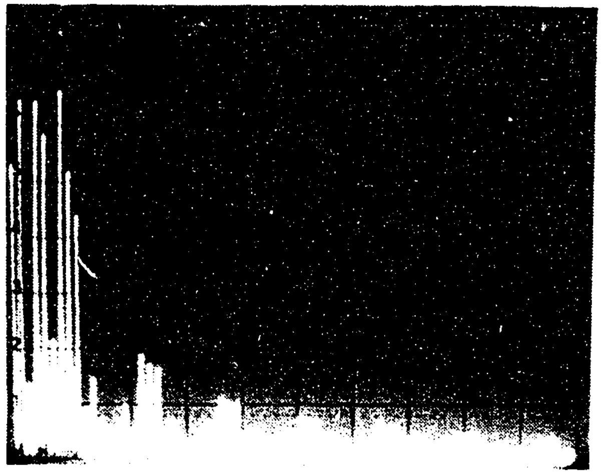

(a)

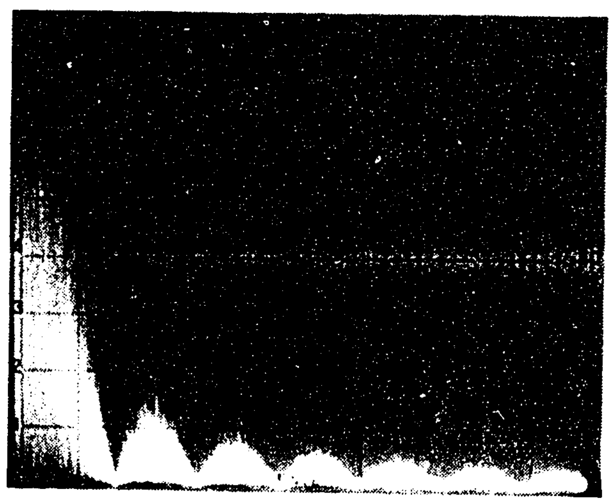

(b)

Fig.5.14 Spectra of the 1.40 Mb/s transmitted data signal.

(horizontal: 1 MHz/DIV, vertical: linear)

(a) 10-bit word data.

(b) 2^{15}-1 PRBS data.

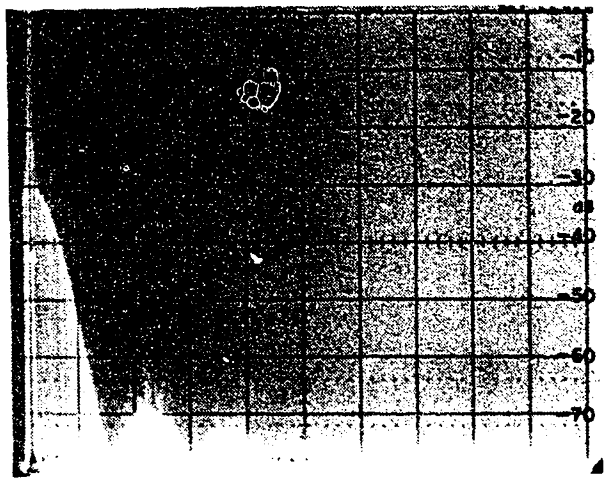

Fig.5.15 Spectrum of the 1.40 Mb/s received PRBS data.

(horizontal: 1 MHz/DIV, vertical: linear)

intended for another station should, ideally, have no effect on the system BER until the power P_{2c} is increased to more than $31 \times P_{1c}$. In the experimental system here, P_{2c} could only go up to $2 \times P_{1c}$ (limited by the range of the LD modulation). Therefore, the poorer BER performance must originate from sources of error other than from user interference, such as the followings:

Firstly, the error introduced by the imperfect correlation in the decoder. This is caused mainly by the incomplete discharge of the integrated-and-dump circuit through the FET switch; also the multiplier does not switch instantaneously, and there may be slight timing errors between received signal and the local keyword).

Secondly, the spikes in the transmitted signal, which is picked by the encoder circuits from the 44.736 Mb/s clock.

Thirdly, the thermal noise added by the PIN detector and the preamplifier to the received signal before decoding [53, 54, 55]. The photo-detector shot noise will vary, depending on the power of the received optical signal, however; it is normally negligible, as we used a PIN photo diode detector [55].

Fourthly, the limitation of the preamplifier bandwidth, which causes distortion of the received signal pulse shape.

Finally, the normal sources of errors in a communication system, such as: power amplitude variations (which may raise the power and cause a 1 to be regenerated when a 0 was sent), timing jitter (which may cause sampling at a wrong time), and intersymbol interference.

6. DISCUSSION AND CONCLUSIONS

This thesis work has investigated and demonstrated the applicability of the Gold code used in an optical fiber multi-user communication network. The code division multiple access technique using Gold codes has conventionally been employed in spread spectrum communication systems, where the main application has been for interference rejection, signal security, or multiple access. Usually, a spread spectrum system requires a large bandwidth, and hence this method is not used in most conventional systems. In an optical fiber communication system, however, the available transmission bandwidth is very large. This makes it attractive to use the CDMA method as the multiplexing technique in an optical fiber network.

Previous researchers [14,15,16] have employed either electrical signal processing or complete optical signal processing, and have all used what has been referred to in this thesis as "asynchronous data slot transmission". The original intent of this thesis was to optimize multi-user system performance, especially to improve a similar transmission system previously developed by S. Tamura, et al. [20], which was an asynchronous data slot transmission using Gold codes for coding, and with electrical signal processing for decoding. Their network could transmit at the relatively low data rate of 20 kb/s, and was limited mainly by the charge-coupled-devices (CCD) in the decoder. Using a set of 127-chip Gold codes, their network could support 6 simultaneous users with a BER of 8.1×10^{-6}.

In order to investigate and optimize the system performance, this thesis work has used Gold codes as the address sequences, electrical signal processing as the decoding method, and synchronous data slot transmission as the transmission pattern.

Computer simulations of BER when using different length Gold sequences were demonstrated in this research work. Assuming that there was only one transmitter for each receiver, with a set of N-chip Gold sequences, ideally, up to N simultaneous transmitters could be supported by the system without any receiving error caused by user interference.

One of the unique features of the reported system is the significant increase in system capacity. This increase came from using the synchronous data slot transmission pattern which takes advantage of the uniform low cross-correlation (-1) of the Gold codes. It was shown by computer simulation that this kind of transmission pattern could support many more users than asynchronous transmission, for the same system BER. For example, for error free transmission, the synchronous case can support 31 users with a set of 31-chip Gold codes, while the asynchronous case with the same set of codes can guarantee only 4 users.

Usually, asynchronous data transmission is favored by communication systems, since synchronous data slot transmission needs extra circuitry to obtain the synchronization. However, as shown in this thesis, synchronous transmission can greatly increase the number of simultaneous users, or it can decrease the necessary length of the code sequences, so as to increase the data speed, given the same number of users and the same BER performance. Therefore, further investigation should be carried out for this kind of transmission.

An experimental CDMA communication system was designed and set up, which consisted of coders, laser transmitters, 3 dB coupler, single mode fiber transmission line, PIN detector, amplifier, and a decoder. The system was operated at a 1.40 Mb/s data rate (44.736 Mb/s DS-3 chip rate). The address sequences used here were Gold sequences { $a \oplus b$, $a \oplus T^1 b$, $a \oplus T^2 b$, $\cdots$, $a \oplus T^{30} b$ } belonging to the set with 31 chips. The 44.736 Mb/s coded signals from two stations were mixed in the 3 dB optical coupler and transmitted by a 1.3 μm single mode fiber channel. Each transmitter and receiver was designed such that it was able to use any one of the 31 Gold sequences, i.e., it was able to function as any one of the 31 possible users. Experimental measurements for the BER were taken, with one and two station transmitting.

An unique feature of the decoder in this system is the use of an analog multiplier to perform the correlation, as well as an integrate-and-dump filter and a decision circuit to obtain the decoded output at the receiver. This allowed an increase in the speed of the system to the 44.736 Mb/s (T3) channel rate. By using the shortest 31-chip Gold codes, a data rate of 1.40 Mb/s was obtained. This speed is considerably higher than the one achieved by S. Tamura et al. [20], who used the CCD in the decoder. The use of surface-acoustic-wave (SAW) devices in the decoder could also allow a higher data speed. However, this would increase the system cost, as SAW devices are comparatively expensive.

Using the experimental system, various BER measurements were carried out for three different system conditions: one station transmission, two station transmission with equal power, and two station transmission with unequal power. The experimental results indicate that the system performance is dependent on the power balance of the network, and is influenced by the interference of the signal from other users and the system noise (produced by the laser sources, the optical detector, the amplifier, and the circuits). A BER of less than 10^{-9} was obtained for one user with a minimum optical power of -3.9 dBμ, or for two users each with a power of 3.3 dBμ. For the worst case, when the interference signal was bigger than the desired signal, up to a difference of 3.0 dB, the BER was less than 10^{-9}; and for a difference of 3.3 dB, the BER was 5.0×10^{-6}.

Electrical signal processing has been used in this thesis work. An optical fiber CDMA system employing electrical signal processing uses both the positive and negative polarity of the signal. For this reason, the address codes for conventional CDMA, which have been investigated thoroughly for many years, can be simply introduced into the optical fiber CDMA system without changing the correlation property of the codes. Otherwise, for a transmission employing optical signal processing, new optical orthogonal codes need to be introduced; such codes have been discussed in the literatures [21, 32], and still require further investigation. It should be pointed out that the allowed data rate in a system employing optical processing can be higher than the data rate in a system using electrical processing, because the latter is limited by the speed of the electronic circuits. However, there are many applications for low cost multi user systems that require a relatively low data rate (1 Mb/s to 100 Mb/s). The optical fiber CDMA electrical processing system reported in this thesis used currently available techniques, and is relatively inexpensive. Further research that can be carried out are outlined below:

(1) This thesis has experimentally investigated the transmission

with two simultaneous users. Further experimental verification of the relationship between the BER and the number of users could be carried out by introducing more users or by simulating the interference from many simultaneous users.

(2) As discussed in Section 5.5, it is possible to improve the experimental system performance of the decoder circuit by optimizing the correlator circuit design and construction. Attention should be paid to further improving the charging and discharging characteristic of the integrate-and-dump circuit, in order to decrease the signal distortion and increase the system speed. Improvement of the circuit properties may also be possible by using a custom IC in the correlator.

(3) This research has considered in detail the interference noise caused by different user signals. However, the white noise and fluctuation introduced by the laser sources, the optical fiber channel, and the optical detector, also play an important part in a communication system. Therefore, an accurate investigation into the effect of the white noise on the system performance needs to be made.

(4) In order to realize synchronous data slot transmission in a real communication system, a method of distributing the clock signal to the different transmitters or some other technique of achieving transmitter synchronization among users needs to be investigated.

Generally speaking, electrical signal processing always limits the data rate. To fully realize the potential of fiber optical CDMA communications, large bandwidth signal processing will be required. An all-optical system could be quite promising for this, and it should provide a substantial improvement in the capacity and signal speed of multi-user systems. Some of the present areas of research in the field of all-optical coding are: the possibility of using the Prime Code or improved pseudo-orthogonal optical codes, the investigation of better correlation techniques and, in the future, utilization of coherent communication.

It is hoped that the work of this thesis will stimulate and help future research of optical fiber multi-user communications in both the theoretical and experimental aspects.

REFERENCES

1. J. Senior, *Optical Fiber Communications*, Prentice-Hall International, Inc., London, 1985, pp.7-9.

2. S. Geckeler, *Optical Fiber Transmission Systems*, Artech House, Inc., Norwood, 1987, pp.253-273.

3. R. E. Ziemer and R. L. Peterson, *Digital Communications and Spread Spectrum Systems*, Macmillan and Collier, New York, 1985, pp.5-7.

4. C. W. Lundgren, "Applications of Video on Fiber Cable," *IEEE Comm. Magazine*, Vol.24, No.5, May 1986, p.33.

5. J. R. Brandsma, "PHILAN: a Fiber Optic Ring for Voice and Data," *IEEE Comm. Magazine*, Vol.24, No.12, May 1986, p.17.

6. G. J. Foschini and G. Vannucci, "Using Spread-Spectrum in a High-Capacity Fiber-Optical Local Network," *J. Lightwave Technol.*, Vol.LT-6, No.3, Mar. 1988, pp.370-379.

7. R. E. Wagner, W. B. Sessa, "16-channel Coherent Broadcast network at 155 Mb/s", *Proc. OFFC'89*, 1989, PD12-1.

8. T. E. Darcie, "Subcarrier Multiplexing for Multiple-Access Lightwave Networks", *J. Lightwave Technol.*, Vol.LT-5, No.8, Aug. 1987, pp.1103-1110.

9. C. P. Tou, "Code Division Multiplexing for Optical Fiber Communications", *Proc. IEEE Pacific Rim Conference on Communication, Computers and Signal Processing*, 1987, pp.327-330.

10. E. G. Rawson and R. M. Metcalfe, "Fibernet: Multimode Optical fibers for local computer networks", *IEEE Trans. Comm.*, 1978, pp.983-990.

11. I. M. Habbab, M. Kavehrad and C. Sundberg, "Protocols for very high speed fiber local area networks using a passive star topology". *J. Lightwave Technol.*, LT-5, Dec. 1987, pp.1782-1794.

12. A. Fapojuwo, D. Irvine-Halliday and W. Chan, "A new multiple access protocol for active star-configured fiber-optical local area networks-starmap", *Proc. ICC'88*, 1988, pp.1509-1513.

13. R. C. Dixon, *Spread Spectrum Systems*, John Wiley & Sons, Inc., New York, 1976, p.4.

14. Ibid., p.16.

15. D. V. Sarwate, and M. B. Pursley, "Cross correlation properties of pseudorandom and related sequences," *Proc. IEEE.*, Vol.68, May 1980, pp.598-619.

16. R. C. Dixon, *Spread Spectrum Systems*, John Wiley & Sons, Inc., New York, 1976, pp.214-248.

17. J. W. MacName, "Noise Tolerant Multiplex System," *U. S. Patent*, No.4., June30, 1981, pp.276 and 640.

18. K. G. Johannsen, "CDMA versus FDMA channel capacity in mobile satellite communication", *International J. of Satellite Comm.*, Vol.6, 1988, pp.29-39.

19. J. A. Salehi and C. A. Brackett, "Fundamental principles of fiber optics code division multiple access (FO-CDMA)", *Proc. ICC'87*, 1987, pp.1601-1609.

20. S. Tamura, S. Nakano, and K. Okazaki, "Optical code-multiplex transmission by Gold sequences," *J. Lightwave Technol.*, Vol.LT-3, No.1, Feb. 1985, pp.121-127.

21. P. R. Prucnal and M. A. Santoro, "Spread spectrum fiber-optic local area network using optical processing," *J. Lightwave Technol.*, Vol.LT-4, No.5, May 1986, pp.547-554.

22. D. J. Blumenthal and P. R. Prucnal, "Performance of an 8x8 LiN3bc Switch matrix as a giga-hertz self-routing switch node", *Electron. Lett.*, Vol.23, 1987, pp.1359-1360.

23. P. R. Prucnal, "Ultra fast fiber-optic networks using all-optical processing", *Proc. ICC'88*, 1988, pp.1485-1489.

24. T. Ishihara, H. Naito, "16-channel digital optical CATV distribution using 1.6 Gbit/s, 3-level optical transmission", *Proc. ECOC'88*, 1988, pp.545-548.

25. R. I. MacDonald, and G. D. Fraser, "Optical code-division Multiplex for high speed transmission," *Proc. 14th Biennial Symposium on Comm.*, Kingston, May 1988, pp.A.4.1-A.4.3.

26. R. L. Pickholtz, D. L. Schilling and L. B. Milstein, "Theory of spread-spectrum communications — a tutorial", *IEEE Trans. on comm.*, VOL.COM-30, NO.5, May 1982, pp.855-884.

27. G. R. Cooper and C. D. McGillem, *Modern Communications and Spread Spectrum*, McGraw-Hill, Inc., New York, 1986, p.279.

28. R. C. Stanley, "Fiber optical local-area networks", *Proc. NFC'88*, Vol.42, No.1, pp.390-396.

29. S. Y. Suh, "Fiber Optical Local Area Network Topology," *IEEE Comm. Magazine*, Vol.24, No.8, Aug. 1986, p.26.

30. R. C. Dixon, *Spread Spectrum Systems*, John Wiley & Sons, Inc., New York, 1976, p.58.

31. R. Gold, "Maximal Recursive Sequences with 3-Valued Recursive Cross-Correlation Functions", *IEEE Trans. Inform. Theory*, Vol.IT-14, Jan. 1968, pp154-156.

32. A. A. Shaar, and P. A. Davies, "Prime Sequences: Quasi-Optimal Sequences for Or Channel Code Division Multiplexing", *Electron. Lett.* Vol.19, No.21, Oct. 1983, pp.888-889.

33. Z. A. Abbasi and F. Ghani, "Multilevel sequences with good auto-correlation properties", *Electron. Lett.*, Vol.24, No.7, Mar. 1988, pp.393-394.

34. J. R. Lee and C. K. Un, "A Code-Division Multiple-Access Local Area Network", *IEEE Trans. Commun.*, Vol.Com-35, No.6, June 1987, pp.667-671.

35. W. W. Peterson, *Error Correcting Codes*, MIT Press, Wiley, New York.

36. P. Z. Peebles, *Probability, Random Variables, and Random Signal Principles*, McGraw-Hill Book Company, New York, 1987, p.44.

37. R. C. Dixon, *Spread Spectrum Systems*, John Wiley & Sons, Inc., New York, 1976, pp.167-175.

38. J. G. Proakis, *Digital Communications*, McGraw-Hill Book Company, New York, 1983, pp43-44.

39. Ibid., p.24.

40. Z. Chen, P. A. Goud, C. G. Englefield, "Fiber optic multi-user access using spread spectrum techniques", *Proc. Canadian Conf. on Electrical and Computer Eng.*, Vancouver, Nov. 1988, pp.B.3.5-B.3.8.

41. *Schottky TTL Data*, Motorola Inc., 1983.

42. *MECL Device Data*, Motorola Inc., 1987.

43. W. R. Blood, *MECL Design handbook*, Motorola Inc., 1983.

44. Technical Staff of CSELT, *Optical Fiber Communication*, McGraw-Hill Inc., Torino, Italy, 1981, pp.780-783.

45. P. R. Gray and R. G. Meyer, *Analysis and Design of Analog Integrated Circuits*, John Wiley & Sons, Inc., New York, 1984, p.238.

46. C. M. Miller, *Optical Fiber Spices and Connectors theory and Method*, Marcel Dekker, Inc., New York, 1986, pp.96-99.

47. Ibid., pp.249-265.

48. J. Gowar, *Optical communication Systems*, Prentic-Hall International, Inc., London, 1984, pp.78-80.

49. G. R. Cooper and C. D. McGillem, *Modern Communications and Spread Spectrum*, McGraw-Hill, New York, Inc., 1986, pp.337-342.

50. A. D. Evans, *Designing with Field-Effect Transistors*, McGraw-Hill, Inc., New York, 1981.

51. H. Taub and D. L. Schill, *Principles of Communication Systems*, McGraw-Hill, Inc., New York, pp.89-91.

52. Z. Chen, P. A. Goud, and C. G. Englefield, "Code Division Multiple Access with Electrical Processing for Fiber Optic Local Area Network Applications", *Proc. 14th Biennial Symposium on Comm.*, Kingston, May 1988, pp.659-662.

53. G. R. Cooper and C. D. McGillem, *Modern Communications and Spread Spectrum*, McGraw-Hill, New York, Inc., 1986, p.65.

54. H. Sobol, "Fundamentals of Transmission Technology", *Proc. NFC'88*, 1988, Vol.42, No.1 pp.427-432.

55. J. Gowar, *Optical Communication Systems*, Prentic-Hall International, Inc., London, 1984, pp.411.

APPENDIX A

GAUSSIAN APPROXIMATIONS FOR BER CAUSED BY MULTI-USER INTERFERENCE

Assume there are k simultaneous users in the system, and the set of 31-chip Gold sequences is used to encode data signals. From Section 3.1.1, ignoring the channel noise, the correlator output at the receiver j is

$$R_j = A_j \Phi_{jj}(0) + \sum_{i \neq j} A_i \Phi_{ij}(T_i) \qquad (A.1)$$

where A_j, A_i = +1 or -1.

Referring to Section 2.3, the auto-correlation of Gold sequences gives

$$\Phi_{ii}(0) = N, \qquad (2.3.3)$$

the in-phase cross-correlation between any pair of sequences { a, $a \oplus b$, $a \oplus Tb$, $a \oplus T^2 b$, $\cdots$, $a \oplus T^{30} b$ } is

$$\Phi_{ij}(0) = -1, \qquad (2.3.4)$$

and the out-of-phase cross-correlations, when the sequences are displaced by ℓ chips, are

$$\Phi_{ij}(T_l) = \begin{cases} -1+2^{(n+1)/2} \\ -1 \\ -1-2^{(n+1)/2} \end{cases}, \qquad (2.3.6.a)$$

with probability respectively to

$$p\ (\ \Phi_{ij}(T_l)) = \begin{cases} (2^{n-2}+2^{(n-3)/2})/N \\ (2^n-2^{n-1}-1)/N \\ (2^{n-2}-2^{(n-3)/2})/N \end{cases} \qquad (2.3.6.b)$$

For asynchronous data slot transmission, (A.1) becomes

$$R_{j,asyn} = N \cdot A_j + \sum_{i \neq j} A_i \cdot \Phi_{ij}(T_i) \qquad (A.2)$$

while for synchronous case, (A.1) becomes

$$R_{j,syn} = A_j \cdot \Phi_{jj}(0) + \sum_{i \neq j} A_i \cdot \Phi_{ij}(0)$$

$$= N \cdot A_j - \sum_{i \neq j} A_i \cdot \Phi_{ij}(0) \qquad (A.3)$$

The first term in (A.2) or (A.3) is the desired signal and other terms are interference terms, which represent signals intended to be received by other stations.

At the receiver, the data is regenerated after decoding. The probability of error, hence the bit error rate (BER), may be broken down into two parts:

$$BER = p(1|0)\ P(0) + p(0|1)\ P(1) \qquad (A.4)$$

where, $p(1|0)$ is the probability of regenerating 1 when 0 is sent,

$p(0|1)$ is the probability of regenerating 0 when 1 is sent,

$P(0)$ is the probability of data 0 is sent, and

$P(1)$ is the probability of data 1 is sent.

Assume equal "a priori" probabilities for the transmitted data symbols 0 and 1, i.e.,

$$P(\mathcal{A}_i) = P(0) = P(1) = 1/2$$

or

$$P(A_i) = P(-1) = P(+1) = 1/2 \qquad (A.5)$$

We have,

$$BER = (1/2)\ [p(1|0) + p(0|1)] \qquad (A.6)$$

When k, the number of simultaneous users, is sufficiently large, the mean value for the interference term $A_i\ \Phi_{ij}(T_l)$, for either asynchronous or synchronous case, is,

$$\mathbb{E}(\ A_i \cdot \Phi_{ij}(T_l)\ ) = \sum_{P} P\ (A_i) \cdot A_i \cdot \Phi_{ij}(T_l)$$

$$= \sum_{P} [1/2 \cdot (1) \cdot \Phi_{ij}(T_l)] + \sum_{P} [1/2 \cdot (-1) \cdot \Phi_{ij}(T_l)]$$

$$= 0 \qquad (A.7)$$

with the variance given by

$$\sigma^2 = \mathbb{E}\,[\,A_i\ \Phi_{ij}(T_l)\,]^2 - [\mathbb{E}(\,A_i\ \Phi_{ij}(T_l)\,)]^2$$

$$= \sum_{P,p}\{\ [A_i\ \Phi_{ij}(T_l)\ ]^2\cdot\ p\ [A_i\ \Phi_{ij}(T_l)\ ]\ \} - 0$$

$$= \sum_{P,p}\{\ [A_i\ \Phi_{ij}(T_l)\ ]^2\cdot\ P(A_i)\cdot p(\Phi_{ij}(T_l))\ \}$$

$$= 2 \times (1/2)\cdot\sum_{p}\{\ [A_i\ \Phi_{ij}(T_l)\ ]^2\cdot p(\Phi_{ij}(T_l))\ \}$$

$$= \sum_{p}\{\ [A_i\ \Phi_{ij}(T_l)\ ]^2\cdot p(\Phi_{ij}(T_l))\ \} \qquad \text{(A.8)}$$

Therefore, for asynchronous case,

$$\sigma^2_{asyn} = (-1+2^{(n+1)/2})^2\cdot(2^{n-2}+2^{(n-3)/2})/N + (-1)^2\cdot(2^n-2^{n-1}-1)/N$$

$$+ (-1-2^{(n+1)/2})^2\cdot(2^{n-2}+2^{(n-3)/2})/N$$

$$= \frac{(\ N^2+N-1)}{N}\ , \qquad \text{(A.9)}$$

and for synchronous case,

$$\sigma^2_{syn} = (1)^2\cdot 1/2 + (-1)^2\cdot 1/2 = 1\ . \qquad \text{(A.10)}$$

When the number of the simultaneous user (k) is large, the overall interference has an almost Gaussian distribution [35, 36], hence, the variance of interference terms in (A.2) or (A.3) is $(k-1)\sigma^2$.

According to the Central Limit Theorem [37], the error probability, hence the system bit error rate, caused by the Gaussian distributed interference with zero mean and variance $(k-1)\sigma^2$, is

$$\text{BER} = \frac{1}{2} - \frac{1}{2}\ \text{erf}\left[\ \frac{N}{\sqrt{2(k-1)}\ \ \sigma}\ \right]\ , \qquad \text{(A.11)}$$

where,

$$\text{erf}(x) = \frac{2}{\sqrt{\pi}}\int_0^x e^{-u^2/2}\,du \qquad \text{(A.12)}$$

is the error function [38].

Therefore, the BER for the asynchronous data slot transmission is

$$BER_{asyn} = \frac{1}{2} - \frac{1}{2}\,\mathrm{erf}\left[\sqrt{\frac{N^{3}}{2(k-1)(N^{2}+N-1)}}\right], \qquad (A.13)$$

and the BER for the synchronous data slot transmission is

$$BER_{syn} = \frac{1}{2} - \frac{1}{2}\,\mathrm{erf}\left[\frac{N}{\sqrt{2(k-1)}}\right]. \qquad (A.14)$$

APPENDIX B

ACCURATE CALCULATIONS FOR BER CAUSED BY MULTI-USER INTERFERENCE

When the number of simultaneous users k is small, the interference of undesired users is not Gaussian distributed, therefore, the BER results from APPENDIX A are no longer right for these situations. Detailed discussions and accurate calculations for these cases are given below.

B.1 The Case of Asynchronous Data Slot Transmission

For asynchronous data slot transmission, the correlator output of receiver j is given in (3.1.1):

$$R_j = A_j \ \Phi_{jj}(0) + \sum_{i \neq j} A_i \Phi_{ij}(T_i) \qquad (3.1.1)$$

where A_j, A_i = +1 or -1.

Look at the interference terms $\Phi_{ij}(T_i)$, from (2.3.6.a), the maximum value of $\Phi_{ij}(T_i)$ is $\pm|1+2^{(n+1)/2}|$. Therefore, the largest interference occurs when the intend data is $A_j = 1$ while the data being sent to other stations are $A_i \equiv -1$ (i = 1, 2, 3, $\cdots$, $i \neq j$) (or $A_j = -1$ while $A_i \equiv 1$), and the largest interference noise in this case will be due to the correlation value $|1+2^{(n+1)/2}|$. Now the correlator output at receiver j is, from (3.1.1),

$$R_j = N\ A_j + \sum_{i \neq j} A_i \ (1+ 2^{(n+1)/2})$$

$$= N + (-1)(k-1)(1+ 2^{(n+1)/2}) \qquad (B.1.1)$$

If the R_j is greater than zero when data $A_j = 1$ is transmitted, or R is less than zero when $A_j = -1$ is transmitted, then there will be no error caused by interference. This requires

$$N - (k-1)\cdot(1 + 2^{(n+1)/2}) > 0, \qquad \text{(B.1.2)}$$

that is,

$$k < K = \frac{2^n + 2^{(n+1)/2}}{1 + 2^{(n+1)/2}} . \qquad \text{(B.1.3)}$$

Therefore, we have

$$BER_{k<K} = 0. \qquad \text{(B.1.4)}$$

Some examples are shown in Table B.1.

Table B.1 Values of N and k when BER=0, asynchronous transmission

k	N-chip Gold code
≤ 4	N=31, n = 5
≤ 8	N=127, n = 7
≤ 16	N=511, n = 9

In fact, even when k is larger than K, it is still possible to get no error caused by interference. The error probability, which is equal to the BER, can be calculated as follows.

For the case of N = 31,

$$\Phi_{jj}(0) = 31 \qquad \text{(B.1.5)}$$

$$\Phi_{ij}(T_l) = \begin{cases} +7 \\ -1 \\ -9 \end{cases}, \text{ with probability of } p(\Phi_{ij}(T_l)) = \begin{cases} 10/31 \\ 15/31 \\ 6/31 \end{cases} \qquad \text{(B.1.6)}$$

Whenever

$$31 + \sum_l \Phi_{lj}(T_l) < 0 \tag{B.1.7}$$

there is a error.

When $k \le 4$, as shown in Table B.1,

$$\text{BER} \equiv 0. \tag{B.1.8}$$

When $k = 5$, the only three cases that produce error, i.e., the correlator outputs R gets wrong polarity (this occurs when the sum of the cross-correlations is larger than the auto-correlation of 31), are:

(1) when the desired signal is $A_j = 1$ and each of the four cross-correlations is -9. This requires that every undesired signal is $A_i = 1$ (which has a probability of 1/2) and its cross-correlation at receiver j is -9 (which has a probability of (6/31)) among the three possible value shown in (B.5).

(2) when the desired signal is $A_j = 1$ and one of the four cross-correlations is -7 (which has a probability of (1/2)×(10/31)) while the other three are all -9 (each has a probability of (1/2)×(6/31)).

(3) when the desired signal is $A_j = 1$ and two of the four cross-correlation are all -7 while the other two are all -9.

These different combinations are shown in Table B.2. Considering these situations, the probability of error (BER) is

$$\begin{aligned} \text{BER } (k=5) &= \left(\frac{1}{2}\cdot\frac{6}{31} \right)^4 + \left(\frac{1}{2}\cdot\frac{6}{31} \right)^3 \cdot \left(\frac{1}{2}\cdot\frac{10}{31} \right)\cdot 4 \\ &\quad + \left(\frac{1}{2}\cdot\frac{6}{31} \right)^2 \cdot \left(\frac{1}{2}\cdot\frac{10}{31} \right)^2 \cdot 6 \\ &= 2.14 \times 10^{-3} \end{aligned} \tag{B.1.9}$$

When $k = 6$, the different situation where error occurs are shown in Table B.3.

Table B.2 The combinations of cross-correlation which cause error for the case of N=31, k=5, $\mathcal{A}_j=1$ and asynchronous transmission

$\Phi_{ij}(T_l)$	Times this will occur
-9 -9 -9 -9	1
-9 -9 -9 -7	4
-9 -9 -7 -7	6

Table B.3 The combinations of cross-correlation which cause error for the case of N=31, k=6, $\mathcal{A}_j=1$ and asynchronous transmission

$\Phi_{ij}(T_l)$	Times this will occur
-9 -9 -9 -9 -9	1
-9 -9 -9 -9 -7	5
-9 -9 -9 -9 -1	5
-9 -9 -9 -9 +1	5
-9 -9 -9 -7 -7	10
-9 -9 -9 -7 -1	20
-9 -9 -9 -7 +1	20
-9 -9 -7 -7 -7	10
-9 -9 -7 -7 -1	30
-9 -9 -7 -7 +1	30 *
-9 -7 -7 -7 -7	5
-9 -7 -7 -7 -1	20 *
-7 -7 -7 -7 -7	1

* Here the sum of cross-correlation is -N, so that the output of the correlator is 0. The probability of decision error is 1/2.

The overall average BER is

$$BER\ (k=6) = \left(\frac{1}{2}\cdot\frac{6}{31}\right)^5 + \left(\frac{1}{2}\cdot\frac{6}{31}\right)^4\cdot\left(\frac{1}{2}\cdot\frac{10}{31}\right)\cdot 5$$

$$+ \left(\frac{1}{2}\cdot\frac{6}{31}\right)^4\cdot\left(\frac{1}{2}\cdot\frac{15}{31}\right)\cdot 10 + \left(\frac{1}{2}\cdot\frac{6}{31}\right)^3\cdot\left(\frac{1}{2}\cdot\frac{10}{31}\right)^2\cdot 10$$

$$+ 40\cdot\left(\frac{1}{2}\cdot\frac{6}{31}\right)^3\cdot\left(\frac{1}{2}\cdot\frac{15}{31}\right)\cdot\left(\frac{1}{2}\cdot\frac{10}{31}\right) + 10\cdot\left(\frac{1}{2}\cdot\frac{6}{31}\right)^2\cdot\left(\frac{1}{2}\cdot\frac{10}{31}\right)^3$$

$$+ 45\cdot\left(\frac{1}{2}\cdot\frac{6}{31}\right)^2\cdot\left(\frac{1}{2}\cdot\frac{10}{31}\right)^2\cdot\left(\frac{1}{2}\cdot\frac{15}{31}\right) + 5\cdot\left(\frac{1}{2}\cdot\frac{6}{31}\right)\cdot\left(\frac{1}{2}\cdot\frac{10}{31}\right)^4$$

$$+ 10\cdot\left(\frac{1}{2}\cdot\frac{6}{31}\right)\cdot\left(\frac{1}{2}\cdot\frac{15}{31}\right)\cdot\left(\frac{1}{2}\cdot\frac{10}{31}\right)^3 + \left(\frac{1}{2}\cdot\frac{10}{31}\right)^5$$

$$= 6.41 \times 10^{-3} \qquad (B.1.10)$$

Similar as the case of N = 31, for the case of N = 127,

$$\Phi_{jj}(0) = 127 \qquad (B.1.11)$$

$$\Phi_{ij}(T_l) = \begin{cases} +15 \\ -1 \\ -17 \end{cases}, \text{ with probability of } \rho(\Phi_{ij}(T_l)) = \begin{cases} 36/127 \\ 63/127 \\ 28/127 \end{cases} \qquad (B.1.12)$$

Whenever

$$127 + \sum_l \Phi_{ij}(T_l) < 0 \qquad (B.1.13)$$

there is a error.

When $k \le 8$, as shown in Table B.1,

$$BER \equiv 0. \qquad (B.1.14)$$

When k =9, the different situations where error occur are shown in Table B.4. The overall average BER is

$$BER\ (k=9) = \left(\frac{1}{2}\cdot\frac{28}{127}\right)^8 + 8\cdot\left(\frac{1}{2}\cdot\frac{28}{127}\right)^7\cdot\left(\frac{1}{2}\cdot\frac{36}{127}\right)$$

$$+ 28\cdot\left(\frac{1}{2}\cdot\frac{28}{127}\right)^6\cdot\left(\frac{1}{2}\cdot\frac{36}{127}\right)^2 + 56\cdot\left(\frac{1}{2}\cdot\frac{28}{127}\right)^5\cdot\left(\frac{1}{2}\cdot\frac{36}{127}\right)^3$$

$$+ 70\cdot\left(\frac{1}{2}\cdot\frac{28}{127}\right)^4\cdot\left(\frac{1}{2}\cdot\frac{36}{127}\right)^4$$

$$= 2.82 \times 10^{-6} \qquad (B.1.15)$$

Table B.4 The combinations of cross-correlation which cause error for the case of N=127, k=9, A_j=1 and asynchronous transmission

$\Phi_{ij}(T_l)$	Times this will occur
-17 -17 -17 -17 -17 -17 -17 -17	1
-17 -17 -17 -17 -17 -17 -17 -15	8
-17 -17 -17 -17 -17 -17 -15 -15	28
-17 -17 -17 -17 -17 -15 -15 -15	56
-17 -17 -17 -17 -15 -15 -15 -15	70

For the case of N = 511,

$$\Phi_{jj}(0) = 511 \tag{B.1.16}$$

$$\Phi_{ij}(T_l) = \begin{cases} +31 \\ -1 \\ -33 \end{cases} \text{,with probability of } p(\Phi_{ij}(T_l)) = \begin{cases} 136/511 \\ 255/511 \\ 120/511 \end{cases} \tag{B.1.17}$$

Whenever

$$511 + \sum_i \Phi_{ij}(T_l) < 0 \tag{B.1.18}$$

there is a error.

When k ≤ 16, as shown in Table B.1, BER ≡ 0. (B.1.19)

When k = 17, the different situations where error occur are shown in Table B.5. The overall average BER is

$$\begin{aligned} \text{BER (k=9)} = {} & \left(\frac{1}{2}\cdot\frac{120}{511} \right)^{16} + 16\cdot\left(\frac{1}{2}\cdot\frac{120}{511} \right)^{15}\cdot\left(\frac{1}{2}\cdot\frac{136}{511} \right) \\ & + 120\cdot\left(\frac{1}{2}\cdot\frac{120}{511} \right)^{14}\cdot\left(\frac{1}{2}\cdot\frac{136}{511} \right)^{2} + 560\cdot\left(\frac{1}{2}\cdot\frac{120}{511} \right)^{13}\cdot\left(\frac{1}{2}\cdot\frac{136}{511} \right)^{3} \\ & + 1820\cdot\left(\frac{1}{2}\cdot\frac{120}{511} \right)^{12}\cdot\left(\frac{1}{2}\cdot\frac{136}{511} \right)^{4} + 2184\cdot\left(\frac{1}{2}\cdot\frac{120}{511} \right)^{11}\cdot\left(\frac{1}{2}\cdot\frac{136}{511} \right)^{5} \\ & + 8008\cdot\left(\frac{1}{2}\cdot\frac{120}{511} \right)^{10}\cdot\left(\frac{1}{2}\cdot\frac{136}{511} \right)^{6} + 11440\cdot\left(\frac{1}{2}\cdot\frac{120}{511} \right)^{9}\cdot\left(\frac{1}{2}\cdot\frac{136}{511} \right)^{7} \end{aligned}$$

$$= 6.86 \times 10^{-11} \quad (B.1.20)$$

Table B.5 The combinations o[illegible] cross-correlation which cause error for the case of N=511, $\mathcal{A}_j$=1 and asynchronous transmission

$\Phi_{ij}(T_l)$																Times this will occur
-33	-33	-33	-33	-33	-33	-33	-33	-33	-33	-33	-33	-33	-33	-33	-33	1
-33	-33	-33	-33	-33	-33	-33	-33	-33	-33	-33	-33	-33	-33	-33	-31	16
-33	-33	-33	-33	-33	-33	-33	-33	-33	-33	-33	-33	-33	-33	-31	-31	120
-33	-33	-33	-33	-33	-33	-33	-33	-33	-33	-33	-33	-33	-31	-31	-31	560
-33	-33	-33	-33	-33	-33	-33	-33	-33	-33	-33	-33	-31	-31	-31	-31	1820
-33	-33	-33	-33	-33	-33	-33	-33	-33	-33	-33	-31	-31	-31	-31	-31	2184
-33	-33	-33	-33	-33	-33	-33	-33	-33	-33	-31	-31	-31	-31	-31	-31	8008
-33	-33	-33	-33	-33	-33	-33	-33	-33	-31	-31	-31	-31	-31	-31	-31	11440

B.2 The Case of Synchronous Data Slot Transmission

For synchronous data slot transmission, the correlator output of receiver j is given in (3.1.2)

$$R_j = A_j N + \sum_{i \neq j} A_i \Phi_{ij}(0) \quad (B.2.1)$$

where A_j, A_i = +1 or −1 corresponding to the data $\mathcal{A}_j$, $\mathcal{A}_i$ = 1 or 0, and the interference $\Phi_{ij}(0)$ is ± 1 as given in (2.3.4). Therefore, the largest interference occurs when the intended data is A_j= 1 while all the other stations are sending $A_i \equiv 1$ (i = 1, 2, 3, ···, $i \neq j$) (or A_j= 1 while $A_i \equiv 1$), and the largest interference noise in this case will be due to the correlation value -1. Now the correlator output at the receiver j is,

$$R_j = N A_j + (-1)(k-1)A_i = N - (k-1) \quad (B.2.2)$$

If R_j is greater than zero when $A_j = 1$ is transmitting, or R is less than zero when $A_j = -1$ is transmitting, then, there will be no error caused by interference. This requires

$$N - (k-1) > 0 \quad (B.2.3)$$

that is,

$$k < N+1 \quad (B.2.4)$$

Therefore, we have

$$BER_{k<k} = 0. \quad (B.2.5)$$

Some examples are shown in Table B.6.

Table B.6 Values of N and k when BER=0, synchronous transmission

k	N-chip Gold Sequence
≤ 31	N=31 (n=5)
≤ 127	N=127 (n=7)
≤ 511.	N=511 (n=9)

Similar as the asynchronous case, when k is larger than K, it is still possible to get no error caused by the interference. The error probability (BER) can be calculated as follows.

According (B.1.2), whenever

$$N + \sum_i (-1) < 0 \quad (B.2.6)$$

there is a error.

Firstly, let us consider N = 31. When $k \le 31$, as shown in Table B.6, BER ≡ 0. When k = 32, 33, 34, 35, 36, the situations where error occur are shown in Table B.7 respectively.

Table B.7 The combinations of cross-correlation which cause error for the case of N=31, A_j=1 and synchronous transmission

k	$\pm\Phi_{ij}(0)$	Times this will occur
	1 2 3 ··· 27 28 29 30 31 32 33 34 35	
32	-1 -1 -1 ··· -1 -1 -1 -1	1*
33	-1 -1 -1 ··· -1 -1 -1 -1 -1	1
34	-1 -1 -1 ··· -1 -1 -1 -1 -1 -1 -1	1
	-1 -1 -1 ··· -1 -1 -1 -1 -1 -1 +1	1*
35	-1 -1 -1 ··· -1 -1 -1 -1 -1 -1 -1 -1	1
	-1 -1 -1 ··· -1 -1 -1 -1 -1 -1 -1 +1	34
36	-1 -1 -1 ··· -1 -1 -1 -1 -1 -1 -1 -1 -1	1
	-1 -1 -1 ··· -1 -1 -1 -1 -1 -1 -1 -1 +1	35
	-1 -1 -1 ··· -1 -1 -1 -1 -1 -1 -1 +1 +1	595*

* See Table B.3.

The overall average BER are

$$\text{BER (k=32)} = \frac{1}{2}\cdot\left(\frac{1}{2}\right)^{31} = 2.33\times10^{-10} \quad \text{(B.2.7)}$$

$$\text{BER (k=33)} = \left(\frac{1}{2}\right)^{32} = 2.33\times10^{-10} \quad \text{(B.2.8)}$$

$$\text{BER (k=34)} = \left(\frac{1}{2}\right)^{33} + 33\cdot\frac{1}{2}\cdot\left(\frac{1}{2}\right)^{33} = 2.04\times10^{-9} \quad \text{(B.2.9)}$$

$$\text{BER (k=35)} = \left(\frac{1}{2}\right)^{34} + 34\cdot\frac{1}{2}\cdot\left(\frac{1}{2}\right)^{34} = 2.04\times10^{-9} \quad \text{(B.2.10)}$$

$$\text{BER (k=36)} = 36\cdot\left(\frac{1}{2}\right)^{35} + 35\cdot17\cdot\frac{1}{2}\cdot\left(\frac{1}{2}\right)^{35} = 8.69\times10^{-9} \quad \text{(B.2.11)}$$

Secondly, for the case of N = 127.

When $k \le 127$, as shown in Table B.6,

$$BER \equiv 0. \qquad (B.2.12)$$

When k = 128, 129, 130, the situations where error occur are shown in Table B.8 respectively. The overall average BER are

$$BER\ (\ k=128\ ) = \frac{1}{2}\cdot\left(\frac{1}{2}\right)^{127} = 2.94\times10^{-39} \qquad (B.2.13)$$

$$BER\ (\ k=129\ ) = \left(\frac{1}{2}\right)^{128} = 2.94\times10^{-39} \qquad (B.2.14)$$

$$BER\ (\ k=130\ ) = \left(\frac{1}{2}\right)^{129} + 129\cdot\frac{1}{2}\cdot\left(\frac{1}{2}\right)^{129} = 9.62\times10^{-38} \qquad (B.2.15)$$

Table B.8 The combinations of cross-correlation which cause error for the case of N=127, A_j=1 and synchronous transmission

k	$\pm\Phi_{ij}(0)$								Times this will occur
	1	2	3	···	127	128	129	130	
128	-1	-1	-1	···	-1	-1			1*
129	-1	-1	-1	···	-1	-1	-1		1
130	-1	-1	-1	···	-1	-1	-1	-1	1
	-1	-1	-1	···	-1	-1	-1	+1	129*

* See Table B.3.

It is seen from (B.2.13)—(B.2.15) that, when using 127-chip Gold codes, up to 130 users, the BER caused by interference signals is less than 10^{-39}. Therefore, in a real communication, the thermal noise becomes the main source of error and the effect of interference signal can be ignored totally.

APPENDIX C

LIST OF COMPUTER PROGRAMS

```
C ************************************************************

C       PROGRAM #1   (1EA)

C ************************************************************

C       BER CAUSED BY INTERFERENCE OF SIGNAL TO OTHER STATIONS
C       FOR ASYNCHRONOUS TRANSMISSION
C       ERROR PROBABILITY USING CENTRAL LIMITED THEORY

C ************************************************************
        REAL A, B, X, ERROR(160)
        INTEGER N, M, K

C       INPUT DATA M=THE NUMBER OF STAGES OF GOLD CODE GENERATOR
C       M = 5, 7, 9, ...
C       N = THE LENGTH OF GOLD CODE USED AS ADDRESS CODE
C       N = 31, 127, 511, ...

        READ(5,*)M
         A=EXP(M*ALOG(2.))-1.0
         N=A+0.5

C       ACCORDING TO THE CENTRAL LIMIT THEORY
C       BER = ERROR(K)
C       K = THE NUMBER OF SIMULTANEOUS STATIONS

        DO 10 K=2,150
         B=(N*N)/SQRT((K-1.0)*(N*N+N-1.0)*N)
         X=B/SQRT(2.0)
         ERROR(K)=0.5*ERFC(X)

         IF ( ERROR(K).GT.0.1E-09.AND.ERROR(K).LE.0.1E+01) THEN
         GOTO 15
         ELSE
         GOTO 10
         ENDIF

15       WRITE (6,20)  K, ERROR(K)
20       FORMAT (6X, I5, 4X, E12.3)
10      CONTINUE
C *********************************************************
C       RESULT IS PUT IN "1EA31", "1EA127", "1EA511"
C       RESPECTIVELY FOR M = 5, 7, 9
C *********************************************************
        STOP
        END
```

```
C ****************************************************************

C       PROGRAM #2  (2ES)

C ****************************************************************

C       BER CAUSED BY INTERFERENCE OF SIGNAL TO OTHER STATIONS
C       FOR SYNCHRONOUS TRANSMISSION
C       ERROR PROBABILITY USING CENTRAL LIMITED THEORY

C ****************************************************************
        REAL A, B, X, ERROR(2500)
        INTEGER N, M, K

C       INPUT DATA M=THE NUMBER OF STAGES OF GOLD CODE GENERATOR
C       M = 5, 7, 9, ...
C       N = THE LENGTH OF GOLD CODE USED AS ADDRESS CODE
C       N = 31, 127, 511, ...

        READ*, M
         A=EXP(M*ALOG(2.))-1.0
         N=A+0.5

C       ACCORDING TO THE CENTRAL LIMIT THEORY
C       BER = ERROR(K)
C       K = THE NUMBER OF SIMULTANEOUS STATIONS

        DO 10 K=2,2500,10
         B=N/SQRT(K-1.0)
         X=B/SQRT(2.0)
         ERROR(K)=0.5*ERFC(X)

          IF ( ERROR(K).GT.0.100E-24.AND.ERROR(K).LE.1.000) THEN
          GOTO 15
          ELSE
          GOTO 10
          ENDIF

15       WRITE (6,20)  K, ERROR(K)
20       FORMAT (6X, I5, 4X, E12.3)
10      CONTINUE
C ***************************************************************
C       RESULT ERROR(K) IS IN "2ES31", "2ES127", "2ES511"
C       RESPECTIVELY FOR M = 5, 7, 9
C ***************************************************************
        STOP
        END
```

```
C *******************************************************

C     PROGRAM #3 (3TA)

C     ASYCHRONOUS TRANSMISSION OF K SIMULTANEOUS STATIONS

C *******************************************************

C *******************************************************

      INTEGER X(70), Z(70), E, Y(70), A, B,C,D, T
      INTEGER X1(70,70),X2(70,70), XC(31,33,33)
      INTEGER S(32,10), SE(32,10), RS(2,10)
      INTEGER SS(32,200), SUM(190)
      INTEGER RSS(190), SS1(190), RS1(190), DDS(190)

C *******************************************************
C     M-SEQUENCE a, b
C     INPUT INITIAL STATE OF THE 5-STAGE SHIFT REGESTER

      DO 5 I=1,5
       X(I)=1
       Y(I)=X(I)
       Z(I)=X(I)
5      CONTINUE

      DO 20 I=5, 61
       A=F(X(3),X(5))
       B=F(Y(4),Y(5))
       C=F(B,Y(3))
       D=F(C,Y(2))
       E=F(Z(2),Z(5))
       DO 10 N=I,1,-1
        X(N+1)=X(N)
        Y(N+1)=Y(N)
        Z(N+1)=Z(N)
10     CONTINUE
       X(1)=A
       Y(1)=D
       Z(1)=E
20    CONTINUE

C *******************************************************

C     M-SEQUENCES
```

```
C      X(I)=[5,3]
C      Y(I)=[5,4,3,2]
C      Z(I)=[5,2]

       DO 22 I=1,31
        X(I)=X(63-I)
        Y(I)=Y(63-I)
        Z(I)=Z(63-I)
22     CONTINUE
25     FORMAT('  ',32(1X,I2))

C **************************************************

C **************************************************
C      GOLD SEQUENCES
C      X1(T,I) LOGYCAL SIGNAL OF THE Ith CHIP OF THE Tth GOLD CODE
C      X1(1,I)= [5,3]
C      X1(T,I)= [5,3]+(T-1)CHIPS SHIFTED [5,4,3,2]

       DO 30 I=1,31
        X1(1,I)=X(I)
30     CONTINUE
       DO 35 T=2,32
        DO 40 I=1,31
         X1(T,I)=F(X(I),Y(I))
40      CONTINUE
        C1=Y(1)
        DO 37 I=1,30
         Y(I)=Y(I+1)
37      CONTINUE
        Y(31)=C1
35     CONTINUE

C      X2(T,I) ELECTRICAL SIGNAL OF X1(T,I)

       DO 1 T=1,32
       DO 2 I=1,31
       IF (X1(T,I).EQ.1) THEN
       X2(T,I)=1
       ELSE
       X2(T,I)=-1
       ENDIF
2      CONTINUE
1      CONTINUE
11     FORMAT('X2(T,I)=[5,3,]+T [5,4,3,2], AC ELECTRICAL SIGNAL')
```

```
500   FORMAT(I2,32(1X,I2))

C ****************************************************************

C ****************************************************************

C     XC(K,J,I) K-1 [illegible] SHIFT OF THE Ith CHIP OF THE Jth GOLD CODE

      DO 400 J=1,32
      DO 401 I=1,31
      XC(1,J,I)=X2(J,I)
401   CONTINUE
400   CONTINUE
      DO 404 K=2,10
      DO 406 J=1,32
      DO 408 I=1,30
       XC(K,J,I)=XC(K-1,J,I+1)
408    CONTINUE
       XC(K,J,31)=XC(K-1,J,1)
406    CONTINUE
404   CONTINUE

C ************************************************************

C ************************************************************

C     S(N,L) INPUT LOGICAL DATA SIGNALS OF M DIFFERENT STATIONS

C     SE(N,L) AC ELECTRICAL SIGNAL OF S(N,L)

      READ*, M
101   FORMAT('S(STATION N, BIT1-6)')
      DO 100 N=1,M
      READ*, S(N,1),S(N,2),S(N,3),S(N,4),S(N,5),S(N,6)
      DO 420 I=1,6
      IF (S(N,I).EQ.1) THEN
      SE(N,I)=1
      ELSE
      SE(N,I)=-1
      ENDIF
420   CONTINUE
102   FORMAT(50X,I3,'th STATION:', 6(1X,I1))
      WRITE (6,102) N,(S(N,I), I=1,6)
100   CONTINUE
```

```
C *****************************************************************
 
C *****************************************************************
 
C     ELECTRICAL SIGNAL ENCODING
C     SS(L,K) Kth CHIP OF ENCODED SIGNAL SENDING TO THE Lth STATION
 
      DO 104 I=1,6
      DO 106 J=1,31
      K=31*(I-1)+J
      SS(1,K)=SE(1,I)*XC(1,1,J)
106   CONTINUE
104   CONTINUE
 
      DO 124 I=1,6
      DO 126 J=1,31
      K=31*(I-1)+J
       SS(2,K)=SE(2,I)*XC(5,2,J)
       SS(3,K)=SE(3,I)*XC(7,3,J)
       SS(4,K)=SE(4,I)*XC(2,4,J)
       SS(5,K)=SE(5,I)*XC(8,5,J)
       SS(6,K)=SE(6,I)*XC(3,6,J)
       SS(7,K)=SE(7,I)*XC(9,7,J)
       SS(8,K)=SE(8,I)*XC(8,8,J)
       SS(9,K)=SE(9,I)*XC(6,9,J)
       SS(10,K)=SE(10,I)*XC(4,10,J)
126   CONTINUE
124   CONTINUE
 
C ***********************************************************
 
C ***********************************************************
 
C     SUM(K) THE Kth CHIP OF RECEIVED MULTILEVEL SIGNAL
 
      DO 116 K=1,186
      SUM(K)=0
116   CONTINUE
      DO 108 K=1,186
      DO 110 N=1,M
      SUM(K)=SUM(K)+SS(N,K)
110   CONTINUE
108   CONTINUE
 
C **************************************************************
```

```
C     CORRELATION OF THE 1st STATION RECEIVER
C     RSS(K) THE Kth CHIP OF INTEGRATE-AND-DUMP INPUT WAVEFORM
C     RS1(K) THE Kth CHIP OF INTEGRATE-AND-DUMP OUTPUT WAVEFORM

      DO 130 I=1,6
       DO 132 J=1,31
        K=31*(I-1)+J
        RSS(K)=XC(1,1,J)*SUM(J+31*(I-1))
        SS1(K)=SE(1,I)
        RS1(K)=0
        DO 131 N=31*(I-1)+1, K
         RS1(K)=RS1(K)+RSS(N)
131     CONTINUE
132    CONTINUE
130   CONTINUE

C     DECODED DATA

      DO 150 N=1,6
       DO 155 M=31*(N-1)+1, 31*N
       IF (RS1(31*N). LE.0) THEN
        DDS(M)=-1
        ELSE
        DDS(M)=1
       ENDIF
155    CONTINUE
150   CONTINUE

C **************************************************************

C                   ~~~~~~~~ RESULT ~~~~~~~~
C     K--NUMBER OF CHIPS
C     SS1(K) THE Kth CHIP OF DATA SIGNAL FROM THE 1st STATION
C     SS(1,K) THE Kth CHIP OF CODED SIGNAL FROM THE 1st STATION
C     SUM(K) THE Kth CHIP OF THE RECEIVED SIGNAL
C     RSS(K) THE Kth CHIP OF THE CORRELATED SIGNAL
C     RS1(K) THE Kth CHIP OF INTEGRATE-AND-DUMP OUTPUT WAVEFORM
C     DDS(K) THE Kth CHIP OF DECODED DATA AT THE 1st RECEIVER

      DO 136 K=1,186
      WRITE (6,138) K, SS1(K), SS(1,K), SUM(K),RSS(K), RS1(K),DDS(K)
138   FORMAT (I4,6(2X,I5))
136   CONTINUE
```

```
      STOP
      END

C *************************************************************

C     MOD-2 SUM OF BINARY SIGNAL A AND B

      FUNCTION F(A,B)
      INTEGER A,B
      F=A*(1-B)+B*(1-A)
      RETURN
      END

C *************************************************************
```

```
C ***********************************************************

C     PROGRAM #4 (4TS)

C     SYNCHRONOUS TRANSMISSION OF K SIMULTANEOUS STATIONS

C ***********************************************************

C ***********************************************************

      INTEGER X(70), Z(70), E, Y(70), A, B,C,D, T
      INTEGER X1(70,70),X2(70,70), XC(2,33,33)
      INTEGER S(32,10), SE(32,10), RS(2,10)
      INTEGER SS(32,200), SUM(200)
      INTEGER RSS(190), SS1(190), RS1(190), DDS(190)

C ***********************************************************

C     M-SEQUENCE a, b
C     INPUT INITIAL STATE OF THE 5-STAGE SHIFT REGESTER

      DO 5 I=1,5
       X(I)=1
       Y(I)=X(I)
       Z(I)=X(I)
 5    CONTINUE

      DO 20 I=5, 61
       A=F(X(3),X(5))
       B=F(Y(4),Y(5))
       C=F(B,Y(3))
       D=F(C,Y(2))
       E=F(Z(2),Z(5))
       DO 10 N=I,1,-1
        X(N+1)=X(N)
        Y(N+1)=Y(N)
        Z(N+1)=Z(N)
 10    CONTINUE
       X(1)=A
       Y(1)=D
       Z(1)=E
 20   CONTINUE

C ***********************************************************
```

```
C      M-SEQUENCES
C      X(I)=[5,3]
C      Y(I)=[5,4,3,2]
C      C(I)=[5,2]

       DO 22 I=1,31
        X(I)=X(63-I)
        Y(I)=Y(63-I)
        Z(I)=Z(63-I)
 22    CONTINUE
 25    FORMAT('  ',32(1X,I2))

C *********************************************************

C *********************************************************
C      GOLD SEQUENCES
C      X1(T,I) LOGYCAL SIGNAL OF THE Ith CHIP OF THE Tth GOLD CODE
C      X1(1,I)= [5,3]
C      X1(T,I)= [5,3]+(T-1)CHIPS SHIFTED [5,4,3,2]

       DO 30 I=1,31
        X1(1,I)=X(I)
 30    CONTINUE
       DO 35 T=2,32
        DO 40 I=1,31
         X1(T,I)=F(X(I),Y(I))
 40     CONTINUE
        C1=Y(1)
        DO 37 I=1,30
         Y(I)=Y(I+1)
 37     CONTINUE
        Y(31)=C1
 35    CONTINUE

C      ELECTRICAL SIGNAL OF X1(T,I)

       DO 1 T=1,32
       DO 2 I=1,31
       IF (X1(T,I).EQ.1) THEN
       X2(T,I)=1
       ELSE
       X2(T,I)=-1
       ENDIF
 2     CONTINUE
 1     CONTINUE
```

```
11     FORMAT('X2(T,I)=[5,3]+T [5,4,3,2], AC ELECTRICAL SIGNAL')
500    FORMAT(I2,32(1X,I2))

C ************************************************************

C ************************************************************

C      XC(1,J,I) Ith CHIP OF THE O CHIPS SHIFT OF THE Jth GOLD CODE

       DO 400 J=1,32
       DO 401 I=1,31
       XC(1,J,I)=X2(J,I)
401    CONTINUE
400    CONTINUE

C ************************************************************

C      M, NUMBER OF SIMULTANEOUS STATIONS

C      S(N,L) THE Lth BIT OF LOGICAL DATA SIGNAL OF THE Nth STATION

C      SE(N, L) AC ELECTRICAL SIGNAL OF S(N,L)

101    FORMAT('S(STATION N, BIT1-6)')
       READ*, M
       DO 100 N=1,M
       READ*, S(N,1),S(N,2),S(N,3),S(N,4),S(N,5),S(N,6)
       DO 420 I=1,6
       IF (S(N,I).EQ.1) THEN
       SE(N,I)=1
       ELSE
       SE(N,I)=-1
       ENDIF
420    CONTINUE
102    FORMAT(50X,I3, 'th STATION:', 6(1X,I1))
       WRITE(6,102) N,(S(N,I), I=1,6)
100    CONTINUE

C ************************************************************

C ************************************************************

C      ELECTRICAL SIGNAL ENCODING
```

```
      DO 105 N=1,M
      DO 104 I=1,6
      DO 106 J=1,31
      K=31*(I-1)+J
      SS(N,K)=SE(N,I)*XC(1,N,J)
106   CONTINUE
104   CONTINUE
105   CONTINUE

C ************************************************************

C ************************************************************

C     SUM(K) THE KthCHIP OF RECEIVED MULTILEVEL SIGNAL

      DO 116 K=1,186
      SUM(K)=0
116   CONTINUE
      DO 108 K=1,186
      DO 110 N=1,M
      SUM(K)=SUM(K)+SS(N,K)
110   CONTINUE
108   CONTINUE

C *************************************************************

C     CORRELATION OF THE 1stSTATION RECEIVER
C     RSS(K) THE Kth CHIP OF INTEGRATE-AND-DUMP INPUT WAVEFORM
C     RS1(K) THE Kth CHIP OF INTEGRATE-AND-DUMP OUTPUT WAVEFORM

      DO 130 I=1,6
      DO 132 J=1,31
      K=31*(I-1)+J
      RSS(K)=XC(1,1,J)*SUM(J+31*(I-1))
      SS1(K)=SE(1,I)
      RS1(K)=0
      DO 131 N=31*(I-1)+1,K
      RS1(K)=RS1(K)+RSS(N)
131   CONTINUE
132   CONTINUE
130   CONTINUE

C     DECODED DATA

      DO 150 N=1,6
```

```
      DO 155 M=31*(N-1)+1, K
      IF (RS1(31*N).LE.O) THEN
       DDS(M)=-1
       ELSE
       DDS(M)=1
      ENDIF
155   CONTINUE
150  CONTINUE

C ************************************************************

C          ~~~~~~~~~~~~~~~~ RESULT ~~~~~~~~~~~~~~~~
     DO 136 K=1,186
     WRITE (6,138) K, SS1(K), SS(1,K), SUM(K),RSS(K),RS1(K),DDS(K)
138  FORMAT (I4,G(2X,I5))
136  CONTINUE

     STOP
     END

C ************************************************************

     FUNCTION F(A,B)
     INTEGER A,B
     F=A*(1-B)+B*(1-A)
     RETURN
     END

C ************************************************************
```